
Lehrstuhl für Biochemie der Technischen Universität München

**Metabolite and isotopologue profiling in plants.
Studies on the biosynthesis of terpenoids and alkaloids.**

Elena Ostrozhenkova

Vollständiger Abdruck der von der Fakultät für Chemie der Technischen Universität München zur Erlangung des akademischen Grades eines Doktors der Naturwissenschaften genehmigten Dissertation.

Vorsitzende:

Univ.-Prof. Dr. S. Weinkauff

Prüfer der Dissertation:

1. Priv.-Doz. Dr. W. Eisenreich

2. Univ.-Prof. Dr. M. Sattler

Die Dissertation wurde am 16.06.2008 bei der Technischen Universität München eingereicht und durch die Fakultät für Chemie am 08.07.2008 angenommen.

To my parents, my friends, and me

**When a thing was new, people said “It is not true”.
Later, when the truth became obvious, people said “Anyway, it is not
important”. And when its importance could not be denied,
people said, “Anyway it is not new”.**

William James (1842-1920).

Experiments were carried out at the Department of Biochemistry, Technische Universität München, Garching from April 2003 to April 2008.

ACKNOWLEDGEMENT

I wish to thank my Doktorvater PD Dr. Wolfgang Eisenreich for suggesting me an exciting and modern scientific theme; for constant and patient guidance and support; for numerous useful discussions (on scientific matters and beyond); for opening me the doors into the world of “big” science, with international conferences and collaborations. My special thanks to Wolfgang for teaching me NMR spectroscopy.

I am thankful to Prof. Dr. Dr. Adelbert Bacher for the opportunity to spend five great years at the Lehrstuhl für Organische Chemie und Biochemie and for his helpful mentorship.

I am very grateful to Prof. Dr. Michael Groll for a friendly atmosphere in the Lehrstuhl für Biochemie, for his encouraging smiles, and for allowing me to finish my Ph.D. study.

I am indebted to Dr. Felix Rohdich for offering enzymes for my experiments.

I wish to thank Mr. Fitz Wendling (Computer-Man) for many beautiful pictures, for his professional assistance with computer and HPLC problems, and for familiarizing me with ‘die hochbayrische Sprache’.

I am thankful to Mr. Richard Feicht, Mrs. Christine Schwarz, Ms. Birgit Keil, Ms. Katrin Gärtner, Mrs. Astrid König, Dr. Melissa Poynor, and Mrs. Ute Kashoa for taking care of my flowers while I was away and for creating and maintaining a nice and friendly atmosphere in the lab. My special thanks to Mrs. Christine Schwarz and Ms. Birgit Keil for HPLC and NMR analysis.

I am indebted to Dr. Tanja Radykewicz, Dr. Ralf Laupitz, Dr. Lilla-Margl-Römisch, Dr. Werner Römisch-Margl, Ms. Silke Marsch, Dr. Monika Joshi for their friendly attitude towards me, and just for being around.

I want to thank Ms. Susan Lauw and Mr. Matthias Lee for helping me to prepare my thesis and concomitant documents, for their assistance in computer matters, and for their friendship.

I am grateful to Dr. Victoria Illarionova and Dr. Boris Illarionov for their great help during my first months in Germany, for their constant friendly support, and for not allowing me to forget the Russian.

It is a pleasure to thank Dr. Stefan Hecht for introducing me into NMR technique, for his patience, and for helping me along.

I thank Ms. Eva Eylert and Dr. Claudia Huber for assisting me with the analysis of my probes by GC-MS spectrometry and for their friendly attitude.

My sincere thanks to Mr. Christoph Graßberger for maintaining a warm and friendly atmosphere in our lab, for helping me with many things, for amazing philosophical disputes, and for everyday encouraging 'Grüß Gott'.

Thanks a lot to Dr. Nicholas Schramek for his collaboration.

Many thanks to Hans-Fischer Gesellschaft and Phytochemical Society of Europe (PSE) for their financial support.

It is my please to thank Dr. Leo Jirovetz (University of Vienna, Austria) for a nice friendship, permanent support, and for constant desire to help.

My very special thanks to 'Frau Professor' Rosa Cusido, Prof. Javier Palazón, and Prof. Mercè Bonfill (University of Barcelona, Spain) for the great time in Barcelona and for our fruitful collaboration, which (I strongly believe) will continue.

Dear Rosa! I am so happy that our virtual acquaintance in 2002 has become real and personal in 2007!

I am grateful to Prof. Avi Golan (Ben Gurion University of Negev, Israel) for an interesting and fruitful year of joint work. I am looking forward for our future collaboration.

I want to say a lot of thanks to Prof. Dr. Maike Petersen (Philipps-Universität Marburg, Germany). Dear Maike! I am so happy that I can call you my Friend!

I am thankful to my dear friend in metabolomics, Prof. Dr. Rob Verpoorte. Dear Rob! Thank you so much for my (our) talk in Cambridge in 2007. As you said me there, "If you are afraid now, you will be afraid forever!" This saying helps me ever since, thank you for believing in me. I deeply thank you for wonderful years of our contacts, for our conversations and meetings, and for our victories!

I'm very grateful to my friends in Munich Dr. Gagik Gurzadyan (Gagarin), Dr. Anatoly Zharikov (Tolik), Dr. Andrey Susha (Andryuha), Dr. Olga Manoilova (Olik). My special thanks to Dr. Maxim Gelin (Maximo). Lots of thanks to all my friends in Russia and elsewhere.

My most sincere thanks to my parents and my family for your love, support, patience, and believing in me.

Publications

Illarionova, V., Kaiser, J., Ostrozhenkova, E., Bacher, A., Fischer, M., Eisenreich, W., Rohdich, F., 2006. Nonmevalonate terpene biosynthesis enzymes as anti-infective drug targets: substrate synthesis and high-throughput methods. *J. Org. Chem.* 71, 8824-8834.

Kaiser, J., Yassin, M., Prakash, S., Safi, N., Agami, M., Lauw, S., Ostrozhenkova, E., Bacher, A., Rohdich, F., Eisenreich, W., Safi, J., Golan-Goldhirsh, A., 2007. Anti-malarial drug targets: screening for inhibitors of 2C-methyl-D-erythritol 4-phosphate synthase (IspC protein) in Mediterranean plants. *Phytomedicine* 14, 242-249.

Ostrozhenkova, E., Eylert, E., Schramek, N., Golan-Goldhirsh, A., Bacher, A., Eisenreich, W., 2007. Biosynthesis of the chromogen hermidin from *Mercurialis annua* L. *Phytochemistry* 68, 2816-2824.

Posters and lectures

The 9th International Congress “Phytopharm 2005 and PSE”, 2005. Saint-Petersburg, Russia. (Poster presentation).

A Young Scientists Symposium “Future Trends in Phytochemistry”, 2006. Olomouc, Czech Republic. (Poster presentation).

Congress “50 Years of the Phytochemical Society of Europe, 2007. Cambridge, UK. (Lecture and poster presentation).

Invited lecture “Biosynthetic flux in plants containing terpenes and alkaloids. Studies with ¹³CO₂ and [U-¹³C₆]glucose”, 2007. Barcelona, Spain.

A Young Scientists Symposium “Future Trends in Phytochemistry Compounds – Enzymes – Genes”, 2008. Bad Herrenalb, Germany. (Poster presentation).

Partnering – Workshop “Plant – KBBE”, 2008. Berlin, Germany. (Participation).

GA Symposium “Plant system biology and medicinal plants”, 2008. Leiden, Netherlands. (Poster presentation).

Table of contents

1. Introduction	1
1.1. Metabolomics and metabolite profiling	1
1.2. Biosynthetic pathways and fluxes	3
1.3. The methods to determine the metabolic pathways and fluxes	12
1.4. Objectives	16
2. Materials and Methods	17
2.1. Instruments	17
2.2. Materials	18
2.2.1. Chemicals	18
2.2.2. Enzymes	19
2.2.3. Media for separation	20
2.2.4. Spray reagents	21
2.2.5.1. Medium for <i>Nicotiana tabacum</i>	21
2.2.5.2. Medium for <i>Allium schoenoprasum</i>	22
2.2.6. Plants	22
2.2.6.1. <i>Allium schoenoprasum</i>	22
2.2.6.2. <i>Hypericum perforatum</i>	22
2.2.6.3. <i>Mercurialis annua</i> L.	23
2.2.6.4. <i>Nicotiana tabacum</i> , var. <i>havanna piperita</i>	23
2.2.6.5. <i>Salvia divinorum</i>	23
2.3. Methods	23
2.3.1. Experiments with <i>Allium schoenoprasum</i>	23
2.3.2. Metabolite profiling in <i>Allium schoenoprasum</i>	24
2.3.3. NMR spectroscopy	24
2.3.4. Experiments with <i>Hypericum perforatum</i>	24
2.3.5. Isolation of hyperforin	25
2.3.6. NMR Spectroscopy	25
2.3.7. Isotopologue abundance by NMR spectroscopy	25
2.3.8. Protein hydrolysis and amino acid derivatization	27
2.3.9. Mass spectrometry	27
2.3.10. Isotopologue abundances by GC-MS	27

2.3.11. Experiments with <i>Mercurialis annua</i> L.	29
2.3.11.1. Metabolite profiling in <i>M. annua</i>	29
2.3.11.2. Experiments with [U- ¹³ C ₆]glucose	29
2.3.11.3. Experiments with ¹³ CO ₂	29
2.3.11.4. Experiments with [1- ¹³ C ₁]glucose	30
2.3.11.5. Experiments with [¹³ C ₄ , ¹⁵ N ₁]aspartate	30
2.3.11.6. Isolation of hermidin	30
2.3.11.7. NMR spectroscopy	30
2.3.12. Experiments with <i>Nicotiana tabacum</i>	30
2.3.13. Isolation of nicotine	30
2.3.14. NMR spectroscopy	31
2.3.15. Isolation of glucose	31
2.3.16. Isolation of glucose from cellulose	32
2.3.17. NMR spectroscopy	32
2.3.18. Experiments with <i>Salvia divinorum</i>	32
2.3.18.1. Experiments with [U- ¹³ C ₆]glucose	32
2.3.18.2. Experiments with ¹³ CO ₂	32
2.3.18.3. Isolation of salvininorin A	33
2.3.18.4. Purification of salvininorin A with column chromatography	33
2.3.18.5. Purification of salvininorin A with HPLC	33
2.3.18.6. Protein hydrolysis and amino acid derivatization	33
2.3.19. Isolation of amino acids	33
2.3.20. Identification of amino acids	34
2.3.21. Enzymatic syntheses	35
2.3.21.1. Preparation of [3,4,5- ¹³ C ₃]1-Deoxy-D-xylulose 5-phosphate ...	35
2.3.21.2. Preparation of [1,3,4- ¹³ C ₃]2C-Methyl-D-erythritol 4-phosphate	35
2.3.21.3. Preparation of [1,3,4- ¹³ C ₃]4-Diphosphocytidyl-2C-methyl-D-erythritol	36
2.3.21.4. Preparation of [1,3,4- ¹³ C ₃]4-Diphosphocytidyl-2C-methyl-D-erythritol 2-phosphate	36
3. Results and discussion	37
3.1. Biological objects	37
3.1.1. <i>Allium schoenoprasum</i> L.	37

3.1.2. <i>Hypericum perforatum</i> L.	38
3.1.3. <i>Mercurialis annua</i> L.	39
3.1.4. <i>Nicotiana tabacum</i>	40
3.1.5. <i>Salvia divinorum</i>	41
3.2. Metabolite profiling	42
3.2.1. Metabolite profiling in <i>Allium schoenoprasum</i>	42
3.2.2. Metabolite profiling in <i>Mercurialis annua</i>	47
3.3. Preparation and properties of isotope-labelled 4-diphosphocytidyl- 2C-methyl-D-erythritol 2-phosphate	52
3.4. Biosynthesis of hyperforin in <i>Hypericum perforatum</i> : experiment with ¹³ CO ₂	59
3.4. Use of ¹³ CO ₂ as metabolic tracer. Biosynthesis of salvinin A	66
3.5. Isotopolog perturbation-relaxation experiments with growing <i>Nicotiana tabacum</i>	72
3.5. Biosynthesis of the chromogen hermidin from <i>Mercurialis annua</i>	74
3.5.1. Experiments with [U- ¹³ C ₆]glucose	74
3.5.2. Experiments with ¹³ CO ₂	80
3.5.3. Experiments with [1- ¹³ C ₁]glucose	83
3.5.4. Experiments with [¹³ C ₄ , ¹⁵ N ₁]aspartate	88
4. Summary	90
References	94

Abbreviations

ADP	Adenosine-5'-diphosphate
AMP	Adenosine-5'-monophosphate
ATP	Adenosine-5'-triphosphate
CDP	Cytidine diphosphate
CMP	Cytidine monophosphate
CTP	Cytidine triphosphate
COSY	Correlated spectroscopy
δ	Chemical shift
d	Doublet
dd	Double doublet
DHAP	Dihydroxyacetone phosphate
DMAPP	Dimethylallyl diphosphate
DMSO	Dimethylsulfoxide
DX	1-Deoxy-D-xylulose
DXP	1-Deoxy-D-xylulose 5-phosphate
DXS	1-Deoxy-D-xylulose 5-phosphate synthase
GAP	Glyceraldehyde 3-phosphate
HMBC	Heteronuclear multiple bond correlation
HMQC	Heteronuclear multiple quantum coherence
HPLC	High performance liquid chromatography
IPP	Isopentenyl diphosphate
IspC	1-Deoxy-D-xylulose 5-phosphate reductoisomerase
IspD	4-Diphosphocytidyl-2C-methyl-D-erythritol synthase
IspE	4-Diphosphocytidyl-2C-methyl-D-erythritol kinase
INADEQUATE	Incredible Natural Abundance Double Quantum Transfer Experiment
J	Coupling constant
LB-Medium	Luria-Bertani Medium
m	Multiplet
MEP	2C-Methyl-D-erythritol 4-phosphate
MS	Mass spectrometry
MS-GC	Mass spectrometry – Gas chromatography

NADP	Nicotinamide adenine dinucleotide phosphate
NADP ⁺	Nicotinamide adenine dinucleotide phosphate
n.d.	Not detected
NMR	Nuclear magnetic resonance
ppm	Partsper million
q	Quadruplet
R _f	Retention factor
RNA	Ribonucleic acid
s	Singlet
t	Triplet
TEMED	Tetramethylethylenediamine
TLC	Thin layer chromatography
TOCSY	Total correlation spectroscopy
TPP	Thiamine pyrophosphate
TSP	3-(Trimethylsilyl)-1-propanesulfonic acid

1. Introduction

1.1. Metabolomics and metabolite profiling

The term metabolomics refers to the systematic study of the unique chemical fingerprints that specific cellular processes leave behind and specifically, the study of their small-molecule metabolite profiles. The subject has been covered in recent reviews (Last *et al.*, 2007; Ward *et al.*, 2007; Lindon *et al.*, 2007; Verpoorte *et al.*, 2007; Aranibar *et al.*, 2006).

In recent years, more and more attention is being paid to the chemical characterization of the phenotype. Chemical characterization can be done on the level of macromolecules (e.g., proteomics and characterization of polysaccharides and lignins) or low molecular weight compounds (the metabolome). The metabolome consists of two types of compounds, the primary metabolites and the secondary metabolites. The primary metabolites are compounds involved in the basic functions of the living cell, such as respiration and biosynthesis of the amino acids and other compounds needed for a living cell. The primary metabolites in plants are important for the growth and agricultural yields. The secondary metabolites are species specific, they play a role in the interaction of a cell with its environment, which can be other cells in the organism or external organisms (Verpoorte *et al.*, 2007). The interest in plant secondary metabolites was in part driven by medicinal aspects. The pure preparations of plant metabolites continue to provide important drugs such as atropine (Facchini, 2001), taxol (Eisenreich *et al.*, 1996), morphine (Novak *et al.*, 2000; Poeknapo *et al.*, 2004), and artemisinin (Covello *et al.*, 2007).

Metabolomics originate from metabolite profiling. The earliest metabolite profiling publications originated from the Baylor College of Medicine in the early 1970s (Devaus *et al.*, 1971; Horning and Horning, 1970, 1971). These authors illustrated their concept through the multicomponent analysis of steroids, acids, and neutral and acidic urinary drug metabolites using GC-MS. They are also credited with coining term “metabolite profiling” to refer to qualitative and quantitative analysis of complex mixtures of physiological origin. Soon afterwards, the concept of using metabolite profiles to screen, diagnose, and assess health began to spread (Cunnick *et al.*, 1972; Mroczek, 1972). Thompson and Markey expanded on the quantitative aspects of using GC-MS for metabolite profiling in 1975 (Thompson and Markey, 1975) and by the late 1970s the methodology had attained enough interest to support a review article

(Gates and Sweeley, 1978). During the early 1980s, results from the application of HPLC and NMR for metabolite profiling (Bales *et al.*, 1984, 1988) began appearing in the literature.

A number of different analytical strategies are employed, as shown in Table 1, with the ultimate goal of analysing a large fraction or all of the metabolites present. Realistically, a range of analytical technologies and not one will be employed to analyse all metabolites present (Dunn *et al.*, 2005; Goodacre *et al.*, 2004; Fiehn, 2002; Sumner *et al.*, 2003).

Table 1. The range of different strategies employed in metabolic experiments (Dunn *et al.*, 2005)

Metabolomics

Non-biased identification and quantification of all metabolites in a biological system. The analytical techniques must be highly selective and sensitive. No one analytical technique, or combination of techniques, can currently determine all metabolites present in microbial, plant or mammalian metabolomes.

Metabonomics

The quantitative measurement of the dynamic multiparametric metabolic response of living systems to pathophysiological stimuli or genetic modification.

Metabolite target analysis

Quantitative determination of one or few metabolites related to a specific metabolic pathway after extensive sample preparation and separation from the sample matrix and employing chromatographic separation and sensitive detection.

Metabolite profiling/metabolic profiling

Analysis to identify and quantify metabolites related through similar chemistries or metabolic pathways. Normally employ chromatographic separation before detection with minimal metabolite isolation after sampling.

Metabolic fingerprinting

Global rapid and high-throughput analysis of crude samples or samples extracts for sample classification or screening of samples. Identification and quantification is not performed. Minimal sample preparation.

Metabolic footprinting

Global measurement of metabolites secreted from the intra-cellular volume into the extra-cellular spent growth medium. High-throughput method not requiring rapid quenching and time consuming extraction of intra-cellular metabolites for microbial metabolomics.

1.2. Biosynthetic pathways and fluxes

Metabolism is based on the enzyme-catalysed interconversion of metabolites, and the resulting network of reactions and transport steps can be characterized in terms of the fluxes between different parts of the network. The plant metabolism is characterized by its varied biosynthetic capacity entailing the presence of multiple pathways for the synthesis of upward of 200 000 secondary metabolites across the plant kingdom (Sumner *et al.*, 2003), by extensive subcellular compartmentation, which imposes a requirement for a substantial number of metabolite transfers between compartments (Knappe *et al.*, 2003), and by the existence of identical metabolic steps and even pathways in different compartments. Thus, there is extensive duplication of the pathways of carbohydrate oxidation in the cytosolic and plastidic compartments of plant cells (Fig. 1; Neuhaus and Emes, 2000) and this is a major complication, for example, in analysing the operation of the oxidative pentose phosphate pathway (Kruger and von Schaewen, 2003).

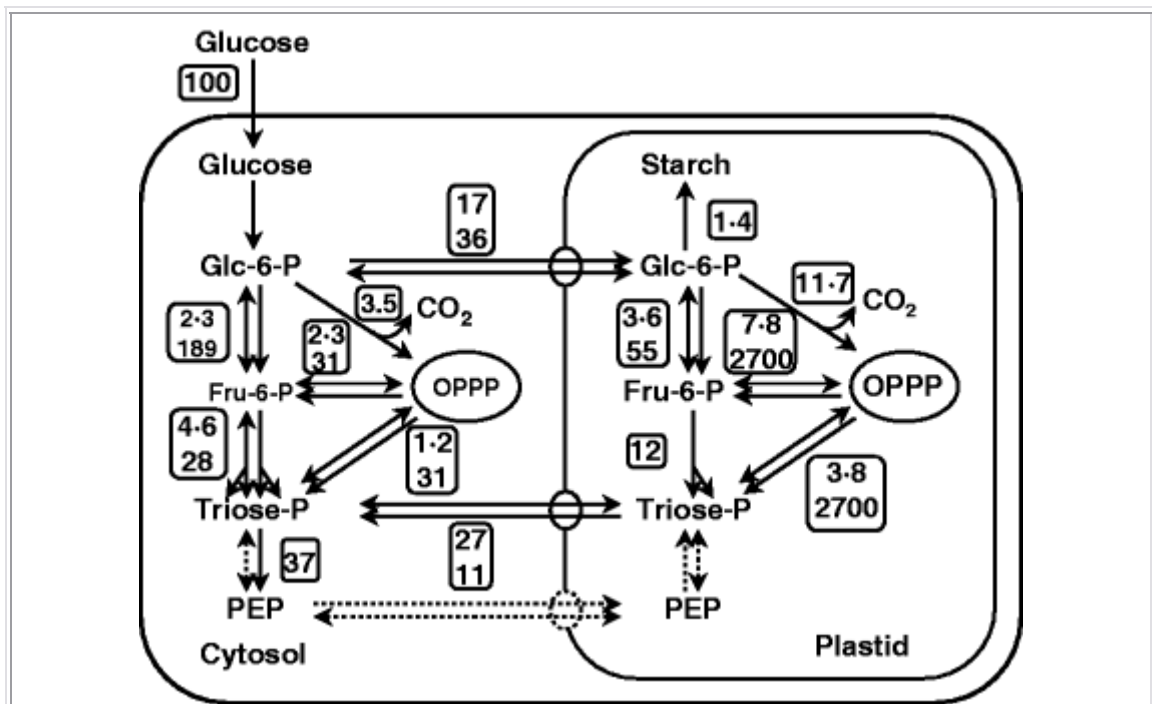


Figure 1. The carbohydrate pathways in cytosolic and plastidic compartments. Most of the steps are reversible and communication between the cytosol and the plastids is facilitated by transporters. OPPP, oxidative pentose phosphate pathway; Fru-6-P, fructose 6-phosphate; Glc-6-P, glucose 6-phosphate; PEP, phosphoenolpyruvate.

Tracer studies using isotopes are among the most important methods for the study of biosynthetic pathways in both primary and secondary metabolism. For decades, the area was dominated by radioactive tracers which could be detected with high-sensitivity and accuracy using comparatively simple techniques. The application for biosynthetic work of stable isotopes had to await sensitive and specific detection methods, i.e. advanced mass spectrometry and high-resolution NMR spectroscopy.

Isotope incorporation studies, irrespective of the radioactive or non-radioactive character of the tracer, are most of the time interpreted in terms of simple source-and-sink models (Fig. 2). If the isotope from the proffered tracer (i.e. source) is diverted to the compound under study (i.e. the sink) there must be some metabolic pathway that explains this result. In fact, the diversion of an isotope from a given source to a given sink can vary over orders of magnitude. If the transfer rate is high or very high, there can be hardly any doubt about the existence of a close metabolic connection. On the other hand, if the transmission is in the low percent range or even lower, the result is open to many different interpretations.

Natural organic matter comprises the two stable isotopes of carbon, ^{12}C and ^{13}C , in approximately ratio of 99:1. The two isotopes are normally distributed to different molecular positions in an almost random (although not strictly random) fashion. The pure organic compound is a complex mixture of different isotopologues¹. Similar considerations apply to the stable isotopes of hydrogen and nitrogen too.

For any organic molecule comprising n carbon atoms, the number of carbon isotopologues is 2^n , and isotopologue space for that molecular species has 2^n dimensions. For example, natural glucose consists of 64 carbon isotopologues, where $[\text{U-}^{12}\text{C}_6]\text{glucose}$ is the most abundant species that accounts for about 93 mol% and each molecular species carrying a single ^{13}C atom accounts for about 1.1 mol%.

A comprehensive isotopologue perturbation/relaxation analysis would involve the assessment of all isotopologues of all low weight metabolites in a given experimental system. The building blocks for complex natural products are extracted from a relatively small set of central metabolic intermediates and primary metabolites, and these are metabolically connected by known pathways of intermediary metabolites. For example, on the basis of known pathways of amino acids biosynthesis, the labelling pattern of central intermediates can be reconstructed from additional amino acids, as shown in Figure 3.

¹Isotopologues are molecules differing in isotopic composition.

Introduction

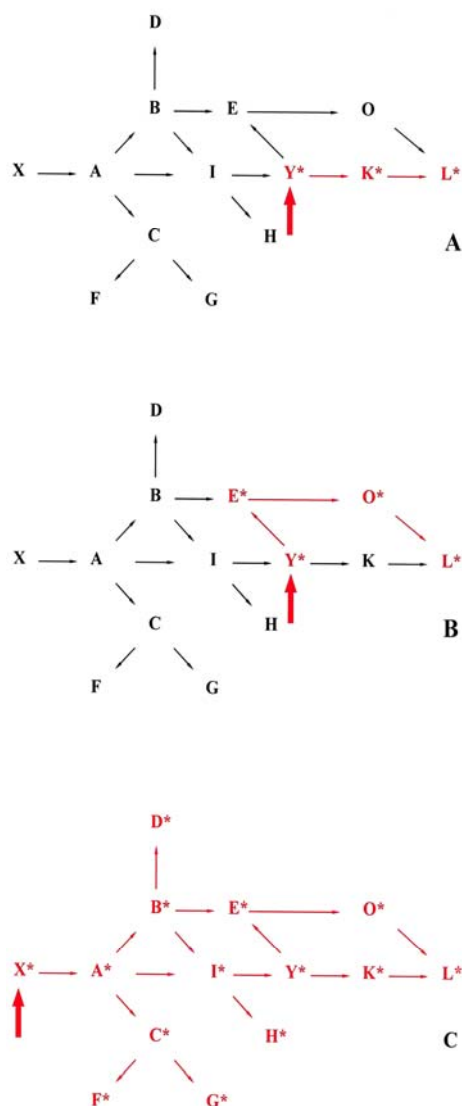


Figure 2. Section of a metabolic network. A and B: In a source-and-sink model, an isotopically-labelled compound Y is applied to an organism. The fact that the target metabolite L acquires label is typically explained by a close biogenetic relationship of Y and L (case A), but can also be a consequence of a more complex biosynthetic history of L where Y is converted into intermediate E that serves as a precursor of L via a completely different pathway (case B). With a general precursor (such as glucose or CO₂) most if not all metabolites in the network acquire label (case C). The complex but specific isotopologue profiles can be deconvoluted by advanced bioanalytical methods (i.e. quantitative NMR spectroscopy and mass spectrometry). With multiple isotopologue profiles at hand, biosynthetic pathways and metabolite flux can be assessed on a quantitative basis.

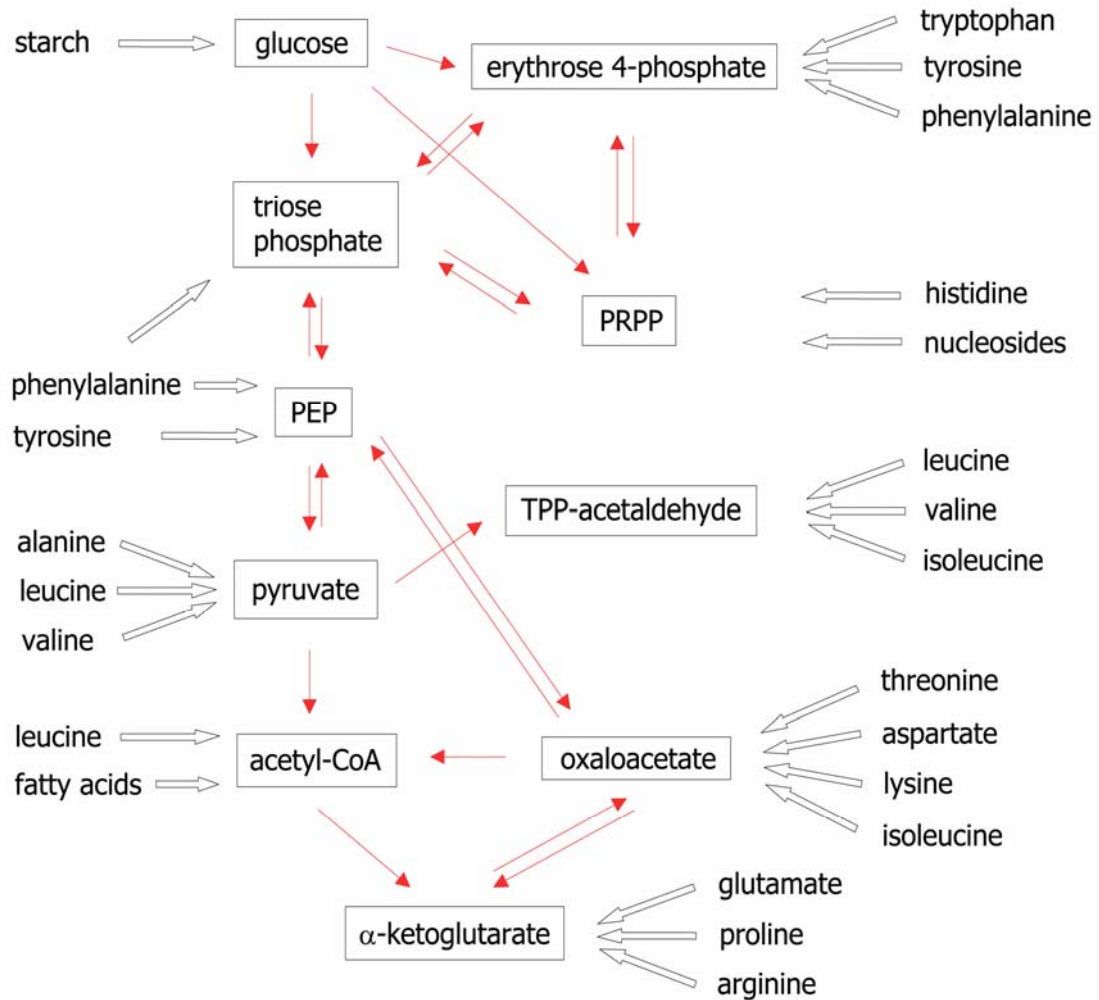


Figure 3. Reconstruction of isotopologue compositions in central intermediates (compounds indicated in boxes) by retrobiosynthetic analysis of sink metabolites (e.g. amino acids) in plants. PRPP, phosphoribosyl pyrophosphate; TPP, thiamine pyrophosphate; PEP, phosphoenol pyruvate.

More recently, stable isotope experiments monitored by NMR spectroscopy and/or mass spectrometry have been adapted to studies with plant systems. A major aim of these studies is to provide a rational basis for the improvement of biomass and/or specific plant products. In recent years several techniques in plant sciences have been reported (Roscher *et al.*, 2000; Ratcliffe and Shachar-Hill, 2001; 2006; Shachar-Hill, 2002; Kruger *et al.*, 2003; Schwender *et al.*, 2004; Krishnan *et al.*, 2005).

The plant cells, tissues or embryos can be immersed or submersed in a nutrient medium, and a variety of isotope-labelled precursors can be used to generate a skewed isotopologue distribution that can subsequently evolve by metabolic processes that are

interpreted as a relaxation process following the initial perturbation. Specifically or uniformly ^{13}C -labelled glucose and sucrose have been used, but in principle any labelled metabolite, such as amino acids, mevalonate and acetate that are absorbed by the cells or tissues, at a sufficient rate is suitable (Fig. 4). The label of the general precursor is diverted through the metabolic network by the reaction of the central metabolism and finally results in specific labelling patterns of metabolic products such as amino acids or secondary metabolites. As examples, metabolic flux patterns have been reported for tobacco plants (Ettenhuber *et al.*, 2005a), and kernel cultures of *Zea mays* (Glawischnig *et al.*, 2003; Ettenhuber *et al.*, 2005b; Spielbauer *et al.*, 2006).

A variety of methods are available for the application of isotope-labelled tracer compounds in studies with plants. (i) Aqueous tracer solutions can be fed to cut plant segments. (ii) Certain tracers such as isotope-labelled glucose can be applied via the root system of plants that have been grown under aseptic conditions. (iii) Cultured plant cells can be grown in medium containing the tracer.

Each of these methods has specific shortcomings. The use of cut segments involves massive traumatization of the plant tissue followed by rapid functional decline. Aseptically grown plants and/or tissue cultures are available for certain plant species but not for others. Moreover, cultured plant cells tend to lose biosynthetic potential and may display metabolic alterations by comparison with whole plants.

The application of labelled precursors presents technical problems for studies with whole plants too. Injection or infiltration of metabolites such as glucose is possible with tall species such as maize, but the dynamics of the distribution of the tracer in the whole plant is hard to control.

By comparison with these techniques, the use of $^{13}\text{CO}_2$ as tracer is absolutely atraumatic. Labelling experiments can be performed with whole plants under a wide variety of experimental conditions, and the extent of labelling can be modulated over a relatively wide range *via* the experimental conditions of the $^{13}\text{CO}_2$ pulse and the length of a consecutive chase period in normal air.

Introduction

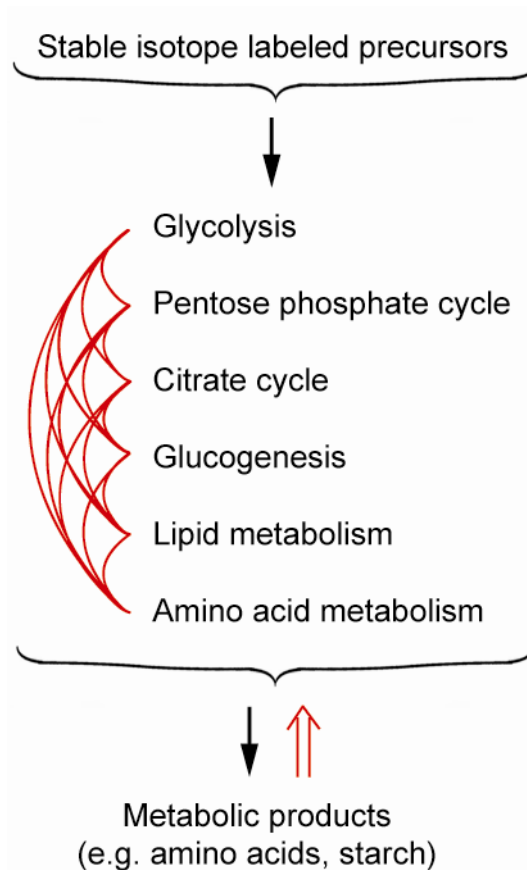


Figure 4. Functional description of biosynthetic pathways and metabolic networks under *in vivo* conditions.

$^{14}\text{CO}_2$ Labelling was a fundamental tool in the pioneering studies on photosynthesis by Calvin, Bassham and their co-workers (for review, see Bassham, 2003). On the other hand, there are hitherto few examples for the use of $^{13}\text{CO}_2$ as tracer in plant physiology (Schaefer *et al.*, 1975, 1980; Hutchinson *et al.*, 1976; Römisch-Margl *et al.*, 2007). The technology is based on the concept that a pool of multiply labelled photosynthate, predominantly in the form of monomeric and polymeric hexose derivatives, can be generated in an atmosphere of synthetic air containing highly enriched $^{13}\text{CO}_2$. Catabolic processing of these second generation tracer compounds (second generation by comparison with the applied $^{13}\text{CO}_2$) can afford a variety of multiply labelled third generation metabolites which can then be combined by anabolic processes with molecular species derived from unlabelled biomass. As a result, one can expect the formation of metabolites which can be interpreted as molecular mosaics assembled at random from labelled as well as unlabelled precursors. In the final outcome, the labelling patterns of the anabolites resulting from these processes may be

Introduction

similar to the patterns expected for experiments with multiply labelled carbohydrate tracers such as [U- $^{13}\text{C}_6$]glucose.

A classical milestone in plant sciences was the elucidation of nicotine biosynthesis in *Nicotiana tabacum*. Source-and-sink experiments clearly indicated that nicotinic acid (**1**) is a building block in the biosynthesis of the alkaloid (Dawson *et al.*, 1960). More recently, three different pathways for the biosynthesis of nicotinic acid have been described in nature, (i) starting from dihydroxyacetone phosphate (**2**) and aspartate (**3**) as building blocks, (ii) starting from *N*-formyl aspartate (**4**) and acetyl-CoA (**5**), and (iii) starting from tryptophan (**6**). It was therefore decided to quantitatively assess possible contributions of the respective pathways in the plant under physiological conditions. A labelling experiment with $^{13}\text{CO}_2$ as precursor showed the presence of multiple ^{13}C -labelled isotopologues in nicotine (Römisch-Margl *et al.*, 2007). Retrobiosynthetic analysis of this labelling pattern was perfectly in line with a prediction by nicotinic acid formation *via* the aspartate pathway (Fig. 5B).

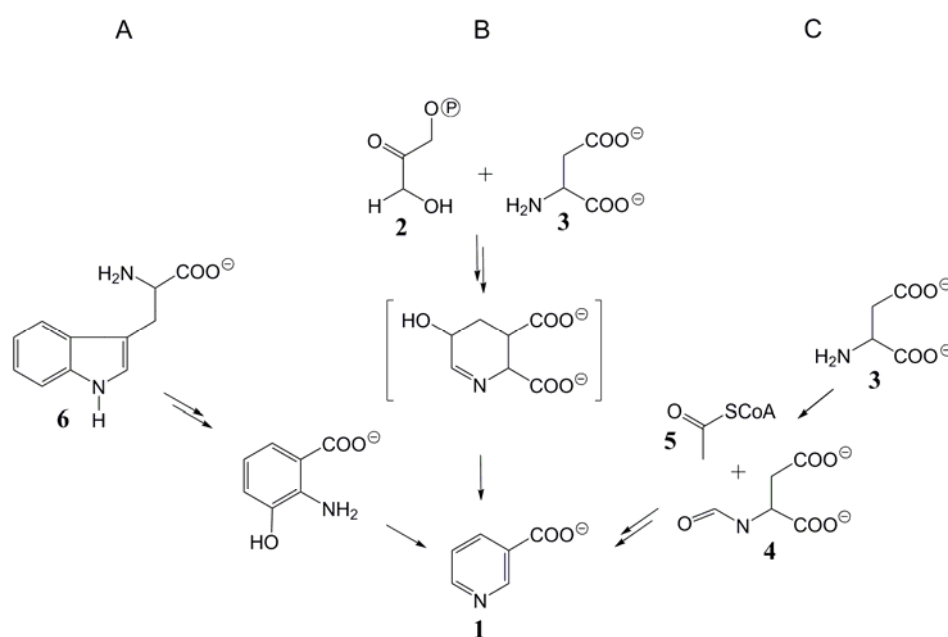


Figure 5. Possible biosynthetic pathways for the formation of nicotinic acid (**1**).

Retrobiosynthetic analysis has also been essential to assign the biosynthetic origin of many plant terpenes and isoprenoids. This class of compounds represents one of the largest groups of natural products, including essential plant metabolites such as sterols, carotenoids or the phytol moiety of chlorophylls.

All plant terpenoids studies up to about 1990 had been assigned a mevalonate origin on the basis of isotope incorporation experiments with mevalonate or acetate. Although these experiments typically proceeded with low incorporation levels attributed to permeability barriers, the label distribution, when analysed carefully, was in line with the mevalonate pathway.

Ultimately, the impossibility to reconcile certain biosynthetic data with the mevalonate paradigm was independently recognized by Rohmer, Arigoni and their co-workers (Rohmer *et al.*, 1993; Schwarz, 1994; Broers, 1994). Rohmer and his co-workers studied the incorporation of various [^{13}C]glucose isotopomers and [^{13}C]acetate isotopomers into hopanoids in certain eubacteria and found the location of the label in the target molecules to be strangely at odds with the mevalonate prediction (Rohmer *et al.*, 1993). Arigoni and Schwarz, observed the joint transfer of three contiguous carbon atoms from [$\text{U-}^{13}\text{C}_6$]glucose into ginkgolides in seedlings of the tree *Ginkgo biloba*. This finding was not compatible with a mevalonate origin, since mevalonate is assembled from two-carbon precursors (Schwarz, 1994). Moreover, with [^{13}C]glucose as a precursor, Arigoni and Broers showed that labeling pattern of ubiquinone formed in *Escherichia coli* cannot be explained in terms of the mevalonate pathway (Broers, 1994). The labeling patterns were in line with 1-deoxy-D-xylulose 5-phosphate as precursor. The role of this intermediate was strongly supported by efficient incorporation of ^2H -labelled 1-deoxy-D-xylulose into ubiquinones of *E. coli* (Broers, 1994). Earlier work had already shown that the carbon skeleton of 1-deoxy-D-xylulose can be incorporated into pyridoxal (vitamin B₆) (Hill *et al.*, 1989) and into the thiazole ring of thiamine (vitamin B₁) (White, 1978; David *et al.*, 1981; David *et al.*, 1982). Thus, 1-deoxy-D-xylulose or a derivative thereof appeared to qualify as the branching intermediate for the biosynthetic pathway of vitamins B₁ and B₆ and a novel, non-mevalonate pathway of isoprenoid biosynthesis.

Follow-up studies using the retrobiosynthetic approach showed that the universal isoprenoid precursors, isopentenyl diphosphate (IPP, **7**, Fig. 6) and dimethylallyl diphosphate (DMAPP, **8**), for the vast majority of plant terpenes and isoprenoids are at least partially contributed from the non-mevalonate pathway (Eisenreich *et al.*, 2001; Eisenreich *et al.*, 2004a; Rohmer, 2006; Rohdich *et al.*, 2005, 2003). Whereas the classical pathway proceeds via acetyl-CoA (**5**) and mevalonate (**9**) in the plant cell cytoplasm, the alternative pathway via 1-deoxyxylulose 5-phosphate (**10**) and 2-C-methylerythritol 4-phosphate (**11**) is operative in plastids (Fig. 6).

The recent studies have established that in plants the compartmental separation between the two isoprenoid pathways is not an absolute one. Minor amounts of metabolites common to both pathways can be exchanged in both directions via the plastid membranes. Thus, label of 1-deoxyxylulose-derived isoprenoid moieties can be diverted to the cytoplasm, where it can become part of sterol molecules (Arigoni *et al.*, 1997). Likewise, a small fraction of isoprenoid moieties derived from the mevalonate pathway find their way into the plastid compartment where they become part of mono- and diterpens which are predominantly obtained via the plastid-based deoxyxylulose pathway (Schwarz, 1994; Nabeta *et al.*, 1995; Piel *et al.*, 1998; Schuhr *et al.*, 2003).

A wide variety of monoterpenes and diterpenes has been shown to be synthesized predominantly *via* deoxyxylulose pathway (Eisenreich *et al.*, 1998). Most notably, the phytol side chain which recruits chlorophylls, the most abundant organic pigment, to the thylakoid membrane, is predominantly formed via deoxyxylulose pathway in higher plants. Carotenoids, which play a central role in all green plants as light-protecting and light-harvesting agents as well as specific roles as pigments in flowers, are derived from the deoxyxylulose pathway.

A powerful strategy for quantitative assessment of the differential contribution of the two isoprenoids pathways for the biosynthesis of individual terpenes uses ^{13}C -labelled glucose as precursor for metabolic studies with whole plants, plant tissues or cultured plant cells (Adam and Zapp, 1998; Yang and Orihara, 2002; Eisenreich *et al.*, 1997; Werner *et al.*, 1997; Eichinger *et al.*, 1999; Adam *et al.*, 2002; Lichtenthaler *et al.*, 1997; Kutrzeba *et al.*, 2007). Since glucose is a general intermediary metabolite, the isotope from the proffered carbohydrate can be diverted to virtually all metabolic compartments and intermediates in plant cells. Using ^{13}C NMR spectroscopy, the ^{13}C enrichment for all non-isochronous carbon atoms can be determined with high precision. Biosynthetic information can then be derived from the positional aspects of the label distribution in the target molecule rather than from the net transfer of isotope. NMR spectroscopy can diagnose the joint transfer of ^{13}C atom groups, even in case an intramolecular rearrangement, by a detailed analysis of the ^{13}C coupling pattern via one- and two-dimensional experiments, and indeed, the NMR detection of $^{13}\text{C}_3$ fragments in plant terpenoids from experiments with $[\text{U-}^{13}\text{C}_6]\text{glucose}$ was crucial for the discovery of the non-mevalonate pathway in plants (Schwarz, 1994; Eisenreich *et al.*, 1996).

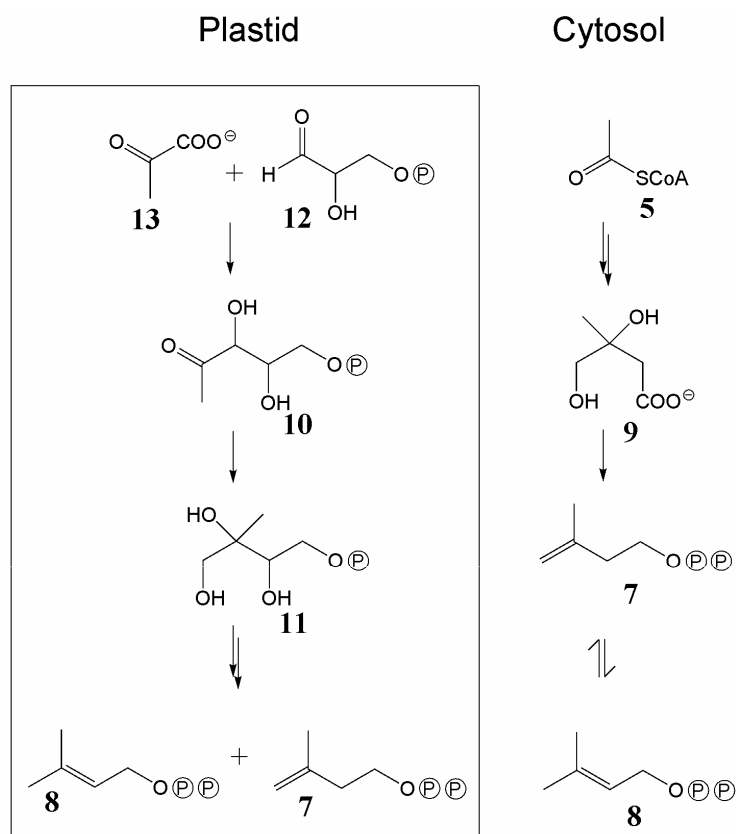


Figure 6. Topology of IPP (7) and DMAPP (8) biosynthesis in plants. For more details see text.

Moreover, the formation of target enzyme products of non-mevalonate pathway was monitored with ^{13}C NMR spectroscopy (Illarionova *et al.*, 2006; Kaiser *et al.*, 2007). Optically monitored assays that are also suitable for high-throughput screening have been reported for three protein of non-mevalonate pathway (Illarionova *et al.*, 2006; Kuzuyama *et al.*, 2000b; Bernal *et al.*, 2005).

1.3. The methods to determine the metabolic pathways and fluxes

In metabolomics studies there are three phases. The first one is a qualitative phase in which as many as possible of the signals observed in the NMR are assigned to compounds. After this phase, it is necessary to determine the biological variation for the system studied, that means measuring a large number of samples, e.g., young and old leaves, different times of the day, and different stages of development of the plant. The last step is to compare the model system under different experimental conditions. An important aspect is the extraction method. Plants contain a wide variety of compounds

with totally different polarities. No single method is able to detect all metabolites in a single operation (Verpoorte *et al.*, 2007).

Many analytical technologies have been enlisted to profile the metabolome. Methods based on infrared spectroscopy (IR) (Oliver *et al.*, 1998), nuclear magnetic resonance (NMR) (Eisenreich and Bacher, 2007; Lewis *et al.*, 2007; Verpoorte *et al.*, 2007), thin layer chromatography (TLC) (Tweeddale *et al.*, 1998), HPLC with ultraviolet and photodiode array detection (LC-UV-PDA) (Fraser *et al.*, 2000), capillary electrophoresis coupled to ultraviolet absorbance detection (CE-UV) (Baggett *et al.*, 2002), capillary electrophoresis coupled to laser induced fluorescence detection (CE-LIF) (Arlt *et al.*, 2001), capillary electrophoresis coupled to mass spectrometry (CE-MS) (Soga *et al.*, 2002), gas chromatography-mass spectrometry (GC-MS), liquid chromatography-mass spectrometry (LC-MS) (Huhman and Sumner, 2002), HPLC coupled with both mass spectrometry and nuclear magnetic resonance detection (LC-NMR-MS) (Bailey *et al.*, 2000) have been used (Sumner *et al.*, 2003).

MS allows the determination of the molecular weight, and in case of high resolution also of the elemental composition, but this is not always sufficient to determine the structure. MS can help to identify in such case the compound through its fragmentation pattern, but in case of novel compounds further spectral data are required (Verpoorte *et al.*, 2007).

By comparison with HPLC, GC, CE, MS, GC-MS and LC-MS, the amount of sample required is much larger in NMR spectrometry.

NMR spectroscopy is a powerful technique for the structural identification of metabolites that have been isolated in pure or at least partially purified form using appropriate techniques. It is also possible to record NMR spectra from crude metabolite mixtures and to extract the relative amounts of different metabolites by systematic signal deconvolution (Choi *et al.*, 2006; Widarto *et al.*, 2006; Yang *et al.*, 2006). Because NMR is based on the fact that nuclei such as ^1H , ^{13}C , ^{31}P can exist at different energy levels in a strong magnetic field because they possess nuclear spin, it can generate valuable structural information (Goodacre *et al.*, 2004). The chemical shift range for ^1H is small, and the ^1H spectra of complex mixtures are necessarily crowded.

The combined application of advanced NMR spectroscopy allows the rapid mapping of spin networks yielding information on the homotopic ^1H - ^1H and ^{13}C - ^{13}C relations, and on the heterotopic ^1H - ^{13}C relations. In order to determine the chemical

structure of an unknown molecule, the information on spin topology must be translated into a plausible chemical structure (Eisenreich and Bacher, 2007).

Although one-dimensional (1D) NMR studies are extremely useful in classifying similar groups of samples, problems with large numbers of overlapping peaks can make actual identification of large numbers of metabolites difficult. Two-dimensional (2D) NMR studies can help to overcome these problems. The use of 2D NMR for metabolomics is usually restricted to the characterization of unidentified compounds from the 1D spectra. The increased resolution provided by the second dimension can allow for the characterization of components in an unfractionated or partially fractionated mixture (Ward *et al.*, 2007).

Two-dimensional NMR methods are used to increase spectral resolution, to establish connections between signals for metabolite identification and other purposes, and to achieve sensitivity enhancement. Homonuclear correlation experiments, such as correlation spectroscopy (COSY) (Piantini *et al.*, 1982) or total correlation spectroscopy (TOCSY) (Braunschweiler and Ernst, 1983; Bax and Davis, 1985a; Davis and Bax, 1985a,b; Griesinger *et al.*, 1988) recorded with different mixing times, are invaluable for analysing the ^1H spectra of complex mixtures, such as root exudates and cell extracts (Fan, 1996), because they allow subsets of peaks in the crowded one-dimensional ^1H spectra to be linked and assigned to specific metabolites. Heteronuclear experiments are similarly informative when the extracted metabolites have been labelled with ^{13}C or ^{15}N . For example, the proton-detected ^1H - ^{13}C correlation experiments with gradient selection of magnetization transfer, e.g. heteronuclear multiple quantum coherence (HMQC) spectroscopy (Müller, 1979; Bax *et al.*, 1983), heteronuclear single quantum coherence (HSQC) spectroscopy (Bodenhausen and Ruben, 1980) or heteronuclear multiple bond coherence (HMBC) spectroscopy (Bax and Summers, 1986) improve metabolite identification by providing information on the relationship between the signals from two different nuclei (Fan, 1996; Shachar-Hill *et al.*, 1996; Mesnard *et al.*, 2000; Ratcliffe and Shachar-Hill, 2005). Two-dimensional experiments, such as nuclear Overhauser effect spectroscopy (NOESY) (Macura and Ernst, 1980) or rotating frame Overhauser effect spectroscopy (ROESY) (Bothner-By *et al.*, 1984; Bax and Devis, 1985b) provide information about dipolar couplings through space. On the basis of these experiments, a set of constraints for the constitution and the configuration of a molecule can be obtained which may provide sufficient information to unambiguously assign the

structure of a typical metabolite (see Fig. 7 for example) (Ostrozhenkova *et al.*, 2007; Eisenreich and Bacher, 2007; Verpoorte *et al.*, 2007).

On the other hand, the chemical shift values of organic molecules in solution are unfortunately not invariable. Rather, they are influenced in subtle ways by a variety of temperature, changes (even minor changes) in solvent makeup, and the concentration of the compound under study as well as all other compounds present in the mixture (Daviss, 2005).

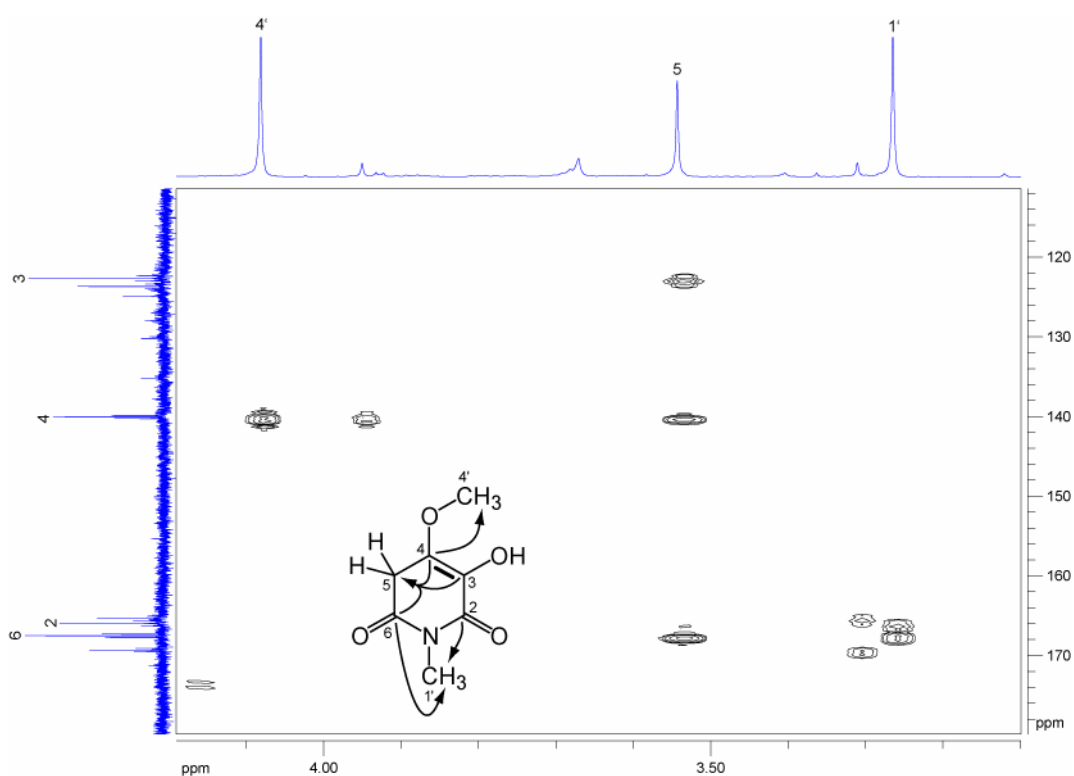


Figure 7. HMBC spectrum of the hermidin from *Mercurialis annua* showing correlations between ^{13}C and ^1H via long-range coupling through bonds.

On the positive side, NMR spectroscopy has numerous advantages by comparison with other methods that should be viewed as complementary rather than competitive. In contrast to GC-MS, extracts can be directly or with little sample preparation steps analyzed by NMR analysis without prior derivatization and metabolite concentration can be determined an unbiased manner (Lindon *et al.*, 2003; Nicholson and Wilson, 2003; Eisenreich and Bacher, 2007). However, the combination of NMR and MS-based technologies coupled with state of the art chromatographic assays presents a chance to fulfil the strived high-flying aim of developing metabolic profiling toward a sturdy

analytical platform indispensable in the comprehensive analysis of complex biological systems (Seger and Sturm, 2007). Hence, a metabolic fingerprinting approach yields data of a similar format: the first list contains mass-to-charge (m/z) ratios, chemical shifts or wave numbers for MS, NMR or Fourier transform-IR (FT-IR), respectively, and the second list contains their relative contribution (Alm and Arkin, 2003).

1.4. Objectives

In this thesis, metabolite profiles of plant extracts were determined by ^1H NMR spectroscopy in order to estimate the impact of stress factors, such as saline and heavy metal ions. More specifically, *Mercurialis annua* (female and male plants) and *Allium schoenoprasum* were supplemented with saline or Cd^{2+} salts. Extracts were then made from various parts of the plants and ^1H NMR spectra were measured. The complex spectra of the mixtures were partially assigned by comparison with reference spectra from a spectral library (Chenomx).

The biosynthetic pathways of the hyperforin from *Hypericum perforatum*, salvinorin A from *Salvia divinorum*, hermidin from *M. annua* and nicotine from *Nicotiana tabacum* wild-type and *N. tabacum* mutants were investigated using labelled precursors such as $^{13}\text{CO}_2$ and $[\text{U}-^{13}\text{C}_6]\text{glucose}$. As a general goal of the thesis, the $^{13}\text{CO}_2$ method should be compared with experimental settings using $[\text{U}-^{13}\text{C}_6]\text{glucose}$ as a precursor.

With the model studies mentioned above, labelling and profiling methods should be developed as general tools for the analysis of plant metabolism.

2. Materials and Methods

2.1. Instruments

Fractions collector	Pharmacia LKB-SuperFrac (Amersham Pharmacia Biotech, Freiburg, Germany)
Thermostat	Psycrotherm (New Brunswick Scientific Corp., New Brunswick, USA)
CO ₂ Incubator	BIOBOX (GWS, Berlin, Germany)
Multi-Purpose equipment for UV 254/366 nm and illumination	DESAGA (Heidelberg, Germany)
HPLC pump	Wellchrom (preparative) (KNAUER, Germany)
Refractometer	(GAT LCD 201, Gamma Analysen Technik GmbH, Bremerhaven, Germany)
Heatblock	Techne DRI. BLOCK DB-2A (Wertheim, Germany)
Lyophilizer	CHRIST ALFA 1-4 (Osterode am Harz, Germany)
NMR	AVANCE DRX500, Spectrometer (Bruker, Karlsruhe, Germany) FT-NMR AM 360, Spectrometer (Bruker, Karlsruhe, Germany)
pH Meter	E512 Metrohm AG CH-9100 (Herisau, Switzerland)
Shaker	Lab Shaker and Certomat MO (B. Braun, Melsungen, Germany)
Spectrophotometer	Ultraspec 2000 (Amersham Pharmacia Biotech, Freiburg, Germany)
Sonifier	Sonifier B-12 (Branson SONIC Power Company, USA)
Scales	SCALTEC SBA 32, max 120 g, d=0,0001 g
Centrifuge	RC2-B with GSA-rotor (Sorvall, Connecticut, USA)
Table-centrifuge	GS-15R, rotor S4180 (Beckman, Fullerton, USA) Eppendorf, Germany
Rotary evaporator	Vacuumpump (Vacuubrand GmbH & Co, Wertheim, Germany) Evaporator RE 120 (Büchi, Germany)
Water bath	(Köttermann, Germany)

Ultra Turax T 25

Jank & Kunkel (IKA Labortechnik, Stauffen, Germany)

2.2. Materials

2.2.1. Chemicals

All chemical substances were purchased from Merck (Darmstadt), Sigma-Aldrich (Deisenhofen), Serva (Heidelberg) and Fluka (Ulm), Isotec (Miamisburg), ChromaDex (Germany).

^2HCl (37%; 99 atom-% ^2H)	Aldrich Chem. Co. (Steinheim, Germany)
$^2\text{H}_2\text{O}$ (99,9% atom-% ^2H)	ISOTEC inc. A Matheson, USA Company (USA)
C^2HCl_3 (99.8% atom-% ^2H)	Cortec (Paris, France)
$\text{DMSO-}^2\text{H}_6$	ISOTEC inc. A Matheson, USA Company (USA)
[U- $^{13}\text{C}_6$]D-glucose	ISOTEC inc. A Matheson, USA Company (USA)
[1- $^{13}\text{C}_1$]D-glucose	Omicron (Soth Bend, Indiana, USA)
[1- $^2\text{H}_1$]D-glucose	Omicron (Soth Bend, Indiana, USA)
L-Asparagine- $^{13}\text{C}_4$, $^{15}\text{N}_2$ (98% atom-% ^{13}C , 98% atom-% ^{15}N)	ISOTEC (Miamisburg, Germany)
Methanol- $^2\text{H}_4$ (99.8% atom-% ^2H)	Aldrich (St. Luis, USA)
Pyridine- $^2\text{H}_5$ (99% atom-% ^2H)	Sigma-Aldrich (Steinheim, Germany)
Salvinorin A	ChromaDex (Germany)
Sodium pyruvate [3- $^{13}\text{C}_3$] (99% atom-% ^{13}C)	Cambridge Isotop Laboratories (Cambridge, UK)
$\text{K}^2\text{H}_2\text{PO}_4$ (~95 atom-% ^2H)	KH_2PO_4 several times extracted with D_2O and

Materials and Methods

lyophilised

Boronate Gel

Bio-Rad Laboratories GmbH, Munich, Germany

*All organic solvents were distilled for analysis and isolations.

2.2.2. Enzymes

All commercial enzymes (Table 1) were purchased from Sigma (Deisenhofen, Germany), Fluka (Steinheim, Germany) and Boehringer (Mannheim, Germany).

Table 1. Commercial enzymes

Enzyme	EC-Number	Origin
Hexokinase	2.7.1.1	Yeast
Glucose-6-phosphateisomerase	1.1.1.49	Yeast
Phosphofruktokinase	2.7.1.11	Rabbit muscle
Aldolase	4.1.2.13	Rabbit muscle
Triosephosphateisomerase	5.3.1.1	Rabbit muscle
Pyruvatekinase	2.7.1.40	Rabbit muscle
Glucosedehydrogenase	1.1.1.47	<i>Bacillus megaterium</i>
Alkaline phosphatase	3.1.3.1	Mucous coat of stomach of bull

Non-commercial enzymes (Table 2) were isolated and purified as described (Wungsintaweekul, 2001; Herz, 2000).

Table 2. Non-commercial enzymes

1-Deoxy-D-xylulose-5-phosphate synthase	<i>B. subtilis</i> (expression in <i>E. coli</i>)
1-Deoxy-D-xylulose-5-phosphate reductoisomerase	<i>E. coli</i>
4-Diphosphocytidyl-2C-methyl-D-erythritol synthase	<i>E. coli</i>
4-Diphosphocytidyl-2C-methyl-D-erythritol kinase	<i>E. coli</i>

2.2.3. Media for separation

Materials for column chromatography:

- Dowex 50 Wx8; Serva (Heidelberg, Germany)
- Dowex 1x8; Serva (Heidelberg, Germany)
- Kieselgel (Silica gel) 60; Merck (Darmstadt, Germany)
- Cellulose microcrystalline for column chromatography Merck (Darmstadt, Germany)

Materials for TLC:

- Microcrystalline cellulose; Stürmer & Schüle GmbH (Germany)
- Kieselgel 60 F₂₅₄; Merck (Darmstadt; Germany)

HPLC:

- Column RP 18, Lichrosorb (preparative, 250 x 7,8 mm)
- Column RP 18, Lichrosorb (analytical, 250 x 4,5 mm)
- Luna-NH₂, Phenomenex (preparative, 250 x 20 mm)

Preparation of Dowex 50 Wx8 (cation exchange, NH₄⁺-form)

Dowex 50 Wx8 material (NH₄⁺-form) (approx. 120 g) was steeped in 400 ml of sodium hydroxide for 3 h. The suspension was washed with water until neutral pH. Then, the material was steeped with 400 ml of 3 M HCl for 3 h, and then washed with water until neutral pH again. Then, the material was steeped in 400 ml of 2 M NH₄HCOO⁻ for 15 h and washed several times with water.

Preparation of Dowex 1x8 (anion exchange, formic-form)

Dowex 1x8 material (Cl⁻-form) (approx. 120 g) was steeped in 400 ml of 1 M HCl for 2 h. The suspension was washed with water until neutral pH. Then, the material was steeped with 400 ml of 1 M NaOH for 1 h, and then washed with water until neutral pH again. Then, the material was steeped in 400 ml of 2 M NH₄HCOO⁻ for 15 h and washed several times with water.

2.2.4. Spray reagents

2.2.4.1. Spray reagents for TLC:

1) *Anisaldehyde reagent* (Jork *et al.*, 1998):

acetic acid/sulphuric acid/anisaldehyde (100:1:2, v/v).

2) *Ninhydrine reagent* (Jork *et al.*, 1998):

Ninhydrine/butanol (3 mg/100 ml).

3) *Spray reagent for sugars*:

5.0 g trichloroacetic acid

2.5 g phthalate acid

0.6 g aminohippuric acid

100 ml ethanol

2.2.5.1. Medium for *Nicotiana tabacum* (B5 medium/l):

3.1 g of salt mixture (Table 3)

10 ml of solution of vitamins (Table 3)

0.9 g of MgSO₄ x 7 H₂O

20 g of sucrose

7.0 g of bacteriological agar

Table 3. Salt and vitamins mixtures for the B5 medium

Mixture	Components	mg/l
Salt	EDTA	40.00
	KJ	0.75
	H ₃ BO ₃	3.00
	MnSO ₄ x H ₂ O	10.00
	ZnSO ₄ x 7H ₂ O	2.00
	Na ₂ MoO ₄ x 2H ₂ O	0.25
	CuSO ₄ x 5H ₂ O	0.025
	CoCl ₂ x 6H ₂ O	0.025
Vitamins	Inosite	100
	Pyridoxine-HCl	1
	Thiamine-HCl	10
	Nicotinic acid	1

2.2.5.2. Medium for *Allium schoenoprasum* (Hoagland medium):

Table 4. Components of Hoagland medium

Components	g/l
MgSO ₄ x 7H ₂ O	36.97
K ₂ SO ₄	34.85
CaCl ₂ x 2H ₂ O	58.81
NaH ₂ PO ₄ x 2H ₂ O	22.71
Na ₂ HPO ₄ x 2H ₂ O	1.91
H ₃ BO ₃	17.2
ZnSO ₄ x 7H ₂ O	9.3
MnSO ₄ x H ₂ O	1.3
Na ₂ MoO ₄ x 2H ₂ O	0.12
CuSO ₄ x 5H ₂ O	1.65
Fe-citrate	1.06
FeSO ₄ x 2H ₂ O	3.28
NaNO ₃	84.98
NH ₄ Cl	53.49
NH ₄ NO ₃	20.01

2.2.6. Plants

2.2.6.1. *Allium schoenoprasum*

Seedlings of *A. schoenoprasum* were grown in the greenhouse using commercial gardening soil mixture (Terreau Professional Gepac Einheits Erde, Germany) (provided by Prof. P. Schröder, GSF, Munich). The growth conditions were: 14 h light per day; day temperature, 25-28 °C; night temperature, 20-23 °C; relative humidity, 50%. Six to eight weeks old seedlings were used for the labelling experiments.

2.2.6.2. *Hypericum perforatum*

The plants of *H. perforatum* 'Elixir' were obtained from Rühlemann's Gärtnerei (Horstedt, Germany).

2.2.6.3. *Mercurialis annua* L.

Seedlings of *M. annua* L. were grown in the greenhouse using commercial gardening soil mixture (Terreau Professional Gepac Einheits Erde, Germany). The growth conditions were: 14 h light per day; day temperature, 25-28 °C; night temperature, 20-23 °C; relative humidity, 50%. Six to eight weeks old seedlings were used for the labelling experiments.

2.2.6.4. *Nicotiana tabacum*, var. *havanna piperita*

N. tabacum wild-type and *N. tabacum* mutants (*rpoA* mutants) were grown under aseptic conditions from sterilised seed or shoot cutting explanted on B5 medium (Manandhar and Gresshoff, 1980) containing 2% (w/v) sucrose and solidified with 0.7% bacteriological agar and a mixture of [U-¹³C₆]glucose and unlabelled sucrose at 25 °C with 8/16 h dark/light illumination cycles at a light intensity of 0.5-1 Wm⁻² (Osram L85W/25 Universal fluorescent lamps) in the Institute of Botany, Ludwig Maximilian Universität München by Prof. Dr. Koop. *rpoA* Mutants lack an active photosynthetic system and display a white phenotype.

2.2.6.5. *Salvia divinorum*

The plants of *S. divinorum* were obtained in 2006 from Blumenschule, Schongau (Schongau, Germany). Notably, the distribution of *S. divinorum* has been restricted by decision of government in Germany from 01.03.2008.

2.3. Methods

2.3.1. Experiments with *Allium schoenoprasum*

Seeds of *Allium schoenoprasum* (Michal cv.) were germinated in commercial gardening soil mixture (Terreau Professional Gepac Einheits Erde, Germany). Experiments were carried out in Hoagland liquid medium. Seedlings were removed from the soil and the roots thoroughly washed in water before putting in the liquid medium. The plants were left to adapt to the medium for seven days, and then various nutritional conditions were applied: control – Hoagland medium; treatment medium: cadmium 50 µM Cd²⁺ was added. The growth conditions were: photoperiod, 14 h light and 10 h dark; day temperature, 25-28 °C and night temperature, approx. 16 °C; relative humidity, 50%. At given intervals samples were taken for analyses.

2.3.2. Metabolite profiling in *Allium schoenoprasum*

Plant material (fresh weight, 1.5 g) each from shoots and roots was triturated with liquid nitrogen. The cold slurry was extracted with 4 ml of 1 M perchloric acid. The slurry was centrifuged at 4000 rpm for 30 min. The supernatant was neutralised with 1 M potassium hydroxide and centrifuged at 4000 rpm for 15 min. The supernatant was lyophilised. The residue was dissolved in the mixture of 700 μl $^2\text{H}_2\text{O}$, and 50 μl of 150mM $\text{K}^2\text{H}_2\text{PO}_4$ and centrifuged at 4000 rpm for 15 min. To the supernatant (550 μl) 10 μl of 3-(trimethylsilyl)-1-propanesulfonic acid, sodium salt (TSP) were added as internal standard.

2.3.3. NMR spectroscopy

The samples were analysed by ^1H NMR and recorded at 500 MHz with presaturation of the solvent (water) signal. The parameters for ^1H -NMR spectra were following: the temperature - 300 K; the frequency - 500,13 MHz; a set of data - 32 K; 45° Pulse-angle 4 μs ; spectral width - 5,5 Hz; watersupression at 4,75 ppm. NMR signals were analysed with “Chenomx NMR Suite 4,6”. With this software, metabolites were assigned and the concentration was calculated using the known concentration of the internal standard, TSP (0.19 mM).

2.3.4. Experiments with *Hypericum perforatum*

Four plants of *H. perforatum* ‘Elixir’ with a height of about 40 cm were placed in a closed plant growth chamber (BIOBOX, GWS, Berlin). During an adaptation light period of 5 hours at 26 °C and a dark period of 12 hours at 22 °C and 66 % humidity, the plants were exposed to synthetic air containing 20.5 % oxygen and 600 ppm CO_2 . Prior to the labelling period, the chamber was flushed with synthetic air containing only oxygen and nitrogen. Then, the plants were exposed to synthetic air containing 600 ppm $^{13}\text{CO}_2$ (Campro Scientific, Berlin, Germany, > 99 % ^{13}C abundance) as the only carbon source and were illuminated with white light (about 20,000 lux) at 26 °C for 5 hours. During this period, the plants consumed about 1.4 L of $^{13}\text{CO}_2$. Subsequently, the plants were kept for 18 hours in the dark and were then allowed to grow under standard greenhouse conditions at ambient temperature for 5 days. After the chase phase, the plants were harvested and lyophilized.

2.3.5. Isolation of hyperforin

Hyperforin was isolated as described previously (Adam *et al.*, 2002). The flowers (fresh weight, 25 g) were triturated with liquid nitrogen. The cold slurry was transferred into a flask and extracted with 150 ml of n-heptane under a nitrogen atmosphere for 15 min. The slurry was filtered. The solution was concentrated to dryness under reduced pressure. The residue was dissolved in 100 ml of n-heptane, which had been saturated with methanol. The yellow solution was extracted three times with 50 ml of methanol saturated with n-heptane. The alcoholic fractions were combined and concentrated to dryness under reduced pressure. The residue (80 mg) was applied to a column of silica gel (Silica Gel 60, Sigma-Aldrich Chemie, Steinheim, Germany, 20 × 1 cm), which was developed with a mixture of hexane and ethyl acetate (9:1; v/v). Aliquots were spotted on thin-layer plates (TLC) (Silica Gel 60 F₂₅₄, Fluka) that were developed with the same solvent mixture. The TLC plates were dried and sprayed with a mixture of anisaldehyde/sulfuric acid/acetic acid (1:2:100, v/v). Hyperforin afforded a blue spot with an R_f value of 0.40. Fractions were combined and concentrated to dryness under reduced pressure affording 60 mg of a colourless oil.

2.3.6. NMR Spectroscopy

Hyperforin was dissolved in C²H₄O. ¹H and ¹³C NMR spectra were recorded at 500 MHz and 125 MHz, respectively, using a Bruker DRX 500 spectrometer at a temperature of 17 °C. The parameters for ¹³C NMR spectra were following: a set of data size 32 K; 30° pulse-angle, 3 μs; spectral width, 5,5 Hz.

2.3.7. Isotopologue abundance by NMR spectroscopy

Relative ¹³C abundance was determined by comparing the signal intensities of the biosynthetic samples with the signals of samples with natural ¹³C abundance measured under identical spectroscopic conditions (Eisenreich and Bacher, 2000) (Equation 1).

$$\%^{13}C_{rel.} = \frac{cI^*}{cI} \times \frac{1}{f} \times 100 \quad \text{Equation 1}$$

$\%^{13}C_{rel.}$: relative ¹³C enrichment;

cI^* : integral of ¹³C signal of labelled sample in NMR spectra;

${}^c I$: integral of ${}^{13}\text{C}$ signal of sample in NMR spectra with natural abundance of ${}^{13}\text{C}$ enrichment:

f : factor of calibration: the smallest data of $\frac{{}^c I^*}{{}^c I}$.

Absolute ${}^{13}\text{C}$ abundances of individual isotopologues were determined as described earlier (Eisenreich and Bacher, 2000) (Equation 2).

$$\%{}^{13}\text{C}_{abs.} = \frac{{}^H I_s}{{}^H I_s + {}^H I_z} \times 100 \quad \text{Equation 2}$$

$\%{}^{13}\text{C}_{abs.}$: absolute ${}^{13}\text{C}$ enrichment;

${}^H I_s$: the sum of integrals of satellites in ${}^1\text{H}$ NMR spectra;

${}^H I_z$: integral of central signal in ${}^1\text{H}$ NMR spectra.

Isotopomers carrying blocks of two or more ${}^{13}\text{C}$ atoms which are connected by one, two or three bonds give rise to satellites by ${}^{13}\text{C}$ coupling. The abundance of multiply-labelled isotopomers can therefore be easily separated from that of single-labelled isotopomers which give rise to central signals (Equation 3).

$$\%{}^{13}\text{C}^{13}\text{C} = \frac{{}^c I_s}{{}^c I_s + {}^c I_z} \times 100 \quad \text{Equation 3}$$

$\%{}^{13}\text{C}^{13}\text{C}$: procent ${}^{13}\text{C}^{13}\text{C}$ coupling;

${}^c I_s$: the sum of integrals of satellites in ${}^{13}\text{C}$ NMR spectra;

${}^c I_z$: integral of central signal in ${}^{13}\text{C}$ NMR spectra.

The multiplication of absolute ${}^{13}\text{C}$ enrichment of ${}^{13}\text{C}$ atom under study with calculated $\%{}^{13}\text{C}^{13}\text{C}$ gives the concentration of isotopologues or isotopologue groups in mol% (Equation 4).

$$mol\% = \frac{\%^{13}C^{13}C \times ^{13}C_{abs.}}{100} \quad \text{Equation 4}$$

$mol\%$: concentration of isotopologue groups in mol %;

$\%^{13}C^{13}C$: $^{13}C^{13}C$ -coupling in the ^{13}C NMR spectrum of a given C-atom;

$^{13}C_{abs.}$: absolute ^{13}C enrichment of a given C-atom.

2.3.8. Protein hydrolysis and amino acid derivatization.

Freeze-dried plant material (100 mg) was suspended in 2 ml of 6 M hydrochloric acid. The mixture was heated at 105 °C for 24 h under an inert atmosphere and was then centrifuged. An aliquot (500 µl) of the supernatant was dried under a stream of nitrogen. The residue was dissolved in 50 µL of acetonitrile. N-(tert-butyldimethylsilyl)-N-methyl-trifluoroacetamide containing 1% tert-butyldimethyl-silylchloride (50 µl) was added. The mixture was kept at 70 °C for 30 min and was used for GC-MS analysis without further work-up.

2.3.9. Mass spectrometry

GC-MS analysis was performed using a GC-17A Gas Chromatograph (Shimadzu, Duisburg, Germany) equipped with a fused silica capillary column (Equity TM-5; 30 m x 0.25 mm x 0.25 µm film thickness; SUPELCO, Bellafonte, PA) and a QP-5000 mass selective detector (Shimadzu, Duisburg, Germany) working with electron impact ionization at 70 eV. An aliquot (1 µl) of a solution containing TBDMS amino acids was injected in 1:5 split mode (interface temperature, 260 °C; helium inlet pressure, 70 kPa). The column was developed at 150 °C for 3 min and then with a temperature gradient of 7 °C/min to a final temperature of 280 °C that was held for 3 min. Data were collected using the Class 5000 software (Shimadzu, Duisburg, Germany). Selected ion monitoring data were acquired using a 0.3 s sampling rate (for details, see also Römisch-Margl *et al.*, 2007). Samples were analysed at least three times.

2.3.10. Isotopologue abundances by GC-MS

Data evaluation was performed using Microsoft Excel Software. Theoretical isotope ratio and numerical deconvolution of the data were computed according to Lee *et al.* (1991) (Equations 5-8) resulting in molar excess of carbon isotopologue groups (X-groups) or isotopologues of the amino acid skeleton. The isotopomer with the base

Materials and Methods

mass (lowest mass) is designated as X_0 , and the other isotopomers are represented by $X_1, X_2, X_3, \dots, X_r$, where the subscripted numbers are the incremental masses of the isotopomer over the base mass, and there are $(r + 1)$ isotopomers of the compound X . The relative abundance (fractional molar abundance) of these isotopic species are represented by $p_0, p_1, p_2, \dots, p_r$, and the sum of all the p s equals to 1 ($\sum p_i = 1$).

The component X is a mixture of these molecules and can be represented by a normalized distribution (Equation 5):

$$(p_0X_0 + p_1X_1 + p_2X_2 + \dots + p_rX_r), \quad \text{Equation 5}$$

and $\sum p_i = 1$.

Similarly, a mixture of the molecules of a component Y can be denoted by (Equation 6):

$$(q_0Y_0 + q_1Y_1 + q_2Y_2 + \dots + q_sY_s) \quad \text{Equation 6}$$

and $\sum q_i = 1$.

For a compound consisting of components X and Y , the mass isotopomer distribution for the compound XY is given by the product (Equation 7):

$$(p_0X_0 + p_1X_1 + p_2X_2 + \dots) \times (q_0Y_0 + q_1Y_1 + q_2Y_2 + \dots) =$$

$$= (p_0q_0X_0Y_0 + p_0q_1X_0Y_1 + p_0q_2X_0Y_2 + \dots) \quad \text{Equation 7}$$

The relationship between the mass isotopomer distribution ($m_0, m_1, m_2, \dots, m(r + s)$) and the individual relative isotope abundance of X ($p_0, p_1, p_2, \dots, p_r$) and Y ($q_0, q_1, q_2, \dots, q_s$) can be represented by matrix multiplication. The set of liner equations resulted from the matrix multiplication is shown below (Equation 8):

$$\begin{aligned} p_0q_0 &= m_0 \\ p_1q_0 + p_0q_1 &= m_1 \\ p_2q_0 + p_1q_1 + p_0q_2 &= m_2 \\ p_3q_0 + p_2q_1 + p_1q_2 + p_0q_3 &= m_3 \\ \dots & \\ p_rq_{s-1} + p_{r-1}q_s &= m(r + s - 1) \end{aligned} \quad \text{Equation 8}$$

The above relationship can be used to predict the mass isotopomer distribution of a compound XY when the mass isotopomer distribution of the components X and Y are known.

2.3.11. Experiments with *Mercurialis annua* L.

2.3.11.1. Metabolite profiling in *M. annua*

Seeds of *M. annua* were germinated in commercial gardening soil mixture (Terreau Professional Gepac Einheits Erde, Germany). The young plants were divided into two groups: control and experimental plants. All plants were grown under the following conditions: photoperiod, 14 h light and 10 h dark; day temperature, 25-28 °C and night temperature, approx. 16 °C; relative humidity, 50%. The plants were poured with 50 mM of 0.9% sodium chloride (salinity) for four days. After four days the plants from both groups were harvested for analysis.

The samples for ¹H NMR were prepared as described under **Methods 2.3.3**.

2.3.11.2. Experiments with [U-¹³C₆]glucose

Cut seedlings of *M. annua* (approximately 15 g, fresh weight) were immersed into a solution containing 0.05% [U-¹³C₆]glucose (99.9% ¹³C enrichment), 0.95% (w/w) unlabelled glucose and 1 mM ascorbic acid. The samples were incubated in the dark for 5 days. The seedlings consumed approximately 100 ml of the solution.

2.3.11.3. Experiments with ¹³CO₂

Growing plants of *M. annua* with a height of about 20 cm were placed in a plant growth chamber (BIOBOX, GWS, Berlin). During an adaption light period of 6 hours at 26 °C and a light period of 12 h at 22 °C and 66% humidity, the plants were exposed to synthetic air containing 20.5% oxygen and 600 ppm CO₂. The chamber was flushed with an oxygen/nitrogen mixture (20:80, v/v), and the plants were then exposed to synthetic air containing 600 ppm ¹³CO₂ under white light (20,000 lux) at 26 °C for 3 h. The plants consumed approximately 0.8 L of ¹³CO₂. Subsequently, the plants were kept in the dark for 18 h and were then allowed to grow under standard greenhouse conditions at ambient temperature for 4 days.

2.3.11.4. Experiments with [1-¹³C₁]glucose

Cut seedlings of *M. annua* (approximately 12 g, fresh weight) were immersed into a solution containing 55 mM [1-¹³C₁]glucose (99.9% ¹³C enrichment) and 1 mM ascorbic acid. The samples were incubated in the dark for 7 days. The seedlings consumed approximately 200 ml of the solution.

2.3.11.5. Experiments with [¹³C₄, ¹⁵N₁]aspartate

Cut seedlings of *M. annua* (approximately 18 g, fresh weight) were immersed into a solution containing 5 mM [¹³C₄, ¹⁵N₁]aspartate (>98% ¹³C and ¹⁵N enrichment) and 1 mM ascorbic acid. The samples were incubated in the dark for 5 days. The seedlings consumed approximately 100 ml of the solution.

2.3.11.6. Isolation of hermidin

Plant material (fresh weight, 15 g) was triturated with liquid nitrogen. To the cold slurry, 150 ml of distilled water and 5 ml of chloroform were added, and the mixture was kept under a nitrogen atmosphere for 45 min. The slurry was filtered, and sodium dithionite (500 mg) was added. The mixture was extracted with two 100 ml portions of chloroform. The organic phase was evaporated to dryness under reduced pressure.

2.3.11.7. NMR spectroscopy

NMR spectra were recorded at 27°C using a DRX 500 spectrometer (Bruker Instruments, Karlsruhe, Germany). Hermidin was measured in C²HCl₃ as solvent. Two-dimensional COSY, HMQC, HMBC experiments were measured with standard Bruker software (TopSpin).

2.3.12. Experiments with *Nicotiana tabacum*

Sterile plants of *N. tabacum* wild-type and *N. tabacum* mutants lacking plastidic RNA polymerase (*rpoA* mutants) were grown on agar containing a mixture of 400 mg of [U-¹³C₆]glucose (99% ¹³C abundance) and 19.8 g of unlabelled sucrose per liter. The plants were grown at 25 °C with 8/16 h dark/light illumination cycles.

2.3.13. Isolation of nicotine

Tobacco leaves (fresh weight, 15 g) were harvested after a growth period of 20 days. They were frozen with liquid nitrogen, pulverized with Ultra Turax and extracted

with 300 ml of methanol. The dark green solution (after filtration) was reduced to approx. 5-10 mL. The solution was extracted with 300 mL of ether. After separation of the ether phase, the pH of the water phase containing nicotine was adjusted to 11 with 25% solution of ammonium hydroxide. Then the water solution was extracted with 300 mL of ether again. Then, after separation of ether phase, the water phase was extracted with 1 ml of C^2HCl_3 . The solution of C^2HCl_3 was separated from the water phase and analyzed by 1H and ^{13}C NMR.

2.3.14. NMR spectroscopy

NMR spectra were recorded at 27 °C using a DRX 500 spectrometer (Bruker Instruments, Karlsruhe, Germany). Nicotine was measured in C^2HCl_3 as solvent.

2.3.15. Isolation of glucose

Tobacco leaves (approx. 15 g wet weight after isolation of nicotine) were extracted with 300 ml of water. The mixture was centrifuged, and 300 ml of methanol were added. The solution was filtered and evaporated to dryness under reduced pressure. The residue was dissolved in 2 ml of water and pH of solution was corrected to 11 by additional of 1 ml of 25% ammonia. The isolation and purification of glucose were described previously (Römisch-Margl *et al.*, 2007). Briefly, the solution was applied to a Boronate Gel column (Bio-Rad Laboratories GmbH, Munich, Germany) which was washed with 0.25% ammonia until all colored components removed. The column was then developed with 1% formic acid. Fractions containing glucose were combined and evaporated to a volume of 5 ml under reduced pressure. The solution was applied to a Dowex 1 x 8 column (Serva Electrophoresis GmbH, Heidelberg, Germany) which was eluted with water. Fractions with glucose were combined and evaporated to a volume of 5 ml under reduced pressure. Aliquots were applied to a Luna NH_4 HPLC column (Phenomenex, TorranceCA, USA, 250 x 20) which was developed with a mixture of acetonitril/water (85:15, v/v) (40°C; flow rate, 30 ml/min). The effluent was monitored refractometrically using a GAT LCD 201 differential refractometer from Gamma Analysen Technik GmbH, Bremerhaven, Germany. Fractions were combined and lyophilised.

2.3.16. Isolation of glucose from cellulose (Sun, *et al.*, 2004)

The plant material (dry weight, 50 mg) was extracted with 2 ml of 80% acetic acid and 0.2 ml of concentrated nitric acid at 120°C for 30 min. 20 ml of ethanol were added and the mixture was centrifuged at 4000 rpm for 15 min. The supernatant was concentrated under reduced pressure. The residue was heated with 1 M sulfuric acid at 120°C for 30 min. The supernatant was neutralized with barium hydroxide, centrifuged and concentrated under reduce pressure. Glucose was isolated and purified with HPLC as described under **Methods 2.3.15**.

2.3.17. NMR spectroscopy

Glucose was dissolved in $^2\text{H}_2\text{O}$. ^1H and ^{13}C NMR spectra were recorded at 27 °C using a DRX 500 spectrometer (Bruker Instruments, Karlsruhe, Germany). Glucose was measured as described under **Methods 2.3.3** and **2.3.6**.

2.3.18. Experiments with *Salvia divinorum*

2.3.18.1. Experiments with [U- $^{13}\text{C}_6$]glucose

Cut seedlings of *S. divinorum* (approx. 30 g, fresh weight) were immersed into a solution containing 0.05% [U- $^{13}\text{C}_6$]glucose (99.9% ^{13}C enrichment), 0.95% (w/w) unlabelled glucose. The samples were incubated in the dark for 14 days. The seedlings consumed approximately 200 ml of the solution.

2.3.18.2. Experiments with $^{13}\text{CO}_2$

A plant of *S. divinorum* with a height of about 20 cm was placed into a plant growth chamber (BIOBOX, GWS, Berlin). During an adaptation light period of 6 hours at 26 °C and a light period of 12 h at 22 °C and 66% humidity, the plant was exposed to synthetic air containing 20.5% oxygen and 700 ppm CO_2 . The chamber was flushed with an oxygen/nitrogen mixture (20:80, v/v), and the plant was then exposed to synthetic air containing 600 ppm $^{13}\text{CO}_2$ under white light (20,000 lux) at 26 °C for 4 h. The plant consumed approximately 0.5 L of $^{13}\text{CO}_2$. Subsequently, the plant was kept in the dark for 18 h and was then allowed to grow under standard greenhouse conditions at ambient temperature for 10 days.

2.3.18.3. Isolation of salvinorin A

Dried leaves of *S. divinorum* (5.0 g) were powdered and steeped with two 150 ml portions of acetone. Filtration and concentration of the filtrate under reduced pressure gave a dark green oil (250 mg).

2.3.18.4. Purification of salvinorin A with column chromatography

The residue (250 mg) was applied to a column of silica gel (Silica Gel 60, Merck, Darmstadt, Germany, 20 x 1 cm), which was developed with a mixture of ether and hexane stepwise from 50 to 90% ether (v/v). Salvinorin A was eluted with ether/hexane (90/10, %). Aliquots were spotted on thin-layer chromatography (TLC) (Silica Gel 60 F₂₅₄, Merck), which was developed with the same solvent mixture. The TLC plates were dried and sprayed with anisaldehyde reagent (anisaldehyde/sulphuric acid/acetic acid; 1:2:100; v/v). Salvinorin A afforded a violet spot with an R_f value of 0.63. Fractions were combined and concentrated to dryness under reduced pressure (yellow oil, 120 mg).

2.3.18.5. Purification of salvinorin A with HPLC

The residue (120 mg) was dissolved in 250 μ l of acetonitril. Aliquots were applied to a HPLC column RP-18 (250 x 4.6 mm) which was developed with acetonitril/water (45:55, v/v) (flow rate, 1 ml/min). Salvinorin A was detected by UV absorption at 208 nm. The R_f value of salvinorin A was approximately 20 ml.

2.3.18.6. Protein hydrolysis and amino acid derivatization

The amino acids were isolated, derivatized and analysed as described under **Methods 2.3.8, 2.3.9, and 2.3.10.**

2.3.19. Isolation of amino acids (Eisenreich *et al.*, 1991)

The labelled plant material was heated with 150 ml of 6 M HCl and 4 ml of thioglycolic acid at 110°C for 24 h. The suspension was filtered and evaporated under reduced pressure to a small volume.

The first column: Dowex 50 Wx8 (NH₄⁺-form)

The first column (200-300 mesh, 2 x 30 cm) was used for separation of neutral amino acids (fraction 1), phenylalanine/tyrosine (fraction 2), lysine (fraction 3), histidine (fraction 4), and arginine (fraction 5).

The sample was applied to the column and washed with 200 ml of water. The column was developed stepwise with: 1000 ml of 0.2 M ammonium formate (pH 4.5); 1500 ml of 0.2 M ammonium formate (pH 6.5), and 1000 ml of 0.5 M ammonium formate (pH 4.5) (flow rate, approximately 18 ml/min). Fractions 1-5 were lyophilised.

The second column: Dowex 1x8 (COO⁻-form)

The dry powder containing neutral and acid amino acids (fraction 1) was dissolved in 20 ml of water and applied to a column of Dowex 1x8 (COO⁻-form) (200-300 mesh, 2 x 35 cm) which was developed with 200 ml of water and 300 ml of 10mM formic acid (flow rate, approximately 18 ml/min). The fractions with glutamate and aspartate were combined and lyophilised. The fractions with neutral amino acids were combined, lyophilised, dissolved in 20 ml of water, and applied to ***the third column***.

The third column: Dowex 50 Wx8 (H⁺-form)

The sample containing neutral amino acids was applied to a column of Dowex 50 Wx8 (H⁺-form) (200-300 mesh, 3 x 30 cm) which was developed with 200 ml of water and 2000 ml of a lineal gradient of 0-3 M HCl (flow rate, approximately 15 ml/min). The fractions containing amino acids: serine/threonine, glycine/alanine, valine, proline, isoleucine and leucine were lyophilised.

2.3.20. Identification of amino acids

Aliquots were spotted on thin-layer chromatography (TLC) (Cellulose, Merck), which was developed with a mixture of n-butanol/acetic acid/water (50/20/30, v/v/v). The TLC plates were dried and sprayed with a ninhydrine reagent. Most amino acids afforded violet spots with the exception of proline (yellow) and tyrosine (brown). The fractions with amino acids were analysed by ¹H and ¹³C NMR spectroscopy using ²H₂O as solvent.

2.3.21. Enzymatic syntheses

2.3.21.1. Preparation of [3,4,5-¹³C₃]1-Deoxy-D-xylulose 5-phosphate (10)

[3,4,5-¹³C₃]1-Deoxy-D-xylulose 5-phosphate (10) was prepared according to published procedures (Illarionova *et al.*, 2006; Hecht, *et al.*, 2001; Rohdich *et al.*, 2000) with some modifications. A reaction mixture containing 150 mM Tris hydrochloride, 10 mM magnesium chloride, 1 g (4.9 mmol) of [U-¹³C₆]glucose, 0.099 g (0.18 mmol) of ATP, 0.23 g (1.5 mmol) of dithiothreitol, 0.3 g (0.65 mmol) of thiamine diphosphate, and 2.2 g (10.6 mmol) of potassium phosphoenolpyruvate in a total volume of 300 ml was adjusted to pH 8.0 by the addition of 5 M sodium hydroxide. To this mixture, 9 mg (750 U) of hexokinase, 1.1 mg (570 U) of glucose 6-phosphate isomerase, 13 mg (50 U) of fructose 6-phosphate kinase, 0.1 mg (620 U) of triose phosphate isomerase, 18 mg (60 U) of fructose 1,6-biphosphate aldolase, 1.7 mg (590 U) of pyruvate kinase, and 12 mg (30 U) of 1-deoxy-D-xylulose 5-phosphate synthase (Dxs) were added. The final volume was 320 ml. The mixture was incubated at 37 °C. Aliquots of 100 µl were retrieved at 1 h intervals; ²H₂O was added to a volume 500 µl and ¹³C NMR spectra were obtained in order to monitor the reaction progress. The reaction was finished after 3 h. The solution was filtered and lyophilised.

Aliquots (8 g) of the crude product were dissolved in 40 ml of 2-propanol/methanol/water (4:2:4, v/v). The solution was placed on a column of microcrystalline cellulose (3 x 50 cm) which was developed with 2 l of 2-propanol/methanol/water (4:2:4, v/v) (flow rate, 1.5 ml/min). Aliquots were spotted on thin-layer chromatography (TLC) (Cellulose, Merck), which was developed with the same solvent. The plates were dried, sprayed with a mixture of acetic acid/sulphuric acid/anisaldehyde (100:1:2, v/v), and heated at 110 °C. The product afforded violet spots ($R_f=0.7$). Fractions were combined and evaporated to a volume of about 100 ml under reduced pressure. The solution was lyophilised. The yield was about 75%. The concentration of product was determined by ¹³C NMR using [1-¹³C₁]glucose as internal standard.

2.3.21.2. Preparation of [1,3,4-¹³C₃]2C-Methyl-D-erythritol 4-phosphate (11)

To a solution of [3,4,5-¹³C₃]1-Deoxy-D-xylulose 5-phosphate (10), 2.25 g (11 mmol) of unlabelled glucose, 250 mg (300 mmol) of NADP⁺, 1.4 mg (150 U) of glucose dehydrogenase, and 24 mg (100 U) of IspC protein were added, and the mixture

was incubated at 37 °C. The formation of [1,3,4-¹³C₃]2C-methyl-D-erythritol 4-phosphate (**11**) was monitored by ¹³C NMR and was found completed after 3 h. The mixture was filtered and lyophilised. Aliquots of the crude product were purified as described for [3,4,5-¹³C₃]1-Deoxy-D-xylulose 5-phosphate (**10**). The concentration of product was monitored by ¹³C NMR using [1-¹³C₁]glucose as internal standard.

2.3.21.3. Preparation of [1,3,4-¹³C₃]4-Diphosphocytidyl-2C-methyl-D-erythritol (14**)**

A reaction mixture containing 150 mM Tris hydrochloride, pH 8.0, 10 mM magnesium chloride, 0.23 g (1.5 mmol) of dithiothreitol, 2.3 g (4.3 mmol) of CTP, 4.2 mmol of [1,3,4-¹³C₃]2C-Methyl-D-erythritol 4-phosphate (**11**), 6 mg (50 U) of IspD protein, and 0.1 mg (100 U) of inorganic pyrophosphatase in a volume of 150 ml was incubated at 37 °C. The formation of product (**14**) was monitored by ¹³C NMR.

2.3.21.4. Preparation of [1,3,4-¹³C₃]4-Diphosphocytidyl-2C-methyl-D-erythritol 2-phosphate (15**)**

A reaction mixture containing 150 mM Tris hydrochloride, pH 8.0, 10 mM magnesium chloride, 0.23 g (1.5 mmol) of dithiothreitol, 2.3 g (4.3 mmol) of CTP, 165 mg (0.3 mmol) of ATP, 1.23 g (6 mmol) of potassium phosphoenolpyruvate, 4.2 mmol of [1,3,4-¹³C₃]2C-Methyl-D-erythritol 4-phosphate (**11**), 6 mg (50 U) of IspD protein, 14 mg (46 U) of IspE protein, 0.8 mg (280 U) of pyruvate kinase, and 0.1 (100 U) of inorganic pyrophosphatase in a volume of 150 ml was incubated at 37 °C. The formation of [1,3,4-¹³C₃]4-Diphosphocytidyl-2C-methyl-D-erythritol 2-phosphate (**15**) was monitored by ¹³C NMR.

3. Results and discussion

3.1. Biological objects

In this thesis, metabolite profiles of *Allium schoenoprasum* and *Mercurialis annua* L. were analyzed by ^1H NMR spectroscopy. The metabolic response of *A. schoenoprasum* upon exposition with heavy metal ions was quantified. The modulation of the metabolite profiles due to gender (female or male) and due to treatment with 0.9% of sodium chloride (salinity) was quantified in plants of *M. annua*.

Biosynthetic pathways and metabolic flux were assessed by labelling experiments with *H. perforatum*, *N. tabacum*, *S. divinorum*.

3.1.1. *Allium schoenoprasum* L.

Chives (*Allium schoenoprasum*), an important Central European spice plant, is morphologically well adapted to dry and sunny habitats (tubiform leaves with a small transpiring surface, geophytic mode of life with a bulb as water reservoir). In urban ecosystems, it occurs (spontaneously or deliberately grown) on green roof tops, which are dry and exposed habitats (Buttschardt, 2001). *A. schoenoprasum* has numerous morphological variations (Poulsen, 1990). In Europe, young leaves are appreciated as an early vitamin source in spring and are used as a condiment for salads, sauces and special dishes (Poulsen, 1990; Hanelt, 2001). The β -carotene and vitamin C contents of chive are the highest among the onion vegetables and are much higher than those of Welsh onion (Loś-Kuczera, 1990). Especially, β -carotene is an important substance: its antioxidant activity might protect against free radical damage and it is potentially anticarcinogenic (Steimetz, 1996; Umehara *et al.*, 2006).

Chive like most *Allium* species is highly rich in pungent sulphur containing volatile compounds which attribute the unique flavour and aroma (Barazani *et al.*, 2004).



Figure 8. *Allium schoenoprasum* L.

3.1.2. *Hypericum perforatum* L. (St. John's wort)

Saint John's wort, also called common or perforate St. John's wort (Fig. 9), belongs to the family Clusiaceae (formerly Hypericaceae or Guttiferae). The species name "perforatum" is Latin for "perforated". The leaves of *H. perforatum*, when held to the light, reveal translucent dots, giving the impression of perforated leaves. The dots are large spherical glands spanning the whole leaf from the upper to the lower epidermis (Weiss, 1988). They contain essential oil comprising caryophyllene, pinenes, limonene, and myrcene as major components.



Figure 9. *Hypericum perforatum* L.

Today, *H. perforatum* is one of the best studied medicinal plants and hyperforin its best characterized constituent (Kurth and Spreemann, 1998; Beerhues, 2006). Phytomedicines based on extracts from the plant's flowering upper parts are widely used as mild antidepressants (Müller, 2003; Butterweck, 2003).

3.1.3. *Mercurialis annua* L.

Mercurialis annua L. (Euphorbiaceae) is an annual dioecious weed, native to the Mediterranean basin. It grows in cultivated areas and wastelands. Aqueous solutions of the plant contain the chromogen, hermidin, on autoxidation rapidly turn blue, then green and finally yellow-brown which suggests that radicals may be implicated in the transformation of hermidin (Forrester, 1984). Indeed, the blue material was identified as a radical anion, cyanohermidin, that is formed from hermidin by reaction with molecular oxygen (Forrester, 1984; Swan, 1984; Boger and Baldino, 1993). Cyanohermidin dimerises spontaneously into a product that is further oxidised with molecular oxygen to the yellow-brown-colored chrysohermidin (Haas and Hill, 1925; Cannan, 1926; Swan, 1985). As reported earlier by Swan (1985), hermidin is present in *Mercurialis* at relatively high concentration.



A



B

Figure 10. *Mercurialis annua* female (**A**) and male (**B**) plants.

3.1.4. *Nicotiana tabacum*

N. tabacum is a very popular plant in the world. *N. tabacum* var. *havanna piperita* is a smaller species of *N. tabacum* (Cheeke and Schull, 1985). Nicotine is biosynthesised in roots and then transported to leaves.



A

B

Figure 11. *Nicotiana tabacum* wild-type (**A**) and *rpoA* mutant (**B**).

Plastids of higher plants operate with at least two distinct DNA-dependent RNA polymerases, which are encoded in the organelle (PEP) and in the nucleus (NEP), respectively. Plastids run-on assays and Northern analyses were employed to analyse gene expression in tobacco mutant plastids lacking the PEP genes *rpoA*, *rpoB* or *rpoC1* (Krause *et al.*, 2000). In comparison to wild-type chloroplast, which are characterized by preferential transcription of photosynthesis-related genes in the light, mutant plastids exhibit a different transcription pattern with less pronounced differences in the hybridisation intensities between the individual genes. The accumulation of large transcripts in the mutant plastids indicates that processing of primary transcripts may be impaired in the absence of PEP (Krause *et al.*, 2000).

3.1.5. *Salvia divinorum*

The genus *Salvia*, containing over 900 species internationally, is one of the largest in the family Lamiaceae (or Labiatae). The largest subgenus is the South American *Calosphace* (or *Jungia*), of which over 300 species are found in Mexico. The plant is a perennial shrub growing to about 1.5 m, preferring moist shady sites at high elevations. While the flowers are distinctive (Fig. 12), the plant's appearance is nondescript during vegetative growth apart from the unusual square stem.



Figure 12. *Salvia divinorum*.

Traditionally, *S. divinorum* is ingested as a quid or smoked for its psychoactive properties and has been reported to have potent hallucinatory actions (Roth *et al.*, 2002). The leaves of *S. divinorum* are used as a traditional medicine by the Mazatec Indians of the Oaxaca region. The disorders treated include gastrointestinal problems, headaches, rheumatism, anaemia and swelling of the stomach.

3.2. Metabolite profiling

3.2.1. Metabolite profiling in *Allium schoenoprasum*

Toxic metal pollution of waters and soils is a major environmental problem, and most conventional remediation approaches do not acceptable solutions. The use of specially selected and engineered metal-accumulating plants for environmental clean-up is an emerging technology called phytoremediation. Three subsets of this technology are applicable to toxic metal remediation: (1) Phytoextraction – the use of metal-accumulating plants to remove toxic metals from soil; (2) Rhizofiltration – the use of plant roots to remove toxic metals from polluted waters; (3) Phytostabilization – the use of plants to eliminate the bioavailability of toxic metals in soils (Salt *et al.*, 1995).

All plants have the ability to accumulate, from soil and water, those heavy metals which are essential for their growth and development. These metals include Fe, Mn, Zn, Cu, Mg, Mo, and possibly Ni. Certain plants also have the ability to accumulate heavy metals which have no known biological function, these include Cd, Cr, Pb, Co, Ag, Se, and Hg (Baker and Brooks, 1989; Raskin *et al.*, 1994). However, excessive accumulation of these heavy metals can be toxic to most plants (Baker and Brooks, 1989; Ernst *et al.*, 1992).

The optimum plant for the phytoextraction process should not only be able to tolerate and accumulate high levels of heavy metals in its harvestable parts but also have a rapid growth rate and the potential to produce a high biomass in the field. Because most of the metal-accumulating wild plants are relatively small in size and have slow growth rates, their potential for phytoextraction may be limited.

An ideal plant for rhizofiltration should have rapidly growing roots with the ability to remove toxic metals from solution over extended periods of time. Mechanisms of toxic metal removal by plant roots include a combination of such physical and chemical processes as chelation, ion exchange and specific adsorption. Metal-chelating proteins, perhaps related to metallothioneins (Robinson *et al.*, 1993) or phytochelatins (Rausser, 1990) may also function as siderophores in plants (Salt *et al.*, 1995).

As an example, cadmium ions accumulate within the vacuole (Vogeli-Lange and Wagner, 1990) where they associate with the family of thiol rich peptides, called phytochelatins (Raus, 1990; Steffens, 1990). The recent discovery of mechanisms for the transport of both Cd²⁺ and Cd-phytochelatin complexes across the tonoplast (Salt

and Wagner, 1993) support the suggestion that Cd detoxification is achieved by the accumulation of Cd^{2+} , associated with phytochelatins, within the vacuole.

Previously, Barazani and co-workers (Barazani *et al.*, 2004) have shown that treatment of *A. schoenoprasum* plants with cadmium ions in the medium at concentrations of 50 μM and 250 μM , respectively, a high concentration of Cd^{2+} was accumulated in the shoots and roots. They have also shown that the concentrations of SH-compounds including glutathione in the roots and in the shoots of Cd treated plants were higher than in control plants.

In our experiments, we have treated plants of *A. schoenoprasum* with cadmium salt as described under **Methods 2.3.1**. After extraction of shoots and roots with perchloric acid, the extracts were analyzed by ^1H NMR spectroscopy (Figs. 13 and 14). The concentrations of polar compounds were assessed by ^1H NMR spectroscopy using a spectral library comprising ^1H NMR spectra (Chenomx NMR Suite 4,6) (Figs. 15 and 16).

The NMR signal assignments were confirmed by titration with reference compounds. For this purpose, 10 μl of 22 standard solutions of sugars and amino acids at concentrations of 10 – 100 mM were added to the NMR samples. NMR spectra of samples after titration were compared with the original spectra. Using this approach, NMR signals could be assigned for 25 compounds (Figs. 15 and 16).

As examples, NMR signals at $\delta = 5.40$ (d, $J = 3.7$ Hz), $\delta = 5.20$ (d, $J = 7.0$ Hz), and 4.10 (d, $J = 7.5$ Hz) were assigned the protons at anomeric carbons of sucrose, α -glucose, and fructose, respectively. In the aromatic region ($\delta = 5.5 - 9.0$), the amino acids, phenylalanine and tyrosine, and unknown compounds were detected at low levels.

Several aliphatic amino acids including asparagine, aspartate, glutamine, glutamate, proline, serine, and threonine were identified as major compounds in the extract.

The concentrations of assigned compounds in the extracts of the shoots and the roots are summarized in Figs. 15 and 16. It turned out that the concentration of asparagine was approximately 7 times higher in the shoots of Cd-treated plants than in the shoots of control plants (Fig. 15). On the other hand, the concentration of asparagine was approximately 2 times higher in the roots of the control than in the roots of plants treated with Cd^{2+} (Fig. 16). We suppose that asparagine serves as a complexing agent for Cd^{2+} ions and is accumulating in the shoots. Moreover, the concentrations of

glutamine and serine were significantly higher in the shoots of Cd-treated plants than in the shoots of control plants (3 and 3.5 times, respectively) (Fig. 15). The concentrations of glycine, malate, proline, sucrose, isoleucine, and valine were also higher by a factor of approximately 2.5 than in the control plants (Fig. 15). The concentrations of those metabolites in the roots of plants grown with Cd²⁺ were similar as in the roots of control plants (Fig. 16).

Most plant species are sensitive to very low concentration of Cd²⁺ (Pietrini *et al.*, 2003) and toxic symptoms as inhibition of plant growth, browning of root tips can be easily seen (Das *et al.*, 1997). Exposure of *A. schoenoprasum* to Cd²⁺ at 50 µM did not have any effect on leaf nor root elongation, thus indicating high tolerance of *A. schoenoprasum* to the metal (Barazani *et al.*, 2004; Masahiro, 2005). On the other hand, the metabolite profile was modulated especially in the shoots of the plants upon treatment with Cd²⁺ via the root system.

It was reported early that one of the mechanisms involved in plant tolerance to Cd²⁺ is the synthesis of the heavy metal binding ligand, phytochelatin (PC) from a reduced glutathione (GSH) (for review see Clemens, 2001). The biosynthetic pathway of phytochelatins (PCs) starts from the precursors, glutamine, cysteine, and glycine (Noctor and Foyer, 1998).

In addition, the stimulation of PC formation by Cd²⁺ has been reported in roots as well as in the leaves of various plant species (Gekeler *et al.*, 1989; Rauser *et al.*, 1990). Our results did not provide evidence of increased levels as of PCs or their precursors GSH, glycine, glutamine and cysteine. In the perchloric acid extract of shoots and roots, the concentration of those and related compounds appeared at similar levels. On the other hand, we detected a large increase of asparagines in the shoots of *A. schoenoprasum* treated with Cd²⁺. This could reflect that PCs are not the prominent agents for Cd-detoxification under the experimental settings used in this study. Rather, the simpler compound asparagine appears to be involved in the process.

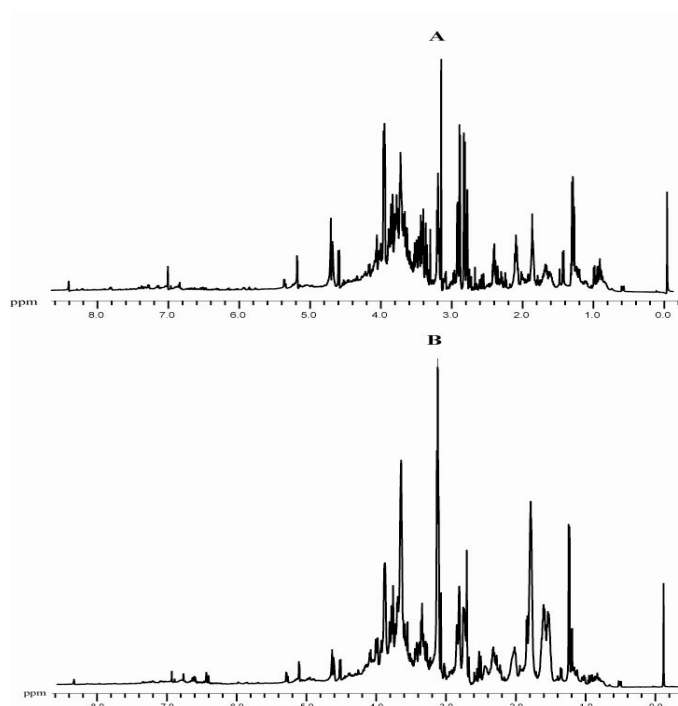


Figure 13. ^1H NMR spectra of the shoot extracts from the control (A) and cadmium treatment (B) plants of *A. schoenoprasum*.

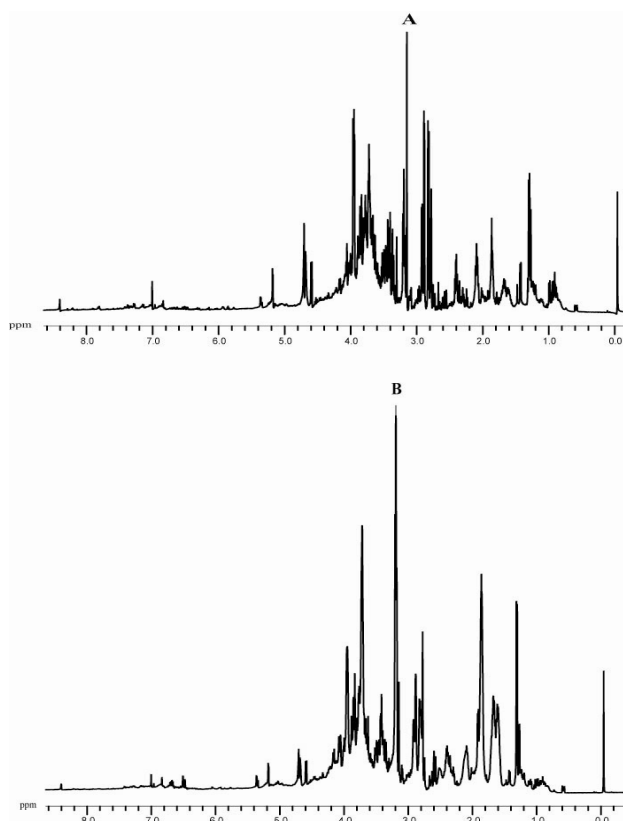


Figure 14. ^1H NMR spectra of the root extracts from the control (A) and cadmium treatment (B) plants of *A. schoenoprasum*.

Results and discussion

Concentration of the metabolites in the shoots of *Allium schoenoprasum*

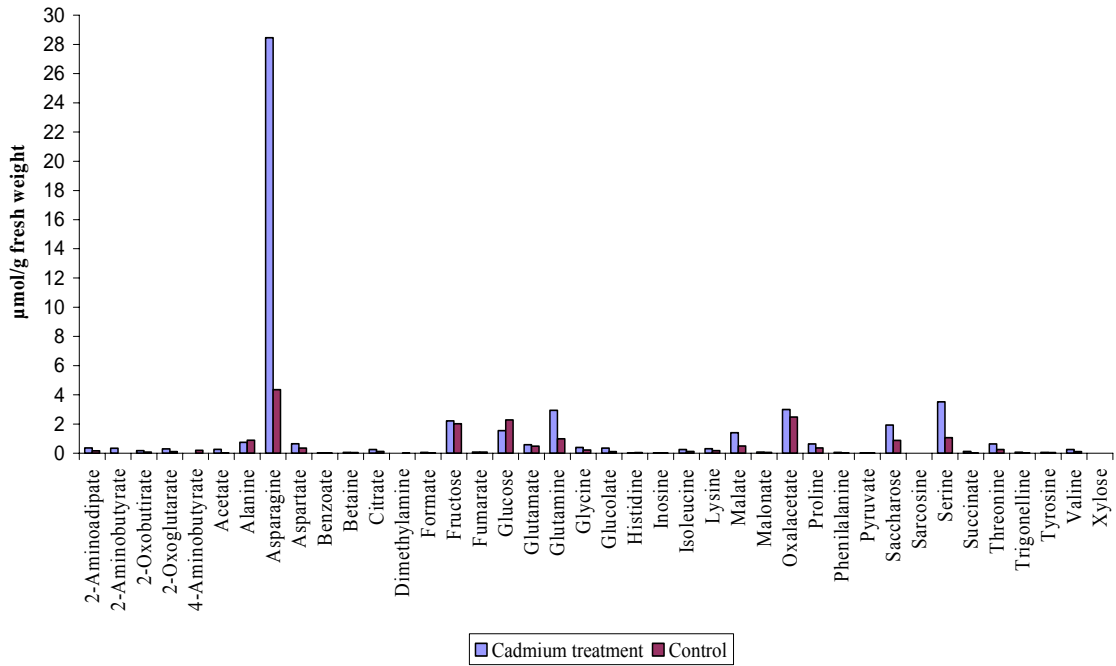


Figure 15. Concentration of the metabolites in the shoots of *A. schoenoprasum*.

Concentration of the metabolites in the roots of *Allium schoenoprasum*

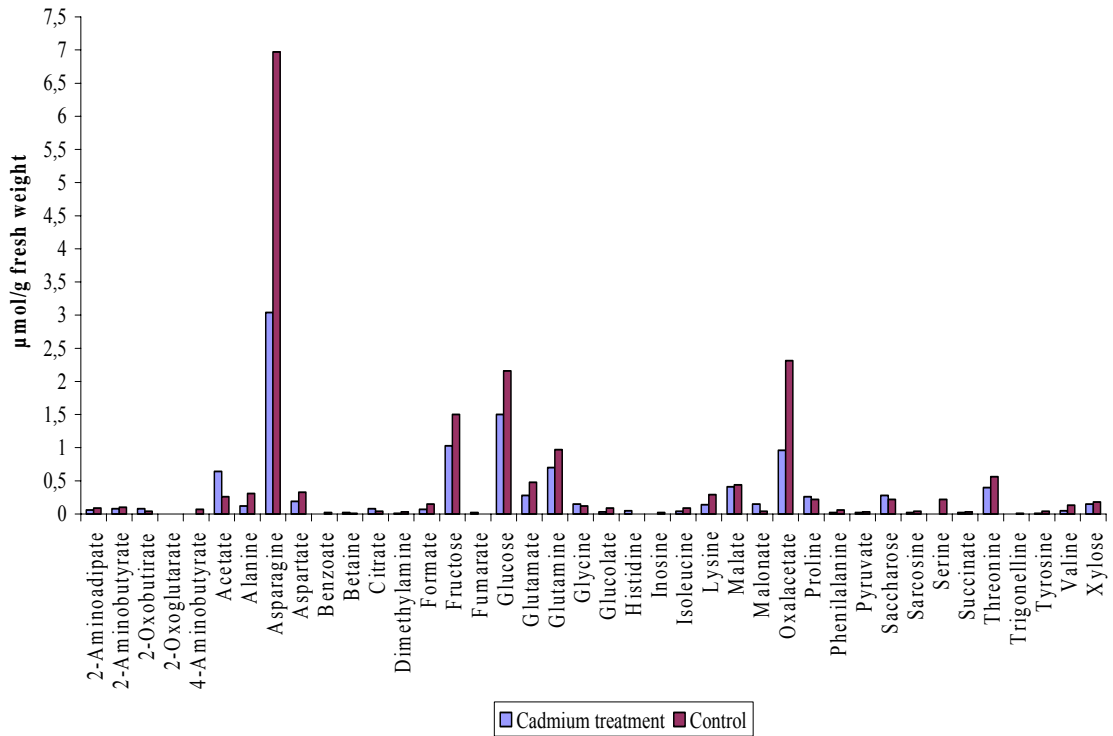


Figure 16. Concentration of the metabolites in the roots of *A. schoenoprasum*.

3.2.2. Metabolite profiling in *Mercurialis annua*

The majority of the research on Na⁺ metabolism in plants has been concerned with the initial uptake across the 'root cell plasmalemma'. At a minimum, it is likely that the plasmalemma and tonoplast have different systems, and though the salt relations of organelles in the cytosolic milieu have not been studied extensively, the apparent control of chloroplast Na⁺ contents suggests an additional system there (Robinson *et al.*, 1983).

Salinity can seriously change the photosynthetic carbon metabolism, leaf-chlorophyll content, as well as photosynthetic efficiency (Seeman and Critchley, 1985). However, salinity is known to boost the nodular carbohydrate content, and sucrose is the predominant carbohydrate in legume root nodules (Fougère *et al.*, 1991; Gordon *et al.*, 1997). In addition, phosphoenolpyruvate carboxylase (PEPC) and malate dehydrogenase (MDH) activities in root nodules produce malate, which is the preferred substrate for supporting nitrogenase activity (Delgado *et al.*, 1993; Kim and Copeland, 1996). The simulation of these activities under saline conditions may be a consequence of the increase in the oxygen-diffusion barrier (Irigoyen *et al.*, 1992; Delgado *et al.*, 1993).

Salt promotes the accumulation of ammonium, nitrate and free amino acids in plants (Hatata, 1982; Pessaraki *et al.*, 1989), and tends to depress the activity of the enzymes involved in ammonium assimilation. It was reported earlier that in *Vicia faba*, glutamine synthetase (GS) activity proved to be more inhibited by salinity than NADH-glutamate synthase activity (Cordovilla *et al.*, 1994). Proline and carbohydrates are accumulated in plant tissues under saline stress, and these substances are suspected of contributing to osmotic adjustment (Fougère *et al.*, 1991; Delauney and Verma, 1993).

The plants of *M. annua* were treated with 50 mM of 0.9% sodium chloride (salinity) as described under **Methods 2.3.11.1**. After extraction with perchloric acid, the concentrations of polar compounds were detected by ¹H NMR spectroscopy (Figs. 17-20).

Specifically, we have compared the concentrations of polar compounds in the leaves and the roots of salt-stressed and control plants, and in the leaves and the roots of female and male plants of *M. annua*. The compounds were again identified by comparison with reference spectra in the "Chenomx" library and titration of several NMR samples with reference compounds. Using this approach, NMR signals were assigned for 30 compounds (Figs. 21-24).

Results and discussion

The concentrations of all polar compounds were similar in female and male plants. The concentrations of glucose and sucrose in the leaves and the roots of female and male salt-treated plants were higher than in control plants (Figs. 21-24). This can be explained by an osmolytic effect. The concentration of malate was approximately 2-5 times higher in the leaves and in the roots of control than in salt-treated plants (Figs. 21-24). On the other hand, the concentrations of aspartate and oxalacetate were higher upon saline stress (Figs. 21-24). This points at rather robust metabolism in *M. annua* which is only modulated by the sex of the plants in a very subtle way. Malate is a precursor of oxalacetate and aspartate. It appears that salinity conditions increase the formation of oxalacetate and aspartate *via* malate. Notably, malate dehydrogenase requires NAD as a co-factor, and it appears that the NAD^+/NADH steady state ratio is modulated by salt stress.

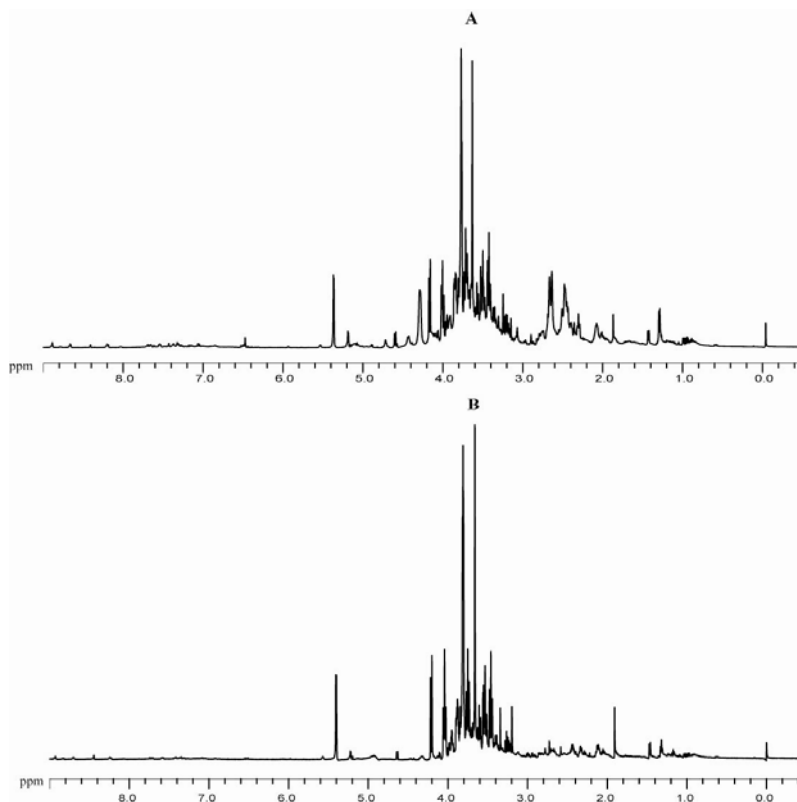


Figure 17. ^1H NMR spectra of the shoots extract from the control (A) and salinity treatment (B) plants of *M. annua* female. .

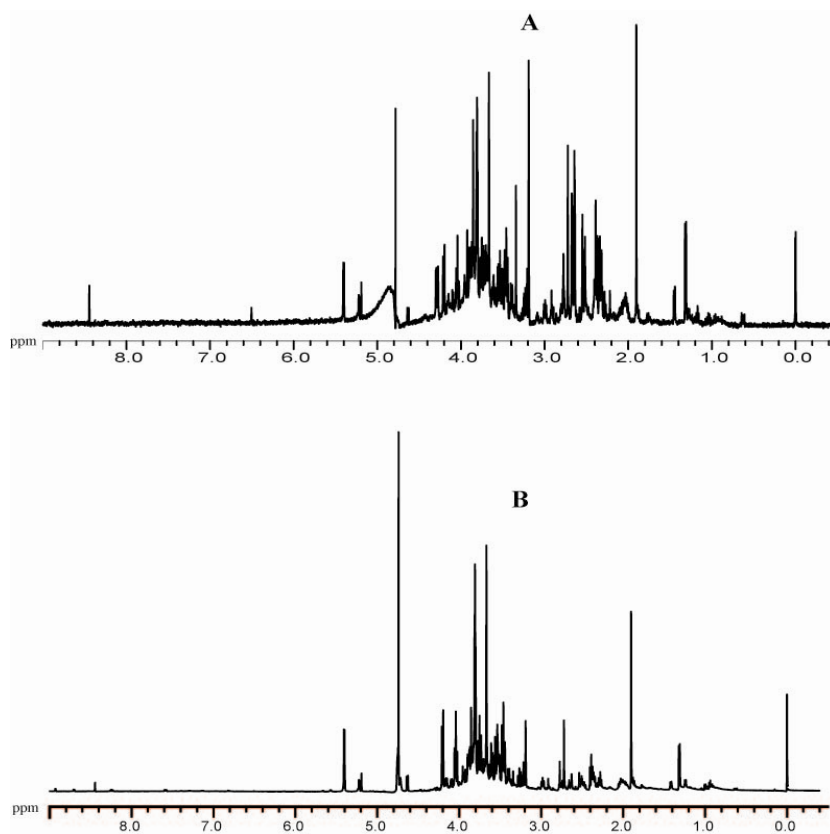


Figure 18. ^1H NMR spectra of the roots extract from the control (A) and salinity treatment (B) plants of *M. annua* female. .

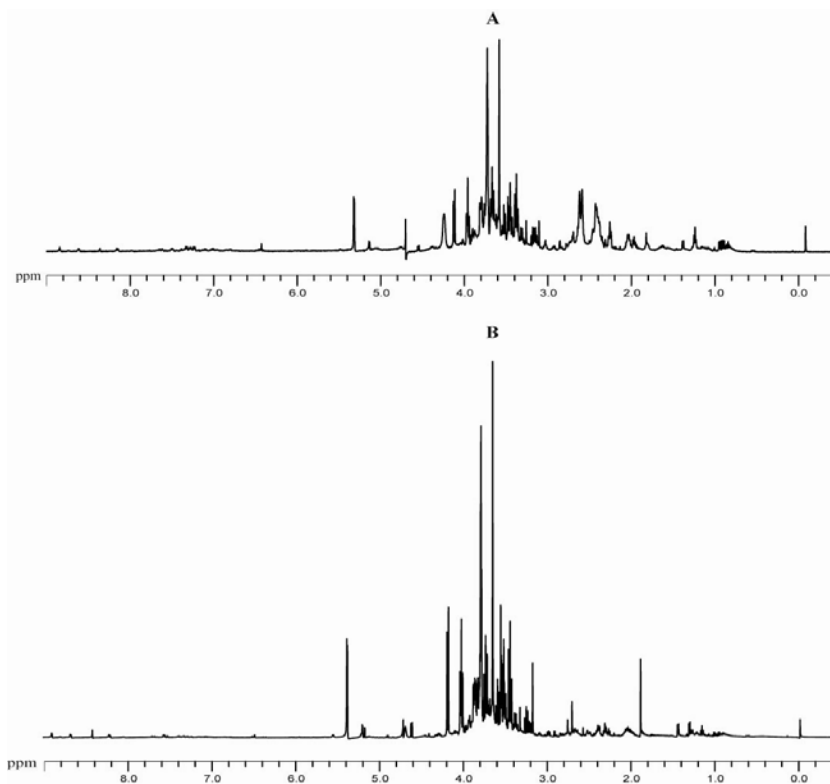


Figure 19. ^1H NMR spectra of the shoots extract from the control (A) and salinity treatment (B) plants of *M. annua* male.

Results and discussion

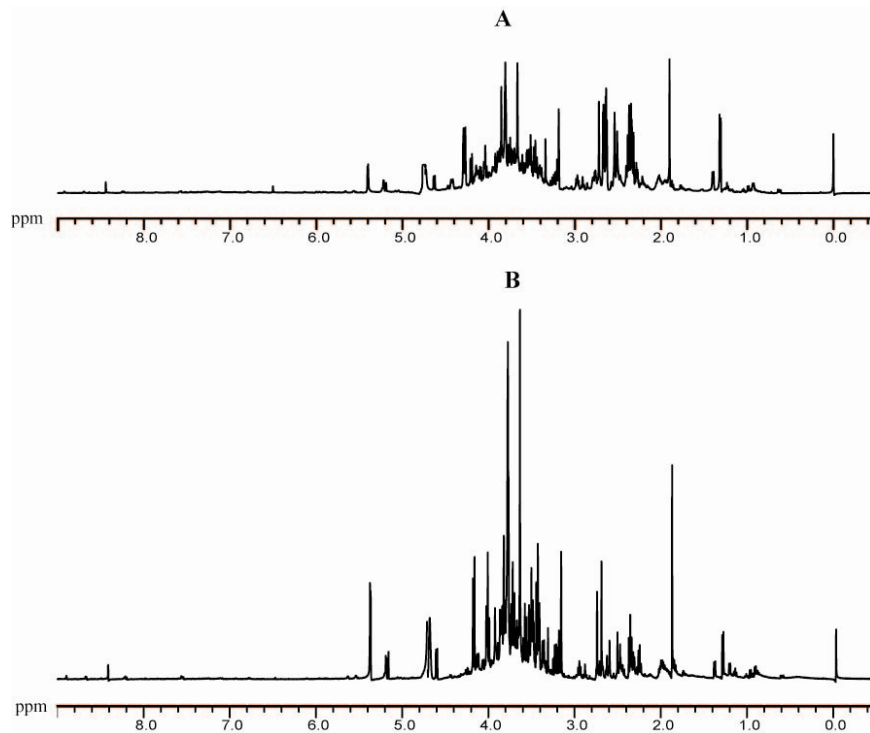


Figure 20. ^1H NMR spectra of the roots extract from the control (A) and salinity treatment (B) plants of *M. annua* male. .

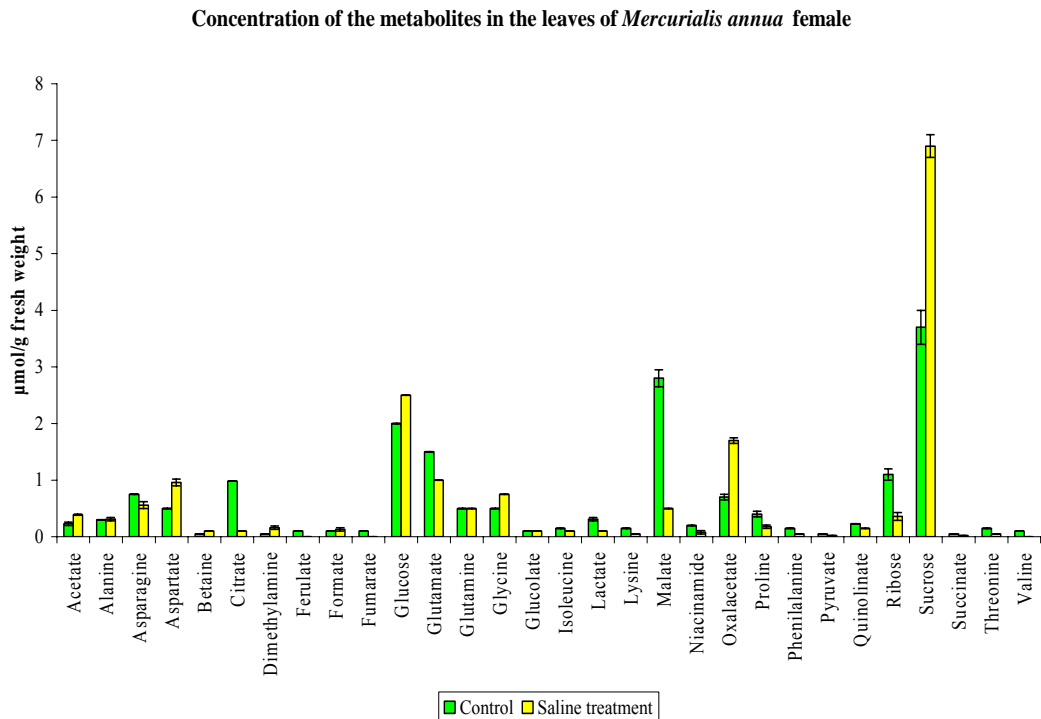


Figure 21. The concentration of the metabolites in the leaves of *M. annua* female in the control and salt-stressed plants.

Results and discussion

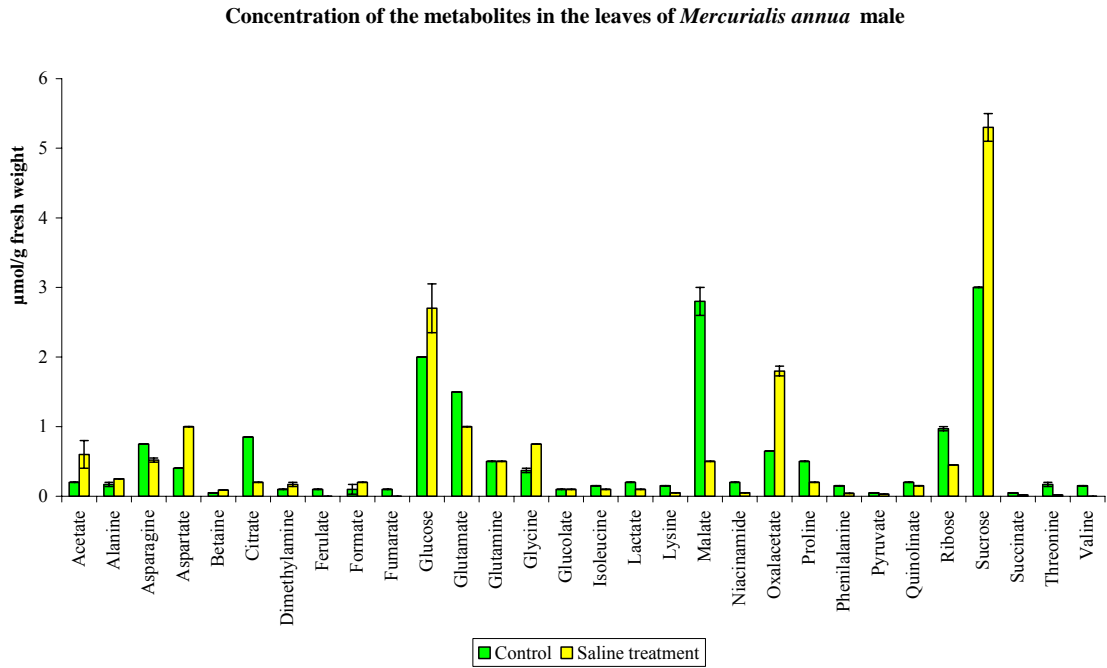


Figure 22. The concentration of the metabolites in the leaves of *M. annua* male in the control and salt-stressed plants.

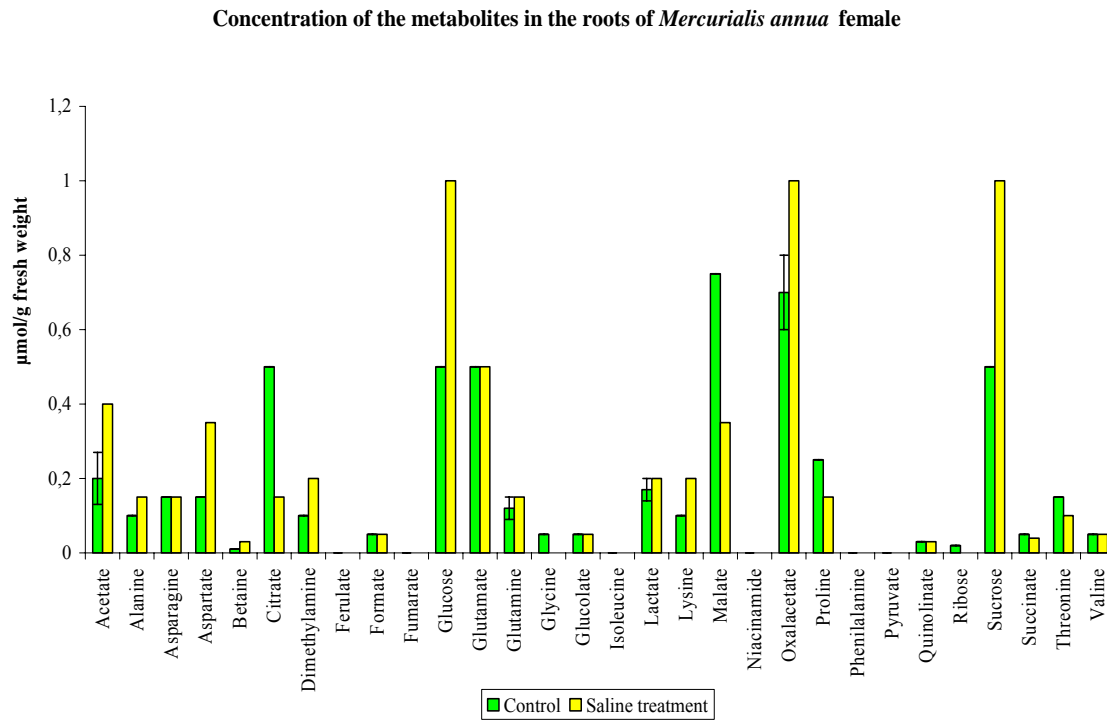


Figure 23. The concentration of the metabolites in the roots of *M. annua* female in the control and salt-stressed plants.

Concentration of the metabolites in the roots of *Mercurialis annua* male

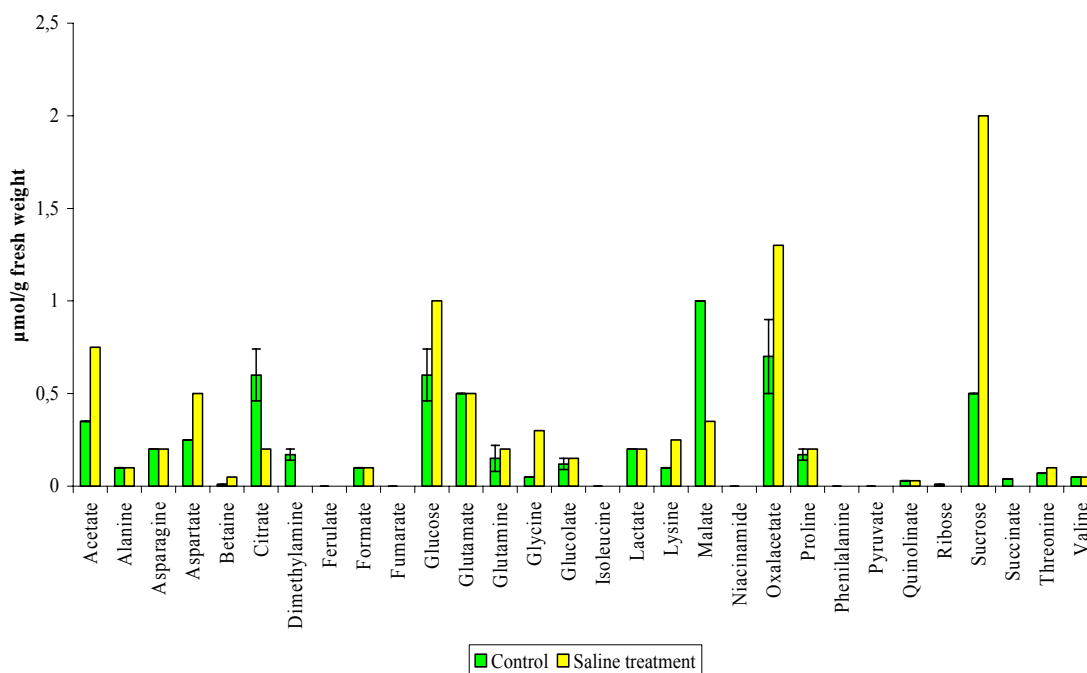


Figure 24. The concentration of the metabolites in the roots of *M. annua* male in the control and salt-stressed plants.

3.3. Preparation and properties of isotope-labelled 4-diphosphocytidyl-2C-methyl-D-erythritol 2-phosphate

Isotope-labelled precursors were crucial in the investigation of the alternative terpenoid pathway. ^{13}C -Labelled 4-diphosphocytidyl-2C-methyl-D-erythritol 2-phosphate was helpful for the studies of identifying downstream metabolites as well as mechanisms of the non-mevalonate pathway enzymes (Rohdich *et al.*, 2000).

The non-mevalonate pathway of isoprenoid biosynthesis (Fig. 25) is a potential target for anti-infective drug development (Bacher *et al.*, 2001). On the basis of the more than 600 completely sequenced genomes in public databases, it is clear that the vast majority of pathogenic bacteria (with the exception of Gram-positive cocci including *Staphylococcus*, *Enterococcus*, and *Streptococcus* spp.) use this pathway for the biosynthesis of essential metabolic products including quinine cofactors required for respiration (for review, see refs Rohdich *et al.*, 2004 and Rohdich *et al.*, 2005; Illarionova *et al.*, 2006).

The preparation of isotope-labelled **15** using recombinant enzymes of the deoxyxylulose pathway has already been described (Rohdich *et al.*, 2000). The ^{13}C -

labelled precursor, in our case [U- $^{13}\text{C}_6$]glucose, is converted into **15** by reactions involving up to 14 enzyme catalysts (Fig. 25). The required enzymes are either commercially available or can be prepared relatively easily from recombinant *Escherichia coli* strains (Sprenger *et al.*, 1997; Lois *et al.*, 1998; Kuzuyama *et al.*, 2000a; Rohdich *et al.*, 1999).

The methods described make extensive use of cofactor recycling (Fig. 25). The formation of D-glyceraldehyde 3-phosphate from glucose requires ATP that can be regenerated by pyruvate kinase using phosphoenolpyruvate as a substrate. Similarly, CTP can be recycled by the inclusion of nucleoside monophosphate kinase and nucleoside diphosphate kinase into the reaction mixture. NADPH can be regenerated in situ by reduction of NADP^+ with glucose and glucose dehydrogenase.

The entire reaction sequence from [U- $^{13}\text{C}_6$]glucose (**16**) to [1,3,4- $^{13}\text{C}_3$]-**15** can be monitored in real time by ^{13}C NMR spectroscopy. Pyruvate is not required for the synthesis of [1,3,4- $^{13}\text{C}_3$]-**15** since it is generated in situ from the phosphoenolpyruvate that is used for the regeneration of ATP. The equilibrium substrate and product concentrations in reaction mixtures containing large amounts of enzymes could also be monitored by ^{13}C NMR spectroscopy using ^{13}C -labelled substrates (Table 5).

The study shows that complex biochemical reaction sequences comprising numerous reaction steps can be executed in vitro with high efficacy. The enzyme-based approach provides unique opportunities for the generation of isotopomers with complex labelling patterns.

The present strategy enables the incorporation of stable isotopes as well as radioisotopes into various positions of **15**. Notably, ^{13}C can be incorporated into virtually any position of the polyol moiety from appropriately labelled glucose and/or pyruvate as starting material.

The data of chemical shifts and coupling constants are summarized in Table 5. Two first precursors (**10** and **11**) were purified by column chromatography as described under **Methods 2.3.21.1**.

Results and discussion

Table 5. ^{13}C NMR data of the reactants used

Position	Chemical shift, ppm	Couplings constant, Hz	
		J_{CC}	J_{PC}
[3,4,5-$^{13}\text{C}_3$]1-deoxy-D-xylulose 5-phosphate (10)			
3	76.9	39.3	
4	70.7	39.8, 43.2	6.7
5	64.1	43.2	4.8
[1,3,4-$^{13}\text{C}_3$]2C-methyl-D-erythritol 4-phosphate (11)			
1	66.5		
3	73.9	42.0	6.2
4	64.8	42.0	4.9
[1,3,4-$^{13}\text{C}_3$]4-diphosphocytidyl-2C-methyl-D-erythritol (14)			
1	66.3		
3	73.4	42.9	7.9
4	66.8	42.9	5.8
[1,3,4-$^{13}\text{C}_3$]4-diphosphocytidyl-2C-methyl-D-erythritol 2-phosphate (15)			
1	65.6		2.2, 1.8
3	73.1	42.9	7.9, 7.9
4	66.9	42.5	5.3

*Referenced to external trimethylsilylpropanone sulfonate.

The procedures described under **Methods 2.3.21** also provide improved technology for the preparation of large amounts (multigram scale) of **10** and **11**. Specifically, the improved procedure affords a yield of about 70-75% of ^{13}C -labelled **10** and **11**.

The non-mevalonate pathway of isoprenoid biosynthesis serves as the unique source of terpenoids in numerous pathogenic eubacteria and apicomplast-type protozoa, most notably Plasmodium, but is absent in mammalian cells. It is therefore an attractive target for anti-infective chemotherapy. The first committed step of the non-mevalonate pathway is catalyzed by 2-C-methyl-D-erythritol 4-phosphate synthase (IspC). Using photometric and NMR spectroscopy assays, we screened extracts of Mediterranean plants for inhibitors of the enzyme. Strongest inhibitory activity was found in leaf extracts of *Cercis siliquastrum*.

The enzyme substrate was multiply labelled with ^{13}C ([3,4,5- $^{13}\text{C}_3$]-**10**). As a consequence of specific ^{13}C -labelling, ^{13}C -signals of C-3, C-4 and C-5 of the substrate and C-1, C-3 and C-4 of the product, [1,3,4- $^{13}\text{C}_3$]-**11**, were detected with high selectivity in the ^{13}C NMR spectrum.

Results and discussion

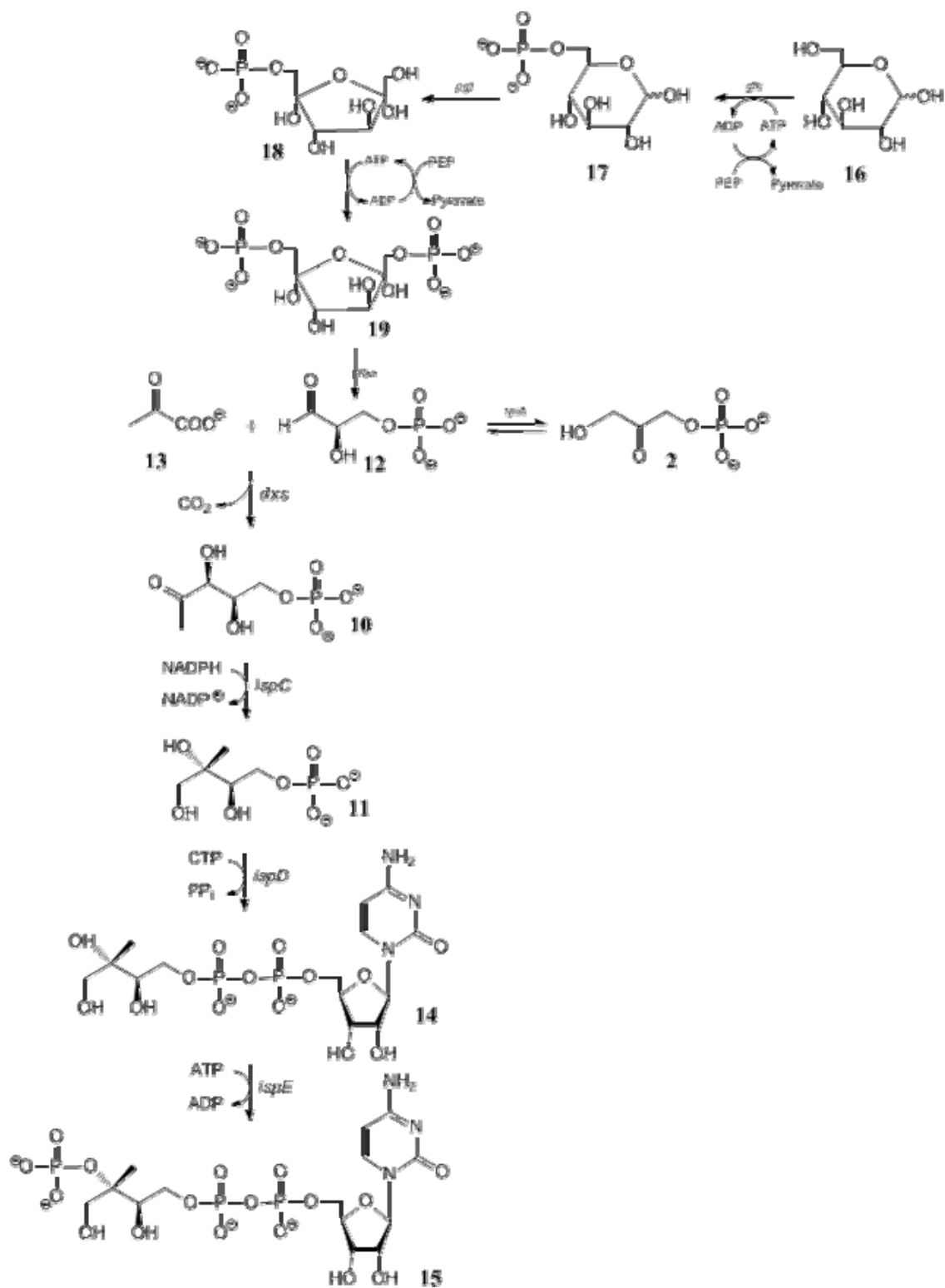


Figure 25. Synthesis of [1,3,4-¹³C₃]4-diphosphocytidyl-2C-methyl-D-erythritol 2-phosphate.

Results and discussion

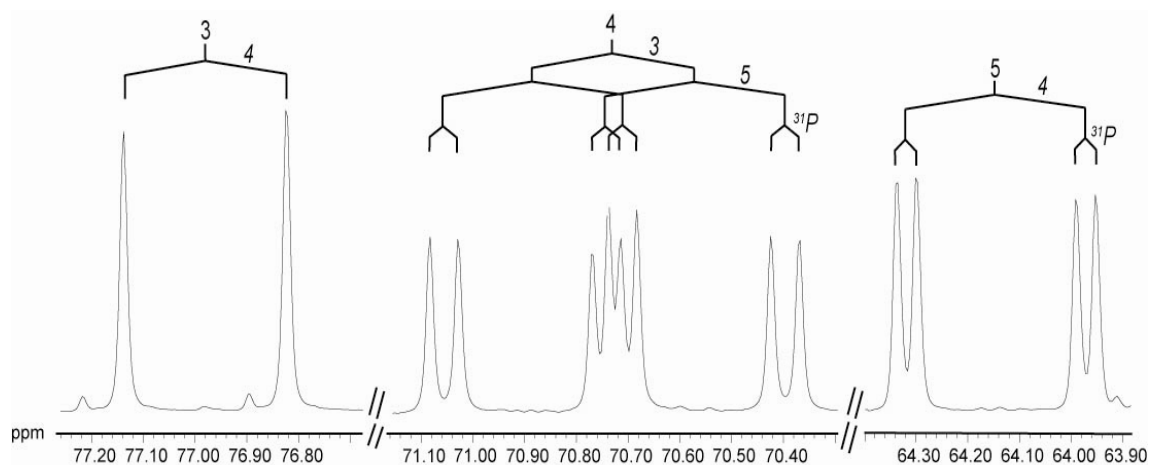


Figure 26. ^{13}C NMR signals of $[3,4,5\text{-}^{13}\text{C}_3]$ 1-deoxy-D-xylulose 5-phosphate (**10**). Coupling patterns are indicated.

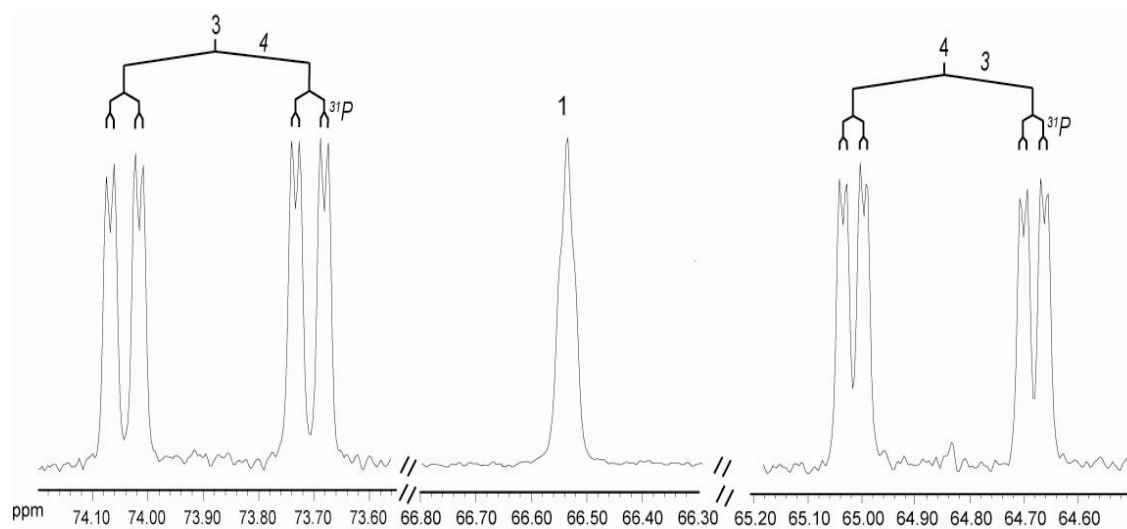


Figure 27. ^{13}C NMR signals of $[1,3,4\text{-}^{13}\text{C}_3]$ 2C-methyl-D-erythritol 4-phosphate (**11**). Coupling patterns are indicated.

Results and discussion

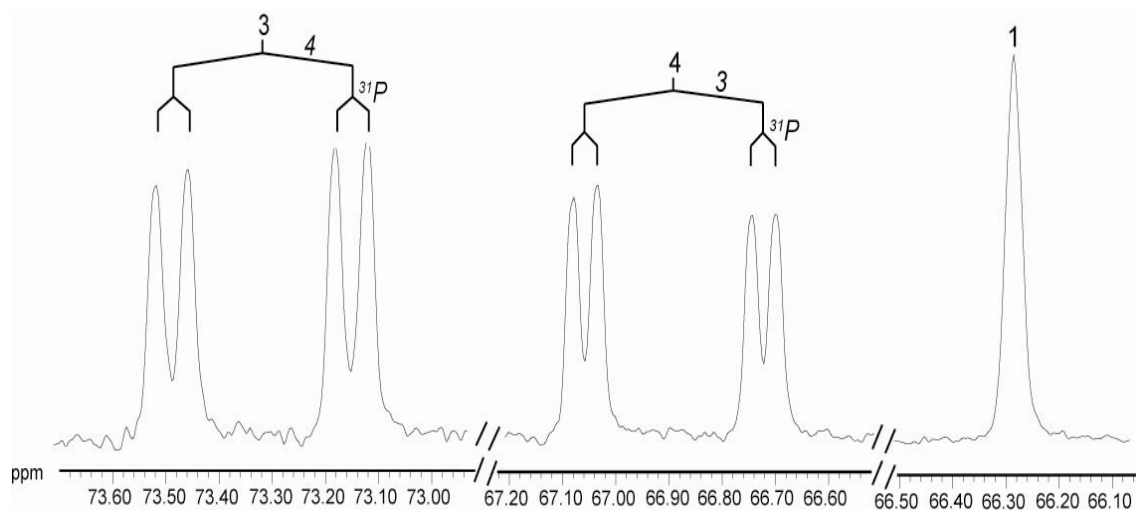


Figure 28. ^{13}C NMR signals of $[1,3,4-^{13}\text{C}_3]$ 4-diphosphocytidyl-2C-methyl-D-erythritol (**14**). Coupling patterns are indicated.

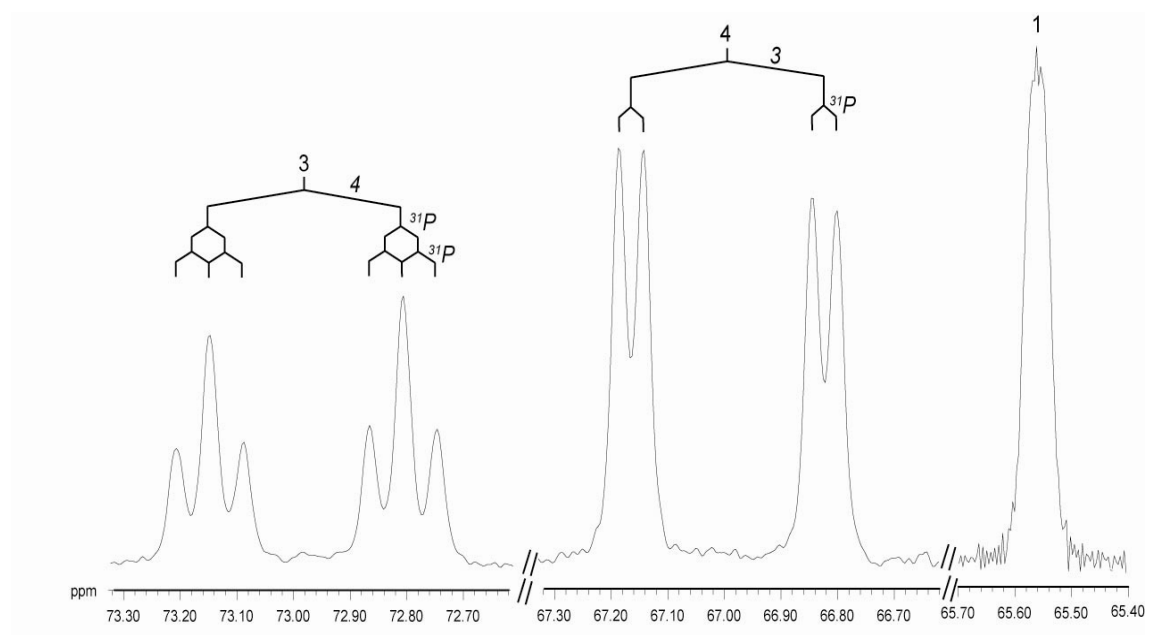


Figure 29. ^{13}C NMR signals of $[1,3,4-^{13}\text{C}_3]$ 4-diphosphocytidyl-2C-methyl-D-erythritol 2-phosphate (**15**). Coupling patterns are indicated.

Results and discussion

The signals of $[3,4,5-^{13}\text{C}_3]$ -**10** in an assay mixture without protein are shown in Figure 30A. The signals detected in a standard assay without an inhibitory agent are in Figure 30B. It is immediately obvious that the signals due to $[3,4,5-^{13}\text{C}_3]$ -**10** disappeared and that three new signals due to $[1,3,4-^{13}\text{C}_3]$ -**11** appeared since the substrate was completely converted into the product. The ^{13}C NMR signals of the same assay mixture in the presence of 6 μl of an extract from *C. siliquastrum* are shown in Figure 30C.

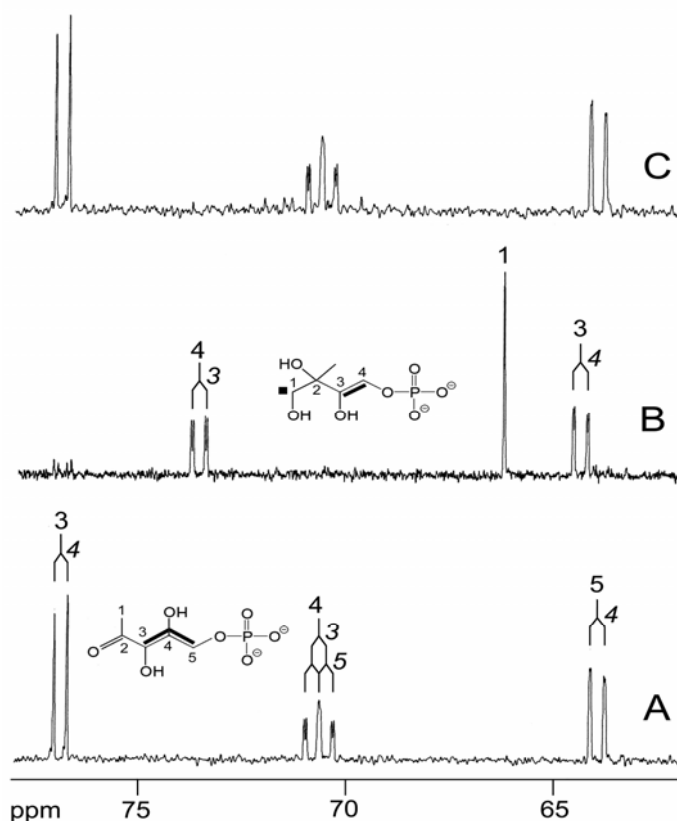


Figure 30. ^{13}C NMR signals observed with IspC reaction mixtures. **A**, reference sample of $[3,4,5-^{13}\text{C}_3]$ 1-deoxyxylulose 5-phosphate; **B**, after inhibition with IspC protein from *E. coli*; **C**, after incubation with IspC protein with IspC protein from *E. coli* in the presence of 6 μl of an extract of *C. siliquastrum*. Multiply ^{13}C -labeling is indicated by filled bars and squares in the formulae of the substrate, $[3,4,5-^{13}\text{C}_3]$ 1-deoxyxylulose 5-phosphate, and the product $[1,3,4-^{13}\text{C}_3]$ 2-methyl-D-erythritol 4-phosphate.

3.4. Biosynthesis of hyperforin in *Hypericum perforatum*: experiment with $^{13}\text{CO}_2$

Tracer experiments can be conducted with single-labelled or multiply labelled precursors. Experiments with single-labelled tracers document the transfer of isotope from a given position in the precursor to one or several positions in each of one or several target compounds. Experiments with multiply labelled precursors document the transfer of individual isotope atoms or contiguous groups of isotope atoms to specific locations in each of one or several target compounds; colloquially the search for transfer of contiguous groups of labelled atom has been attributed as “bond labelling”.

Whereas the early pioneers of the CO_2 labelling technology were limited to radioactivity measurements using $^{14}\text{CO}_2$, there are now powerful NMR and mass spectrometry methods that allow the use of non-radioactive $^{13}\text{CO}_2$ as tracer. Even more important, whereas the $^{14}\text{CO}_2$ technique could only detect the transfer of single ^{13}C atoms from CO_2 to more complex organic molecules, it is now possible to diagnose the incorporation of multiple ^{13}C atoms into a given metabolite and to follow a block of contiguous ^{13}C atoms through a series of biosynthetic transformations affording a complex natural product.

In order to further establish the possibilities and potential limitations of this approach, the isotopologue patterns of hyperforin (Fig. 31) obtained by labelling with $^{13}\text{CO}_2$ and $[\text{U-}^{13}\text{C}_6]\text{glucose}$ were compared (as observed in earlier study).

The earlier study using $[\text{U-}^{13}\text{C}_6]\text{glucose}$ and cut plant segments showed that the prenyl side chains of hyperforin are predominantly biosynthesized *via* the non-mevalonate pathway and that the carbocyclic moiety has a polyketide origin (Adam *et al.*, 2004).

Hypericum perforatum plants with a height of approximately 40 cm were exposed to an atmosphere containing 600 ppm $^{13}\text{CO}_2$ for five hours (see **Materials and Methods 2.3.4**). The ratio of $^{12}\text{C}:^{13}\text{C}$ in the incubation chamber (Fig. 32) was monitored online and was approximately 1:8 (80 ppm $^{12}\text{CO}_2$ and 600 ppm $^{13}\text{CO}_2$) during the incubation period. During the subsequent chase phase, the plants were kept in the greenhouse under ambient conditions for 5 days. 10 mg of hyperforin were isolated from 25 g fresh weight of flowers from labelled plants and then were analyzed by ^{13}C NMR spectroscopy.

The ^{13}C signals of biosynthetic hyperforin displayed intense satellites caused by $^{13}\text{C}^{13}\text{C}$ couplings (Fig. 33). On the basis of the coupling constants (Table 6), these

signals can be attributed to specific multiple ^{13}C -labelled isotopologues. As an example, the ^{13}C NMR signal of C-9 comprised a central line and two pairs of ^{13}C -coupled satellites with considerable intensity that were caused by ^{13}C coupling with C-1 (coupling constant 38.7 Hz) and C-5 (coupling constant 35.2 Hz) reflecting the presence of [1,9- $^{13}\text{C}_2$]- and [5,9- $^{13}\text{C}_2$]-isotopologues, respectively. The signal intensities of the satellite signals for [1,9- $^{13}\text{C}_2$]- and [5,9- $^{13}\text{C}_2$]-isotopologues were identical (19.0 % of the overall signal intensity for each isotopologue group) (Table 6).

Some of the satellites showed couplings via two or three carbon bonds. For example, each of the satellite signals for C-21, C-22, C-26 and C-27, showed three lines (Fig. 33). The central signals in each satellite patterns reflected the coupling between C-21 and C-22, or C-26 and C-27, respectively. The fine splitting of the satellite signals was caused by simultaneous coupling to an additional ^{13}C -atom *via* two or three bonds (long-range coupling). On the basis of the coupling constants (i.e., one large coupling via one bond with a coupling constant of 43.4 Hz and one long-range coupling *via* two or three bonds with coupling constants of 3.1 and 4.5 Hz respectively), these signals can be tentatively assigned to [26,27,30- $^{13}\text{C}_3$]- and [21,21,25- $^{13}\text{C}_3$]hyperforin. Notably, the same signal patterns were also found in the experiment with [U- $^{13}\text{C}_6$]glucose (Adam *et al.*, 2002).

The analysis of all carbon signals is summarized in Table 6. It became obvious that the isotopologue composition of hyperforin labelled from $^{13}\text{CO}_2$ was highly complex and a complete isotopologue deconvolution was not possible on the basis of the observed ^{13}C -pattern. Notably, hyperforin comprises 35 carbon atoms and, in principle, $2^{35} = 3.4^{10}$ different carbon isotopologues can be present in the compound.

However, the number of possible carbon isotopologues can be drastically reduced by looking at given biosynthetic modules, such as the prenyl moieties or the phloroglucinol ring system.

Results and discussion

Table 6. NMR data of hyperforin from the $^{13}\text{CO}_2$ experiment monitored by NMR spectroscopy

Position	Chemical shift, ^{13}C , (ppm)	Coupling constant, (Hz)	% $^{13}\text{C}^{13}\text{C}$
1	n.d.	n.d.	n.d.
2	n.d.	n.d.	n.d.
3	122.3	63.7 (2 or 4) 68.1 (2 or 4)	36.9 (2 or 4)
4	n.d.	n.d.	n.d.
5	n.d.	n.d.	n.d.
6	49.7	n.d.	n.d.
7	43.2	n.d.	n.d.
8	40.9	n.d.	n.d.
9	208.9	38.7 (1 or 5) 35.2 (1, 5)	38.7 (1 or 5) 13.1 (1 and 5)
10	211.8	40.7 (5 or 11)	22.2 (5 and 11)
11	43.2	n.d.	n.d.
12	22.2	43.6 (11) 1.3 (10)	24.9 (11 and 11, 10)
13	21.4	34.1 (11)	43.3 (11)
14	15.5	36.0 (6)	44.8 (6)
15	38.1	33.4 (6or16) 31.2 (6,16)	27.5 (6 or 16) 8.6 (6 and 16)
16	25.6	40.5 (17) 4.8 (20)	37.9 (17, 17 and 20) 15.7 (15 and 17)
17	126.2	43.6 (16) 3.1 (16,20) 72.3 (18)	17.9 (16) 15.6 (16 and 18) 11.9 (16 and 20) 8.8 (18)
18	131.9	42.2 (19or20) 74.3 (17)	26.0 (19 or 20) 11.6 (17) 13.7 (17and19or17and20or19and20)
19	18.3	44.2 (18)	42.0 (18)
20	26.1	n.d.	n.d.
21	28.8	43.2 (22) 4.5 (25)	36.5 (22, 22 and 25) 13.6 (7 and 22)
22	123.9	44.0 (21) 3.1 (21,25) 73.4 (23)	18.2 (21) 16.7 (21 and 23) 12.2 (21 and 25) 8.1 (23)
23	134.4	42.5 (24 or 25) 74.5 (22)	32.9 (24 or 25) 8.9 (22) 6.5 (22and25or22and24or24 and 25)
24	18.3	42.2 (23)	42.0 (23)
25	26.2	n.d.	n.d.
26	22.7	43.6 (27) 4.6 (30)	39.2 (27, 27 and 30) 13.6 (3 and 27)
27	122.7	43.1 (26) 3.1 (26, 30) 72.7 (28)	17.9 (26) 17.1 (26 and 28) 11.9 (26 and 30) 13.3 (28)
28	133.8	42.0 (29 or 30) 74.7 (27)	27.1 (29 or 30) 12.0 (27) 9.0 (27and29or27and30or29 and 30)
29	26.3	42.5 (28)	43.2 (28)
30	18.0	n.d.	n.d.
31	30.8	44.4 (32) 4.4 (35)	39.2 (32, 32 and 35) 13.1 (1 and 32)
32	121.0	44.4 (31) 74.9 (33) 3.1 (31, 35)	18.7 (31) 11.2 (31 and 35) 16.7 (31 and 33) 8.2 (33)
33	134.8	42.2 (34 or 35) 73.6 (32)	24.5 (34 or 35) 9.0 (32) 7.7 (32and34or32and35or34and 35)
34	18.5	42.5 (33)	45.0 (33)
35	26.4	41.2 (33)	n.d.

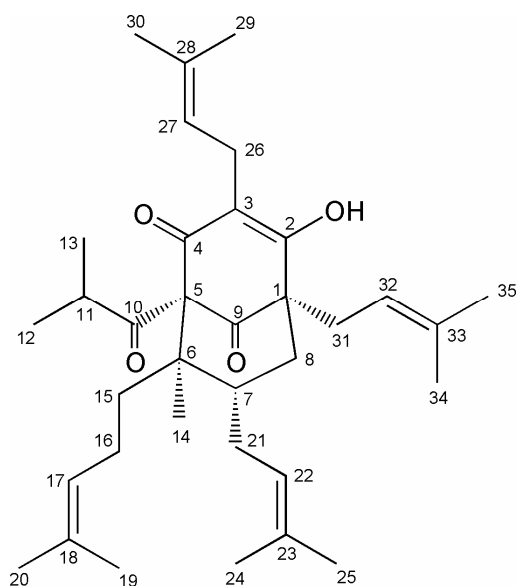


Figure 31. Structure of hyperforin.

As already mentioned above, an earlier experiment using cut sprouts of *H. perforatum* immersed into a solution containing $[U-^{13}C_6]$ glucose indicated that the major fraction of the C5 precursors of the terpenoid units in hyperforin was formed *via* the non-mevalonate pathway and that the phloroglucinol moiety is derived from the polyketide pathway (Adam *et al.*, 2002). Nevertheless, it remained open whether the same pathways are operative in the whole plant under undisturbed (i.e. physiological) conditions.

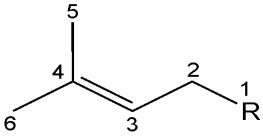
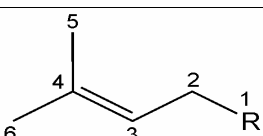
To answer this question, the isotopologue composition of the prenyl moieties in hyperforin isolated from the experiment with $^{13}CO_2$ was analysed. In order to describe the complex isotopologue space of prenyl moieties, we use a notation where the carbon skeleton of prenyl moiety is represented by a six-digit binary number with the first digit representing C-1, the second digit representing C-2, etc.; 1 signifies ^{13}C , 0 (zero) signifies ^{12}C , and X or Y signifies either ^{12}C or ^{13}C . In the present example, C-1 represents the carbon where the respective isoprenyl unit attached (see Table 7). For example, {011XXX} designates a set of isotopologues carrying ^{12}C in the C-5 prenyl attaching carbon, ^{13}C in positions 1 and 2 of the isoprenyl moiety, and ^{13}C or ^{12}C in any of the positions 3-5 of the isoprenyl unit (see also structure inset in Table 7); isotopologue sets of this type are subsequently designated as XY-groups (Römisch-Margl *et al.*, 2007). While the labelling status of X positions is totally undefined, the overall number of ^{13}C -labelled atoms in all Y-positions, given outside the brackets of

Results and discussion

the X-group, is a known parameter. For example, in cases of the carbon where the NMR data can only be assigned to the sum of two simple X-groups, {011XXX and 110XXX} and {Y1YXXX}¹ (Römisch-Margl *et al.*, 2007).

To simplify the analysis, the X-group abundances detected for each prenyl moiety were averaged (Table 7). Indeed, the low standard deviations indicate that all prenyl units in hyperforin originate from common precursor units. This provided a data set consisting of 14 averaged X-group abundances for the prenyl units (Table 7).

Table 7. Relative abundance of X groups in prenyl moieties of hyperforin from the experiments with ¹³CO₂ and [U-¹³C₆]glucose

Experiments with ¹³CO₂					
	Relative abundance of X groups in prenyl moieties, %				
	C 15-20	C7, 21-25	C3, 26-30	C1, 31-35	average SD
{011XXX}	37.9	36.5	39.2	39.2	38.2 ± 1.1
{111XXX}	15.7	13.6	13.6	13.1	14.0 ± 0.7
{010XXX}	46.4	49.9	47.1	47.7	47.7 ± 0.3
{0110XX}	17.9	18.2	17.9	18.7	18.2 ± 0.3
{0110YY} ¹	11.9	12.2	11.9	11.2	11.8 ± 0.4
{0011X0}	8.8	8.1	13.3	8.2	9.6 ± 0.9
{0111XX}	15.6	16.7	17.1	16.7	16.5 ± 0.7
{X010XX}	45.8	44.8	39.8	45.2	43.9 ± 2.1
{XX01YY} ¹	26.0	32.9	27.1	24.5	27.6 ± 3.7
{XX1100}	11.6	8.9	12.0	9.0	10.4 ± 1.9
{XXY1YY} ²	13.7	6.5	9.0	7.7	9.2 ± 3.5
{XX010X}	48.7	51.7	51.9	58.8	52.8 ± 1.2
{XXY11Y}	13.0	16.5	13.6	12.5	13.9 ± 0.5
{XXX01X}	86.3	93.5	91.0	92.3	90.8 ± 1.7
Experiments with [U-¹³C₆]glucose					
	Relative abundance of X groups in prenyl moieties, %				
	C 15-20	C7, 21-25	C3, 26-30	C1, 31-35	average SD
{011XXX}	35.0	35.4	35.8	37.3	35.9 ± 1.0
{111XXX}	0	0	0	0	0
{010XXX}	65.0	64.6	64.2	62.7	64.1 ± 1.0
{0110XX}	8.4	10.2	10.0	9.2	9.5 ± 0.8
{0110YY} ¹	24.9	23.7	24.9	25.4	24.7 ± 0.7
{0011X0}	0	0	0	0	0
{0111XX}	0	0	0	0	0
{X010XX}	66.7	62.5	65.1	65.4	64.9 ± 0.8
{XX01YY} ¹	32.1	33.0	32.2	34.9	33.1 ± 1.3
{XX1100}	0	0	0	0	0
{XXY1YY} ²	0	0	0	0	0
{XX010X}	67.9	67.0	67.8	65.1	66.9 ± 1.3
{XXY11Y}	0	0	0	0	0
{XXX01X}	100	100	100	100	100

Results and discussion

The X-groups profiles of hyperforin from the labelling experiments using $^{13}\text{CO}_2$ and $[\text{U-}^{13}\text{C}_6]\text{glucose}$ as tracer, were now compared from the prenyl and polyketide moieties, respectively. The X-groups $\{011\text{XXX}\}$ and $\{\text{XX}01\text{YY}\}^1$ in the prenyl moieties and $\{\text{XY}1\text{YX}\}^1$ in the polyketide moiety, respectively, were highly similarly (Tables 7 and 8) in both experiments. On the other hand, the relative abundances of $\{0110\text{XX}\}$ and $\{0110\text{YY}\}^1$ in the prenyl moieties were different (Table 7). The relative abundances of $\{0110\text{YY}\}^1$ were approximately 2 time higher than $\{0110\text{XX}\}$ in the experiments with $[\text{U-}^{13}\text{C}_6]\text{glucose}$. On the other hand, the relative abundances of $\{0110\text{XX}\}$ were lightly higher than $\{0110\text{YY}\}^1$ in the experiments with $^{13}\text{CO}_2$.

Table 8. Relative abundance of X groups in the polyketide moiety of hyperforin from the experiments with $^{13}\text{CO}_2$ and $[\text{U-}^{13}\text{C}_6]\text{glucose}$.

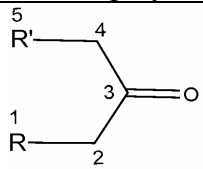
Experiments with $^{13}\text{CO}_2$	
Relative abundance of X groups in the polyketide moiety, %	
	C1, C5, C9
$\{\text{XY}1\text{YX}\}^1$	38.7
$\{\text{X}111\text{X}\}$	13.1
$\{\text{X}010\text{X}\}$	48.2
Experiments with $[\text{U-}^{13}\text{C}_6]\text{glucose}$	
Relative abundance of X groups in the polyketide moiety, %	
$\{\text{XY}1\text{YX}\}^1$	31.4
$\{\text{X}111\text{X}\}$	
$\{\text{X}010\text{X}\}$	



Figure 32. The chamber for incubation of plants with $^{13}\text{CO}_2$.

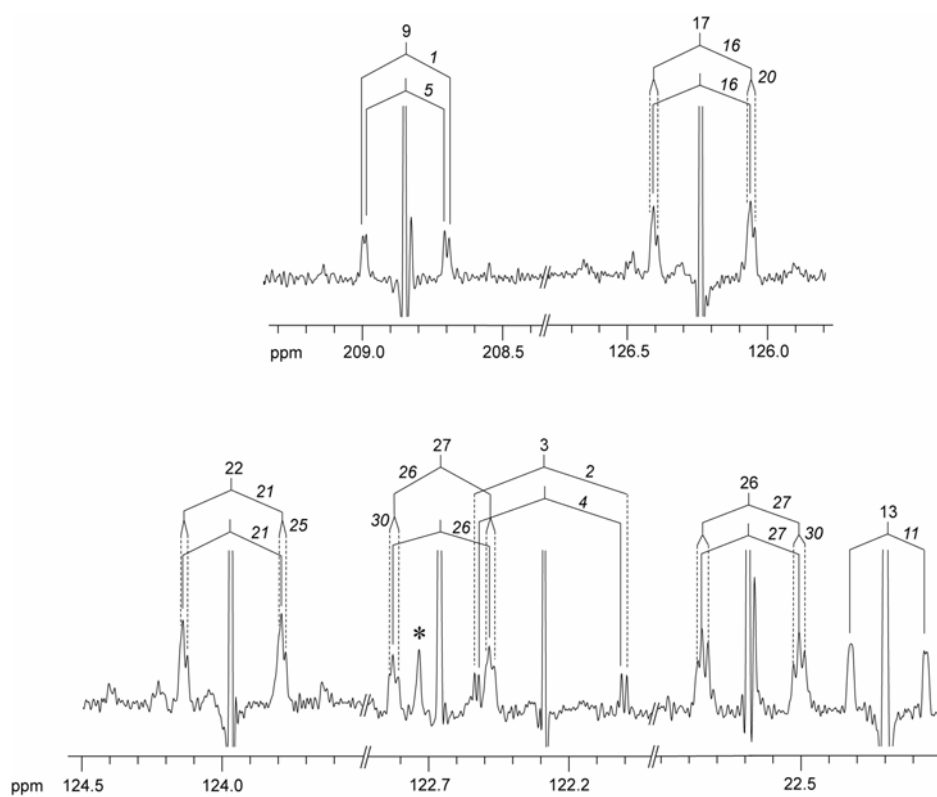


Figure 33. ^{13}C NMR signals of hyperforin from the experiments with $^{13}\text{CO}_2$. Coupling patterns are indicated. The asterisks indicate signals from impurities.

In conclusion, the labelling patterns of the isoprenyl moieties were found to be similar indicating that the isoprenoid units used in the biosynthesis of hyperforin are predominantly of non-mevalonate origin in both settings. However, due to the large number of hypothetical isotopologues in $^{13}\text{CO}_2$ experiments, a concise isotopologue deconvolution is not possible and experimental factors need to be optimized in order to photosynthetically generate a high level of coherent multilabelling in precursor pools during the pulse period with $^{13}\text{CO}_2$. In case of biosynthesis of hyperforin using $[\text{U-}^{13}\text{C}_6]$ glucose as precursor, the labelling patterns of hyperforin can be interpreted on the basis of the known utilization of exogenous glucose by plants (Margl *et al.*, 2001; Goese *et al.*, 1999).

The result of the present study conducted with unperturbed whole plants under strictly physiological conditions is well in line with the earlier results and can serve as a basis for the critical evaluation of the $^{13}\text{CO}_2$ labeling technology as opposed to studies with more complex organic tracer compounds.

3.4. Use of $^{13}\text{CO}_2$ as metabolic tracer. Biosynthesis of salvinorin A

Salvia divinorum whose main active ingredient is the neoclerodane diterpene salvinorin A, is a hallucinogenic plant of the mint family that has been used in traditional spiritual practices for its psychoactive properties by the Mazatecs of Oaxaca, Mexico. More recently, *S. divinorum* extracts and salvinorin A have become more widely used in the USA, as legal hallucinogens (Roth *et al.*, 2002). In Germany, *S. divinorum* is an illegal plant since March 2008 (841. Sitzung des Bundesrates, 2008).

During our experimental work, results from labelling experiments with *in vitro* sterile cultures of *S. divinorum* microshoots using $[1\text{-}^{13}\text{C}]$ glucose, $[\text{Me-}^{13}\text{C}]$ methionine, and $[1\text{-}^{13}\text{C}; 3,4\text{-}^2\text{H}_2]$ -1-deoxy-D-xylulose as precursors were published (Kutrzeba *et al.*, 2007). NMR spectroscopic analysis suggested that salvinorin A is biosynthesized via 1-deoxy-D-xylulose 5-phosphate. In addition, analysis of salvinorin A produced by plants grown in the presence of $[\text{Me-}^{13}\text{C}]$ methionine indicated that methylation of the C-4 carboxyl group is catalyzed by a type III *S*-adenosyl-L-methionine-dependent *O*-methyltransferase (Kutrzeba *et al.*, 2007).

In this thesis, different experimental settings were used. More specifically, cut stems of *S. divinorum* were immersed for 14 days into a solution of $[\text{U-}^{13}\text{C}_6]$ glucose as described under **Methods 2.3.18.1**. Those labelling experiments were conducive to ^{13}C enrichment of the acetyl moiety of salvinorin A (Fig. 35). More specifically, the ^{13}C

NMR spectrum of salvinorin A showed satellite signals for C-21 and C-22 due to $^{13}\text{C}^{13}\text{C}$ coupling, whereas the signals of the diterpene moiety including carbon atom C-11 showed only central lines (Fig. 35). The signal intensities of the satellite signals for [21,22- $^{13}\text{C}_2$]-salvinorin A was calculated (Table 9) and gave approximately 20% in the overall signal intensity of C-21 or C-22, respectively. This means that approximately 0.2 mol% [21,22- $^{13}\text{C}_2$]salvinorin A was present. The data implied that salvinorin A can be obtained from unlabeled salvinorin B by acetylation involving a $^{13}\text{C}_2$ -labelled acetyl donor. However, the approach was not successful for delineation of the core moiety in the diterpene. Obviously, the early steps and/or cyclisation reactions were not active in the cut plant system. For this reason, we used the $^{13}\text{CO}_2$ approach which is based on the labelling of a whole plant under “undisturbed” conditions, where plant metabolism should be fully active.

In this experiment, *S. divinorum* plants were exposed to a synthetic atmosphere containing 600 ppm $^{13}\text{CO}_2$ for 4 hours as described under **Methods 2.3.18.2**. The isotopologue composition of salvinorin A was analysed by ^{13}C NMR spectroscopy. As shown in Figure 36 certain signals of salvinorin A appeared as multiplets comprising 3 to 5 lines due to $^{13}\text{C}^{13}\text{C}$ coupling. The presence of multiply ^{13}C -labelled isotopologues in considerable excess over their natural occurrence showed that the ^{13}C labelling pulse had afforded multiply ^{13}C -labelled compounds. This signifies the presence of isotopologues comprising groups of ^{13}C atoms which were biosynthesized from multiply labelled metabolic intermediates. All NMR lines (central signals and coupling satellites) were integrated separately.

The interpretation of the satellite signatures in Figure 37 depends crucially on unequivocal signal assignments for all 20 carbon atoms of the salvinorin A skeleton. Giner and co-workers (Giner *et al.*, 2007) have assigned the ^1H and ^{13}C NMR spectra of salvinorin A (Fig. 34) in three different NMR solvents using HSQC, HMBC and COSY. They confirmed the spectral data published early by Ortega (Ortega *et al.*, 1982). The detailed analysis of the coupling constants detected in the ^{13}C -enriched sample was in line with these ^{13}C NMR assignments (Table 10).

On basis of the ^{13}C assignments, the coupling patterns summarized in Table 10 indicate the presence of 6 pairs of directly adjacent ^{13}C atoms. For example, the satellite signatures of C-14 and C-15 are more complex but can be easily explained by the superposition of the signatures of molecular species carrying 2 and 3 ^{13}C atoms, respectively. More specifically, both signal groups feature a doublet component

Results and discussion

indicating the presence of the [14,15- $^{13}\text{C}_2$]-isotopologue at significant abundance. A second signal component can be easily interpreted as a triplet arising by coupling of C-14 and C-15 to each other with a coupling constant of 70.3 Hz and by coupling to a third ^{13}C atom with a smaller coupling constant of 3.0 or 3.7 Hz, respectively, which indicates coupling via 2 to 3 bonds. The ^{13}C that can couple to C-14 and C-15, respectively, via long-range coupling must be located only in position 12.

The presence of triple labelled isotopologues demonstrated that a significant fraction of salvinorin A, is biosynthesized *via* IPP and DMAPP precursors the non-mevalonate pathway (Fig. 6) because a bloc of three labelled carbon atoms (Fig. 37A) can be transferred only by the deoxyxylulose pathway (i.e. *via* [$^{13}\text{C}_3$]glyceraldehyde 3-phosphate). On the other hand, the mevalonate pathway can at best transfer blocks of two labelled atoms (i.e. *via* [$^{13}\text{C}_2$]acetyl-CoA. A cyclisation mechanism is proposed on basis of the isoprenoide dissection (Fig. 37).

Table 9. NMR data of the acetyl moiety of salvinorin A from the experiment with [$^{13}\text{C}_6$]glucose

Position	^{13}C abundance % $^{13}\text{C}^{13}\text{C}$
21	19 (22)
22	21 (21)

The clerodane class of diterpenes is biosynthesized from geranylgeranyl diphosphate (GGPP) (**21**) through enzymatic cyclization initiated by electrophilic protonation, followed by a series of methyl and hydride shifts (Akhila *et al.*, 1991; Merritt and Ley, 1992; Eguchi *et al.*, 2003) (Fig. 37A). As depicted in Figure 37A, the cyclization of GGPP (**21**) followed by a series of methyl and hydride shifts to form an intermediary C-4 cation (**23**). The methyl groups C-19 or C-20 are shifted to ring in an allylic diphosphate intermediate (**24**). Conversion of C-21 gives the final diterpene, salvinorin A, in a complex sequence of hitherto unknown steps involving the introduction of O-atoms and the acyl moiety.

The labelling data of the $^{13}\text{CO}_2$ experiment were in line with the suggested cyclase mechanism with C-19 methyl shift (originally the *cis*-configured methyl group in C-21).

Results and discussion

As shown in Figure 37, it can be proposed that cyclization of salvinorin A in α -methyl at C-10 and a β -H at C-5 is generated. A C-19 methyl shift to C-5 produces *trans*-clerodane skeleton.

Table 10. NMR data of salvinorin A from the experiment with $^{13}\text{CO}_2$

Position	Chemical shift		Coupling constant J_{CC} , Hz	^{13}C
	^{13}C δ , ppm	^1H δ , ppm		abundance % $^{13}\text{C}^{13}\text{C}$
1	202.0		42.0(6)	20 (6)
2	75.0	5.16(~ddt)	36.5(3)	24 (3)
3	30.7	2.34-2.3(m)	36.0(2) 2.9(18)	23 (2)
4	53.5	2.8(dd)	35.7(19)	10 (19)
5	42.0		36.0(6)	18 (6)
6,6'(α)	38.1	1.82(dt)	34.7(5) 3.1(1)	23 (5)
7(β)	18.1	2.17-2.14(m)	33.4(11) 3.3(9)	20 (11)
8	51.3	2.08(dd)	52.6(17)	16 (17)
9	35.4		32.3(11) 3.0(7)	18 (11)
10	64.0	2.19(br s)	n.d.	n.d.
11(α)	43.3	2.52(dd)	33.4(9) 3.0(7)	18 (9)
12	72.0	5.54(dd)	n.d.	n.d.
13	125.2		72.6(16)	30 (16)
14	108.3	6.39(dd)	70.3(15) 3.0(12)	22 (15)
15	143.7	7.37(t)	70.3(14) 3.7(12)	28 (14)
16	139.4	7.42(dt)	73.8(13)	22 (13)
17	171.1		51.1(8)	22 (8)
18	171.5		3.5(3)	12 (3)
19	16.4	1.13(s)	35.1(4)	16 (4)
20	15.2	1.47(s)	35.1(10)	10 (10)
21	169.9		59.7(22)	31 (22)
22	20.5	2.18(s)	59.9(21)	31 (21)
23	51.9	3.74(s)		

Results and discussion

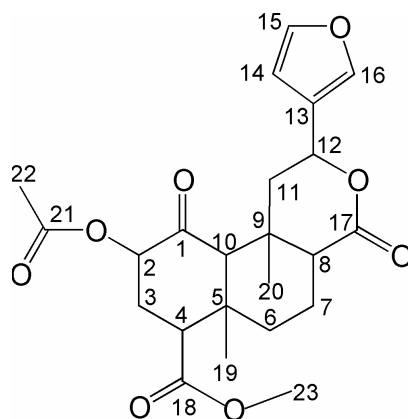


Figure 34. Structure of salvinorin A.

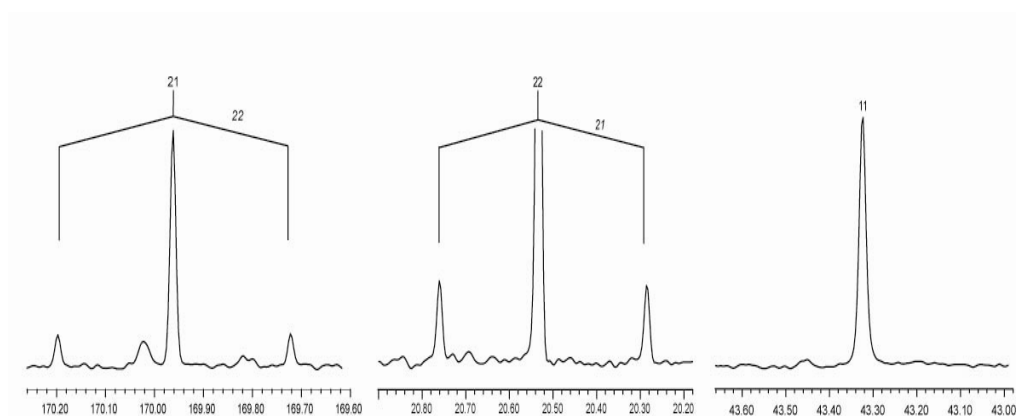


Figure 35. ^{13}C NMR signals of salvinorin A from the experiment with $[\text{U-}^{13}\text{C}_6]\text{glucose}$.

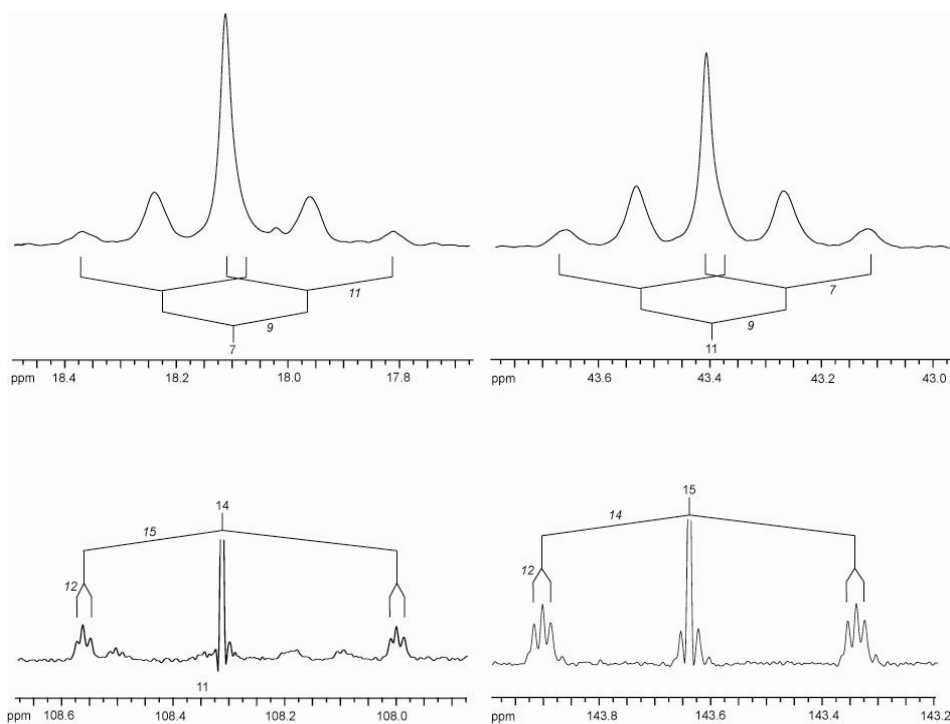


Figure 36. ^{13}C NMR signals of salvinorin A from the experiment with $^{13}\text{CO}_2$.

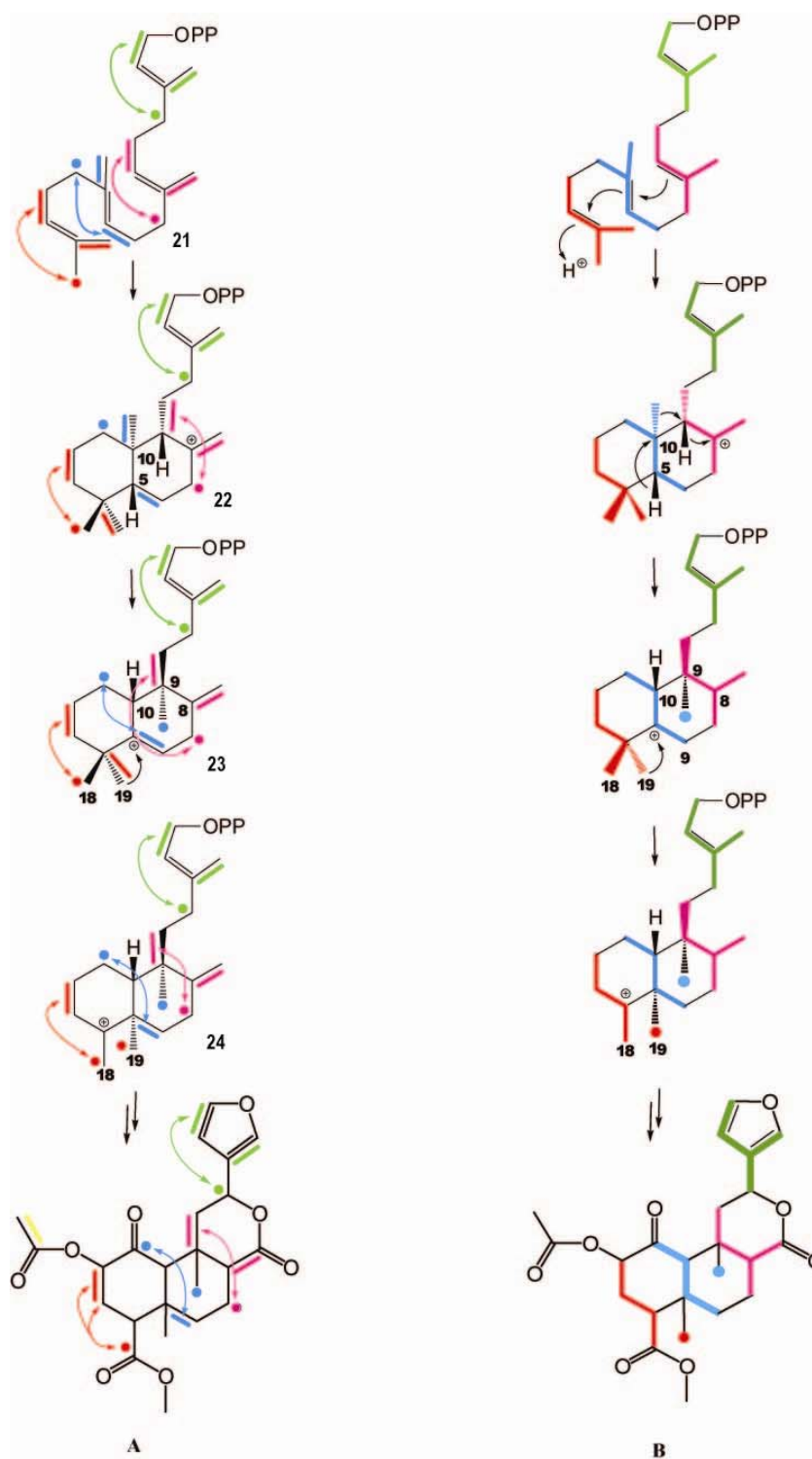


Figure 37. Mechanism of biosynthesis of salvinorin A and isotopologue composition of salvinorin A and its precursors (**A**); isoprenoide moieties of salvinorin A and its precursors (**B**). Multiple ^{13}C -labelled isotopologues are indicated by bars, single-labelled isotopologues by filled dots. Arrows connect three ^{13}C atoms (indicated by filled dots).

3.5. Isotopolog perturbation-relaxation experiments with growing *Nicotiana tabacum*

In our experiments, sterile plants of *Nicotiana tabacum* wild-type and *N. tabacum* mutants lacking plastidic RNA polymerase (*rpoA* mutants) were grown on agar containing a mixture of [U-¹³C₆]glucose and unlabelled sucrose as described under **Methods 2.3.12**. Nicotine was isolated and analyzed by ¹³C NMR spectroscopy as described under **Methods 2.3.13 – 2.3.17**.

The isotopologue profiles of nicotine were also determined by ¹³C NMR spectroscopy (Fig. 38). The signals were characterized by coupling satellites reflecting the presence of multiply ¹³C-labelled isotopologues. Analysis of the coupling patterns revealed the isotopologue composition shown in Figure 39. The isotopologue profile confirms the formation of the pyridine ring of the alkaloid from aspartate (**3**) and glyceraldehyde 3-phosphate (**12**) *via* nicotinic acid (**1**) and formation of the pyrrolidine ring from putrescine (**20**) (Fig. 40). Interestingly, the isotopologue patterns of the glyceraldehyde phosphate building blocks were different in nicotine from both plant materials. Specifically, no [3,4-¹³C₂]-isotopologue of nicotine (reflecting [2,3-¹³C]glyceraldehyde 3-phosphate) was detected in the *rpoA* mutant plants. This indicates that the transketolase reaction of the pentose phosphate pathway (conducive to the formation of [2,3-¹³C₂]glyceraldehyde 3-phosphate from [U-¹³C₆]glucose) does not contribute to glucose cycling in the root system of the wild-type plant. Therefore, it appears that an active photosynthetic system modulates the carbohydrate fluxes in the metabolic network of the roots.

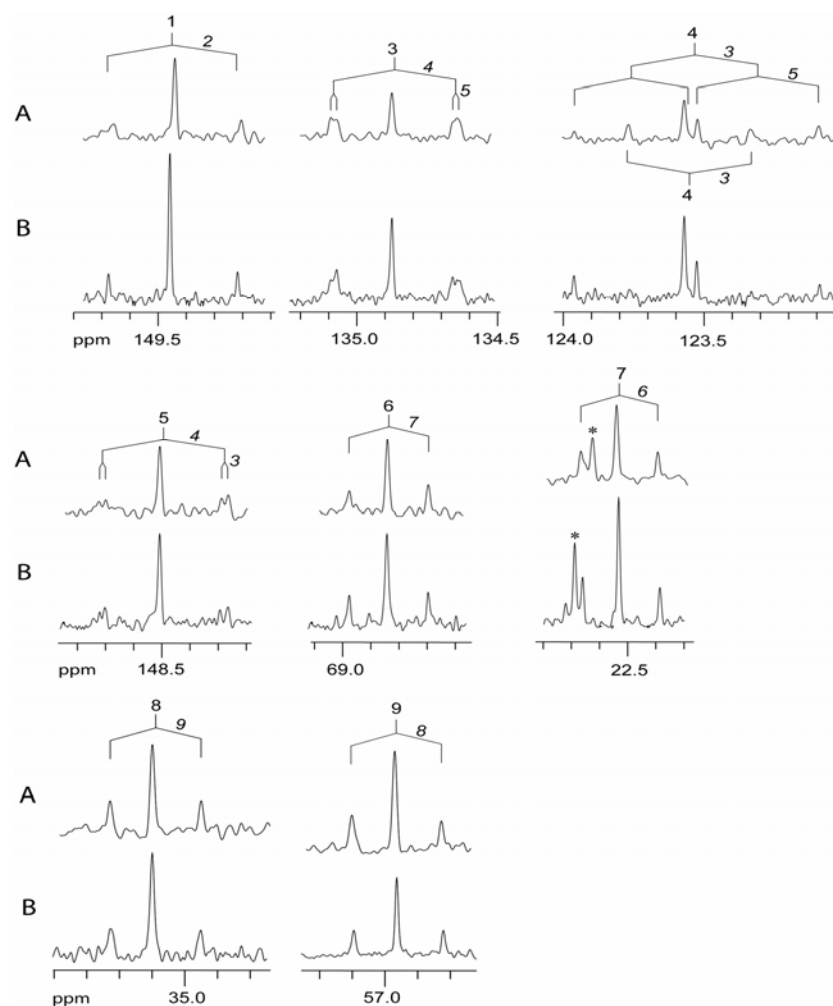


Figure 38. ^{13}C -NMR signals of nicotine from the *rpoA* mutant (A) and wild-type (B); *- indicate signals from impurities.

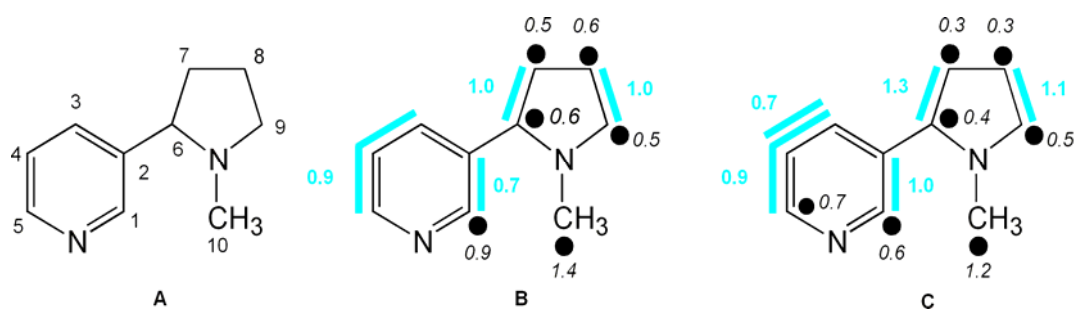


Figure 39. A, structure of nicotine; B, ^{13}C isotopologue composition of nicotine from *N. tabacum* wild-type; C, ^{13}C isotopologue composition of nicotine from the *rpoA* mutant of *N. tabacum*. Multiple ^{13}C -labelled isotopologues are indicated by bars. ^{13}C -Enrichments of single ^{13}C -labelled isotopologues are indicated by filled dot. Numbers indicate the corresponding ^{13}C -enrichments values in mol%.

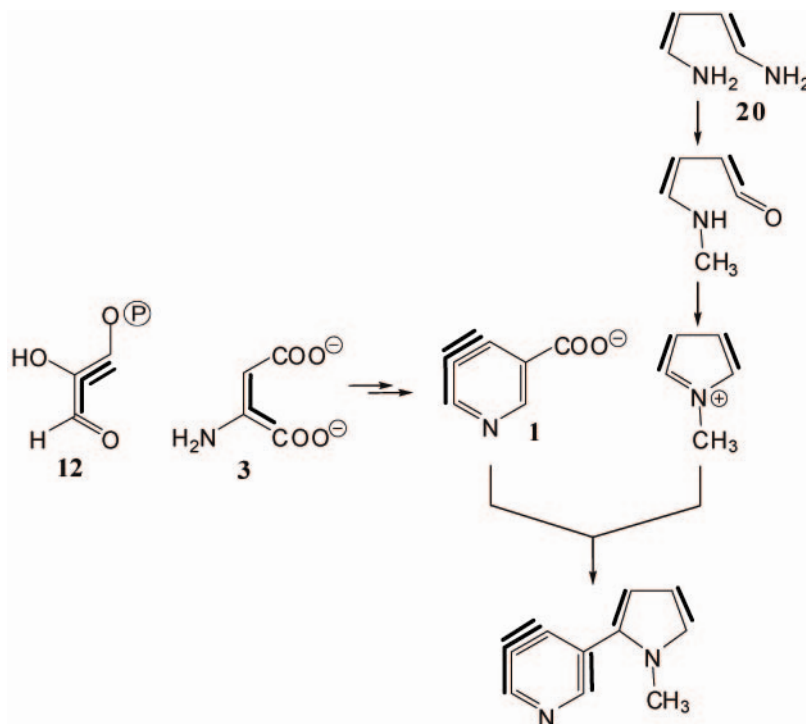


Figure 40. Isotopologue profiling of nicotine from the *rpoA* mutant in the experiment with [U-¹³C₆]glucose. For other details, see Figure 39 and text.

The example shows that perturbation-relaxation analysis of isotopologue abundance using ¹³C-labelled glucose is well qualified to determine the impact of mutations on metabolite flux in central intermediary metabolism of plants. Generally, the comparison of isotopologue relaxation in central metabolites with the relaxation behaviour of secondary metabolites constitutes a multi-dimensional analytical tool for the assessment of the metabolome in compartmented plant systems.

3.5. Biosynthesis of the chromogen hermidin from *Mercurialis annua*

3.5.1. Experiments with [U-¹³C₆]glucose

In these experiments, cut seedlings of *M. annua* were supplied with solutions containing 5 mM [U-¹³C₆]glucose and 50 mM unlabelled glucose as described under **Methods 2.3.11.2**. The survival of the plant material was improved considerably by the addition of ascorbic acid to the glucose solution; the vitamin is believed to act as an antioxidant that reduces damage to the cut plant material.

Hermidin was isolated from the labelled plant material as described under **Methods 2.3.11.6**. The compound turned out to be highly unstable, and it was essential to run ^{13}C NMR experiments immediately after isolation.

Since only ^1H NMR assignments for hermidin were available from the literature (Swan, 1984), the ^{13}C signals were assigned by HMQC and HMBC experiments. Moreover, multiply ^{13}C labelled samples from the labelling experiments afforded $^{13}\text{C}^{13}\text{C}$ coupling constants that confirmed the assignments and were required for the subsequent biosynthetic studies. Data are summarized in Table 11 and Figure 7.

^{13}C Signals of the hermidin sample from the experiment with $[\text{U-}^{13}\text{C}_6]\text{glucose}$ are shown in Figure 41A. The signal of C-5 comprises a central line and 4 satellite lines of considerable intensity that arise by $^{13}\text{C}^{13}\text{C}$ coupling in multiply labelled molecular species. The other ^{13}C signals appear with relatively low intensity that is due to slow relaxation in the absence of directly bound protons. Even so, satellites resulting from $^{13}\text{C}^{13}\text{C}$ coupling can be identified for C-4 and C-6 (Table 12).

The labelling pattern shows unequivocally that up to three ^{13}C atoms can be incorporated *en bloc* into carbon atoms 4 - 6 of the pyridinone ring. A more detailed analysis shows the presence of a triple-labelled as well as two different double-labelled isotopologues in the hermidin sample. The data are summarized in Figure 42A where abundances of individual isotopologues are indicated by the width of the bars connecting jointly transferred clusters of ^{13}C atoms. Isotopologue abundances are indicated numerically in mol%.

Biomass remaining after hermidin isolation was hydrolyzed with 6 M hydrochloric acid, and alanine and aspartate from the hydrolysate were chemically converted into the tert-butyl-di-methylsilyl derivatives, respectively, that were then analysed by mass spectrometry.

On the basis of the known fragmentation pattern of the derivative (Dauner and Sauer, 2000), isotopologue abundances can be determined for ions comprising all carbon atoms of the original amino acid (corresponding to a fragment with $m/z = 260$ from TBDMS-alanine; cf. Table 13), and for ions comprising the carbon atoms of the original amino acids without the carboxylic acid atom ($m/z = 158$ or 232 from TBDMS-alanine). After correcting the detected intensities of the mass peaks using the method described by Lee *et al.* (1991), molar abundances for carbon isotopologues of the amino acid moiety can be calculated (Table 13). The isotopologue pattern is derived from the

Results and discussion

abundances of isotopologue groups (XY-groups) as described elsewhere (Römisch-Margl *et al.*, 2007).

Table 11. ^1H and ^{13}C NMR data of hermidin

Position	Chemical shifts, ppm		J_{CC} Coupling constants ^a , Hz	Correlation	
	^1H	^{13}C	$^{13}\text{C}^{13}\text{C}$	HMQC	HMBC
1'	3.2	26.9	-	1'	2, 6
2		165.9	73.0 (3)		OH (3)
3		122.7	73.4 (2)		OH (3), 5
4		140.1	49.1 (5)	4	3, 4'
5	3.5	35.8	50.0 (4), 50.0 (6)	5	3, 4, 6
6		167.5	50.9 (5)		1', 5
4'	4.1	58.8	-		4
OH (3)	5.6	-	-	-	-

^a observed with ^{13}C -enriched samples. The coupling partner of the index carbon atom is given in parentheses.

The data summarized in Table 14 showed the presence of the universally labelled $[\text{U-}^{13}\text{C}_3]$ alanine and a double-labelled $[\text{2,3-}^{13}\text{C}_2]$ alanine (cf. also Fig. 42A). On the other hand, protein-derived aspartate analysed by the same method showed no significant ^{13}C labelling.

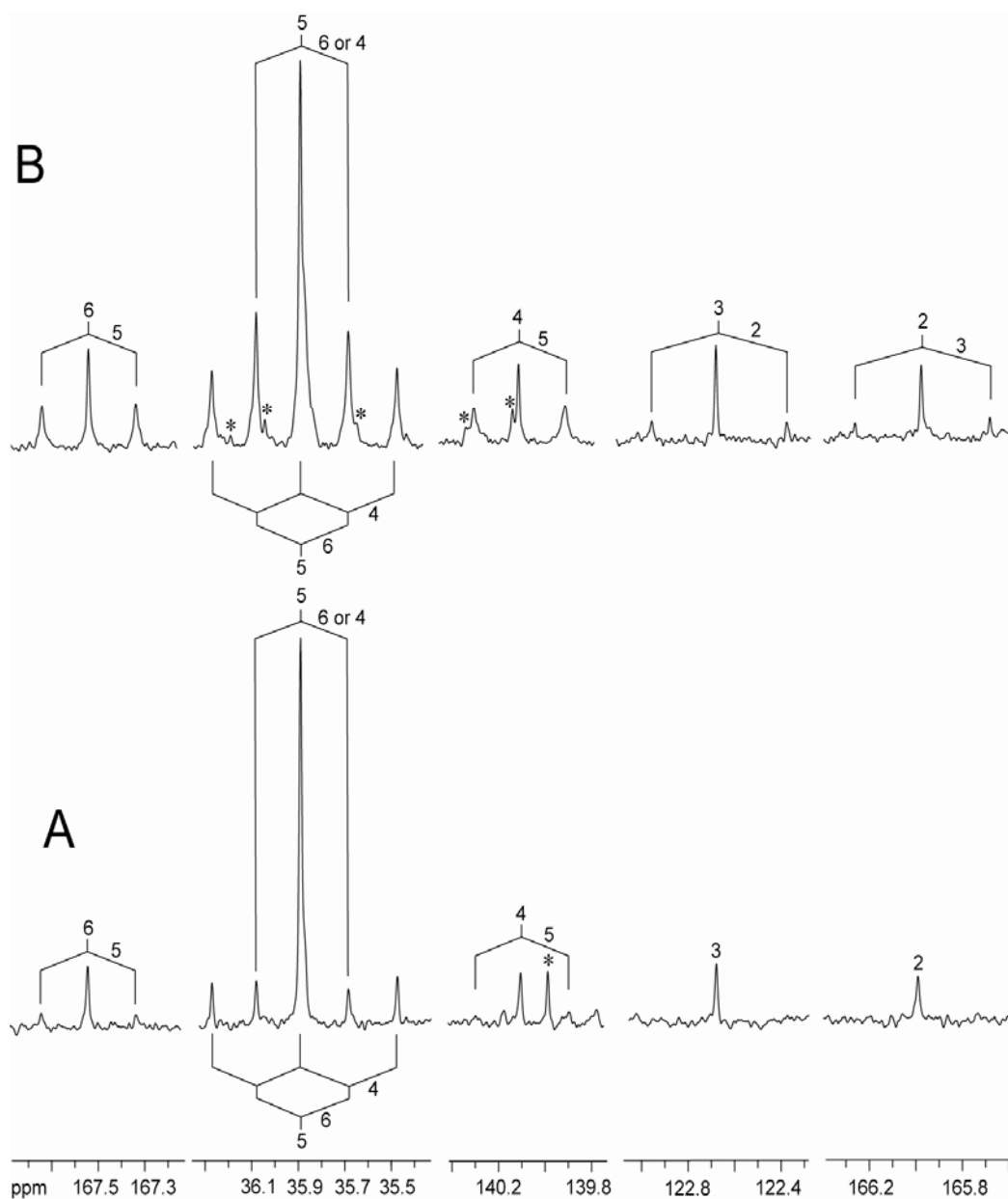


Figure 41. ^{13}C NMR signals of hermidin from the experiments with $[\text{U-}^{13}\text{C}_6]\text{glucose}$ (A) and $^{13}\text{CO}_2$ (B). Coupling patterns are indicated. The asterisks indicate signals from impurities.

Results and discussion

Table 12. Labelling data of hermidin from the experiment with [U-¹³C₆]glucose monitored by NMR spectroscopy.

Position	% ¹³ C ¹³ C ^a	% ¹³ C	Abundance of multiple labelled isotopologues, mol%
1'		< 1.3	
2	-	< 1.3	-
3	-	< 1.3	-
4	32.4 (5)	n.d.	1.0 [4,5,6- ¹³ C ₃] + [4,5- ¹³ C ₂]
5	25.5 (4 and 6)	2.9	0.7 [4,5,6- ¹³ C ₃]
	14.0 (4 or 6)		0.4 [4,5- ¹³ C ₂] + [5,6- ¹³ C ₂]
6	34.2 (5)	2.3	0.8 [4,5,6- ¹³ C ₃] + [5,6- ¹³ C ₂]
4'		1.9	

^a Fraction of ¹³C coupled satellite signals in the overall signal integral of a given carbon atom. ¹³C Atoms that give rise to the coupling signature are indicated in parentheses.

Table 13. GC/MS analysis of TBDMS-alanine. The derivative was made from alanine obtained from protein hydrolysates of seedlings of *Mercurialis annua* labelled with [U-¹³C₆]glucose.

Fragment ^a m/z	Isotopologue / X-group ^b	mol[%]	SD[%]
232	{X00}	98.40	0.42
232 + 1	{XYY} ¹	0.56	0.26
232 + 2	{X11}	1.04	0.25
158	{X00}	97.96	0.41
158 + 1	{XYY} ¹	0.56	0.51
158 + 2	{X11}	1.48	0.10
260	{000}	90.92	4.69
260 + 1	{YYY} ¹	7.69	4.73
260 + 2	{YYY} ²	0.76	0.23
260 + 3	{111}	0.63	0.25

^a Fragment 232: loss of the tert-butyl group from the TBDMS derivate and the CO unit from the amino acid (M-85)⁺; fragment 260: loss of the tert-butyl group from the TBDMS derivative (M-57)⁺; fragment 158: loss of C(O)-TBDMS ion (M – 159)⁺.

^b The XY-group notation of isotopologues is adapted from Römisch-Margl et al. (2007).

Results and discussion

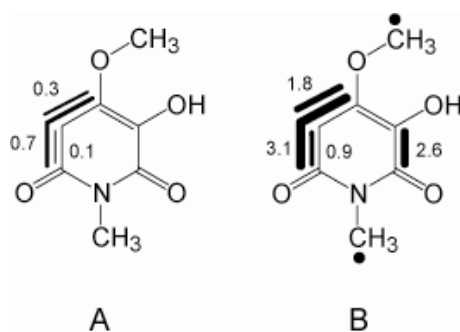


Figure 42. **A**, ^{13}C Isotopologue composition of hermidin from *M. annua* in the experiment with $[\text{U-}^{13}\text{C}_6]\text{glucose}$; **B**, ^{13}C isotopologue composition of hermidin from *M. annua* in the experiment with $^{13}\text{CO}_2$. Multiple ^{13}C -labelled isotopologues are indicated by bars, single labelled isotopologues by filled dots. The numbers indicate ^{13}C -enrichments values in mol%.

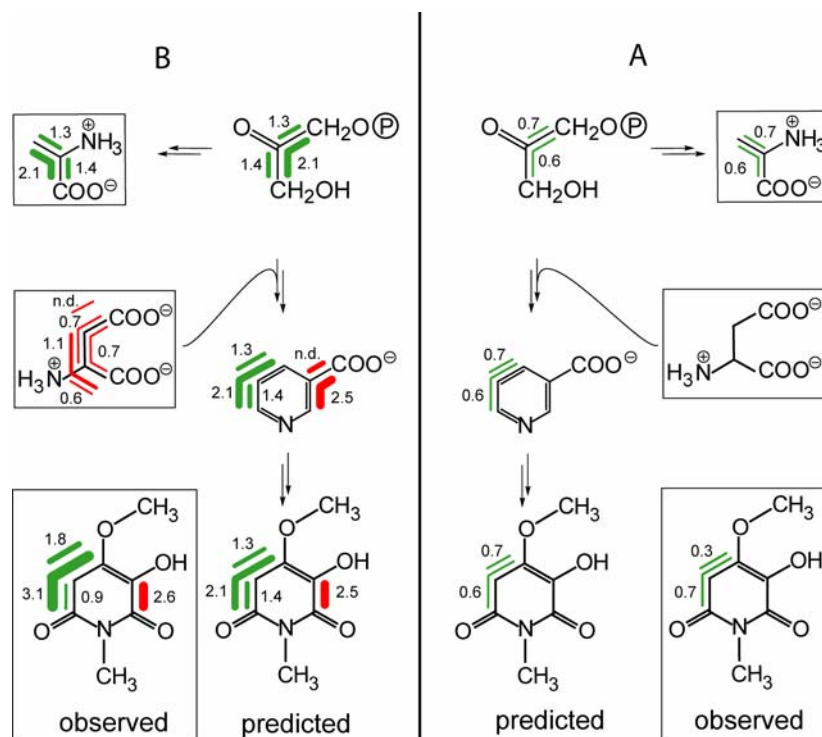


Figure 43. Comparison of the labelling patterns in hermidin labelled with $[\text{U-}^{13}\text{C}_6]\text{glucose}$ (**A**) and $^{13}\text{CO}_2$ (**B**) as precursors observed by quantitative NMR spectroscopy with predicted patterns *via* the aspartate route. The prediction is based on

the observed profiles in alanine and aspartate (shown in boxes). For details see Results and legend to Figure 42.

3.5.2. Experiments with $^{13}\text{CO}_2$

In our experiments, we exposed *M. annua* plants to a synthetic atmosphere containing 600 ppm $^{13}\text{CO}_2$ as described under **Methods 2.3.11.3**.

Carbon NMR signals of hermidin from the $^{13}\text{CO}_2$ experiment are shown in Figure 41B. The relative intensity of the satellite signals indicative of multiply labelled hermidin isotopologues are generally larger in the $^{13}\text{CO}_2$ experiment as compared to the experiment with $[\text{U-}^{13}\text{C}_6]\text{glucose}$ (cf. also Table 14). The satellite patterns of carbon atoms 4 – 6 are similar in the two experiments. Carbon atoms 2 and 3 appear as pseudotriplets with satellites signalling the joint transfer of two ^{13}C atoms to these adjacent positions, in contrast to the experiment with the $[\text{U-}^{13}\text{C}_6]\text{glucose}$ experiment where these carbon signals were devoid of apparent satellites. The isotopologue patterns in the $^{13}\text{CO}_2$ experiment are summarized in Figure 42B.

Table 14. Labelling data of hermidin from the $^{13}\text{CO}_2$ experiment monitored by NMR spectroscopy.

Position	Abundance of multiple labelled isotopologues, mol%		
	% $^{13}\text{C}^{13}\text{C}^a$	% ^{13}C	
1'		5.4	
2	35.0 (3)	7.4	2.6 [2,3- $^{13}\text{C}_2$]
3	38.3 (2)	7.0	2.7 [2,3- $^{13}\text{C}_2$]
4	60.6 (5)	8.0	4.9 [4,5,6- $^{13}\text{C}_3$] + [4,5- $^{13}\text{C}_2$]
5	39.2 (4 and 6)	7.9	3.1 [4,5,6- $^{13}\text{C}_3$]
	32.5 (4 or 6)		2.6 [4,5- $^{13}\text{C}_2$] + [5,6- $^{13}\text{C}_2$]
6	54.1 (5)	7.7	4.2 [4,5,6- $^{13}\text{C}_3$] + [5,6- $^{13}\text{C}_2$]
4'		6.6	

^a Fraction of ^{13}C coupled satellite signals in the overall signal integral of a given carbon atom. ^{13}C Atoms that give rise to the coupling signature are indicated in parentheses.

Results and discussion

Table 15. GC/MS analysis of TBDMS-alanine. The derivative was made from alanine obtained from protein hydrolysates of leaves of *Mercurialis annua*. The leaves were cut from plants grown in the presence of $^{13}\text{CO}_2$. For more details, see also footnotes of Table 15.

Fragment <i>m/z</i>	Isotopologue / X-group	<i>mol</i> [%]	<i>SD</i> [%]
232	{X00}	92.59	0.22
232 + 1	{XYY} ¹	3.81	0.03
232 + 2	{X11}	3.60	0.18
158	{X00}	92.86	0.21
158 + 1	{XYY} ¹	3.70	0.25
158 + 2	{X11}	3.44	0.22
260	{000}	85.74	1.55
260 + 1	{YYY} ¹	9.39	1.58
260 + 2	{YYY} ²	2.73	0.06
260 + 3	{111}	2.14	0.11

Table 16. GC/MS analysis of TBDMS-aspartate obtained from protein hydrolysates of leaves of *Mercurialis annua*. The leaves were cut from plants grown in the presence of $^{13}\text{CO}_2$.

Fragment ^a <i>m/z</i>	Isotopologue / X-group	<i>mol</i> [%]	<i>SD</i> [%]
302	{00XX}	93.90	0.17
302 + 1	{YYXX} ¹	3.76	0.10
302 + 2	{11XX}	2.34	0.11
316	{X000}	91.08	0.33
316 + 1	{XYYY} ¹	5.02	0.17
316 + 2	{XYYY} ²	2.79	0.15
316 + 3	{X111}	1.11	0.05
390	{X000}	91.52	0.39
390 + 1	{XYYY} ¹	5.60	0.15
390 + 2	{XYYY} ²	1.49	0.74
390 + 3	{X111}	1.39	0.39
418	{0000}	89.51	0.25
418 + 1	{YYYY} ¹	4.85	0.22
418 + 2	{YYYY} ²	3.10	0.28
418 + 3	{YYYY} ³	1.84	0.20
418 + 4	{1111}	0.71	0.09

^a Fragment 390: loss of the tert-butyl group from the TBDMS derivate and the CO unit from the amino acid (M-85)⁺; fragment 418: loss of the tert-butyl group from the TBDMS derivative (M-57)⁺; fragment 316: loss of C(O)-TBDMS ion (M - 159)⁺; fragment 302: double silylated C₁-C₂ fragment (302)⁺.

Results and discussion

The isotopologue pattern derived from the mass spectral data of biosynthetic alanine from the $^{13}\text{CO}_2$ experiment is summarized in Table 15 and Figure 43B and appears similar to that observed in the labelling experiment with $[\text{U-}^{13}\text{C}_6]\text{glucose}$, except that the amino acid from the $^{13}\text{CO}_2$ experiment shows a higher level of label, in line with the observed isotopologue pattern of hermidin. Several multiply ^{13}C -labelled aspartate isotopologues were detected at significant abundance (Table 16 and Fig. 43B), whereas aspartate had been found to be virtually without label in the experiment with $[\text{U-}^{13}\text{C}_6]\text{glucose}$. It may reflect the breakdown of aspartate biosynthesis under the experimental conditions with cut seedlings.

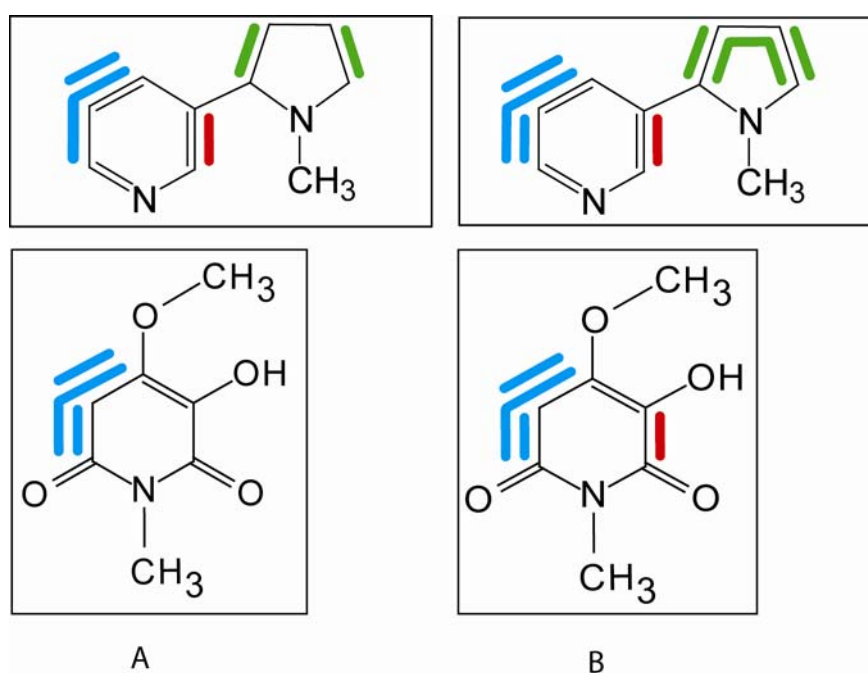


Figure 44. Comparison of labelling patterns in hermidin and nicotine from the $[\text{U-}^{13}\text{C}_6]\text{glucose}$ experiment (A) and the $^{13}\text{CO}_2$ experiment (B). The bars indicate multiple labelled isotopologues. Due to the different scaling factors the labelling patterns are shown only qualitatively. The nicotine pattern from the $^{13}\text{CO}_2$ experiment is published in Römisch-Margl *et al.*, 2007. The pattern from the $[\text{U-}^{13}\text{C}_6]\text{glucose}$ experiment is unpublished.

In order to analyze the biosynthesis of hermidin, which was previously unknown, the data from two labelling experiments using $[\text{U-}^{13}\text{C}_6]\text{glucose}$ and $^{13}\text{CO}_2$ were compared. The pattern of hermidin reminds of the biosynthesis of the pyridine ring in nicotinic acid where also a three carbon unit coming from dihydroxyacetone

phosphate and a two carbon unit coming from aspartate are found as biosynthetic units. In order to verify this hypothesis, we predicted the labelling pattern of hermidin via the nicotinic acid pathway (Figs. 44 and 45). Notably, the ^{13}C abundance is considerably lower in the experiment with ^{13}C -labelled glucose, and that is easily explained by the fact that the tissue segments undergo rapid attrition. However, both experiments unequivocally show the diversion of up to three ^{13}C atoms in tandem to carbon atoms 4 - 6 of hermidin. Significant pairwise incorporation of adjacent ^{13}C atoms into carbon atoms 2 and 3 was only observed in case of the $^{13}\text{CO}_2$ experiment, but this difference may be due to the generally low label transfer in the experiment with labelled glucose.

Nicotinic acid biosynthesis in plants, which was already known in considerable detail, (for reviews see Leete, 1992) is assumed to start from dihydroxyacetone phosphate and iminoaspartate (derived from aspartate by aspartate oxidase, NadB protein, cf. Fig. 45) which undergo a condensation affording quinolate catalysed by quinolate synthase (NadA protein) (Fig. 45) (for review, see Noctor et al., 2006). Using the experimentally determined labelling patterns of the amino acids from the experiments with $^{13}\text{CO}_2$ or $[\text{U-}^{13}\text{C}_6]\text{glucose}$ as tracers, the labelling patterns of hermidin can be simulated using the retrobiosynthetic concept (Bacher *et al.*, 1999). The retrobiosynthetic reconstruction agrees well with the experimentally observed labelling patterns of hermidin. Notably, aspartate from the $^{13}\text{CO}_2$ experiment shows multiply labelled isotopologues in significant abundance, whereas these isotopologues are below the detection limit in the experiment with $[\text{U-}^{13}\text{C}_6]\text{glucose}$. This finding corresponds very well with the presence of $[2,3\text{-}^{13}\text{C}_2]\text{hermidin}$ in the sample from $^{13}\text{CO}_2$ labelling and its absence in the sample from $[\text{U-}^{13}\text{C}_6]\text{glucose}$ labelling.

3.5.3. Experiments with $[\text{1-}^{13}\text{C}_1]\text{glucose}$

Cut seedlings of *M. annua* L. were supplied with solutions containing 55 mM $[\text{1-}^{13}\text{C}_1]\text{glucose}$ and 1 mM ascorbic acid as described under **Methods 2.3.11.4**. The pyridinone type chromogen, hermidin, was again isolated and analyzed by NMR spectroscopy as described under **Methods 2.3.11.6** and **2.3.11.7**.

The ^{13}C abundances for carbon atoms were calculated on the basis of the ^{13}C NMR signal intensities using a reference value of 1.1% for carbon atom C-5. The signals of C-2, C-3 and C-4 comprised a central line and four satellites lines with considerable intensity. The signals of C-5 and C-6 comprised only two satellites with low intensity. The labelling data are summarized in Table 17.

Results and discussion

Several multiply ^{13}C -labelled hermidin isotopologues were detected at significant abundance (Table 17 and Fig. 47). As shown in Figure 47, the ^{13}C -enrichment of carbon C-4 was higher than at carbons C-2, C-3 or C-5 (for details see Figure 46).

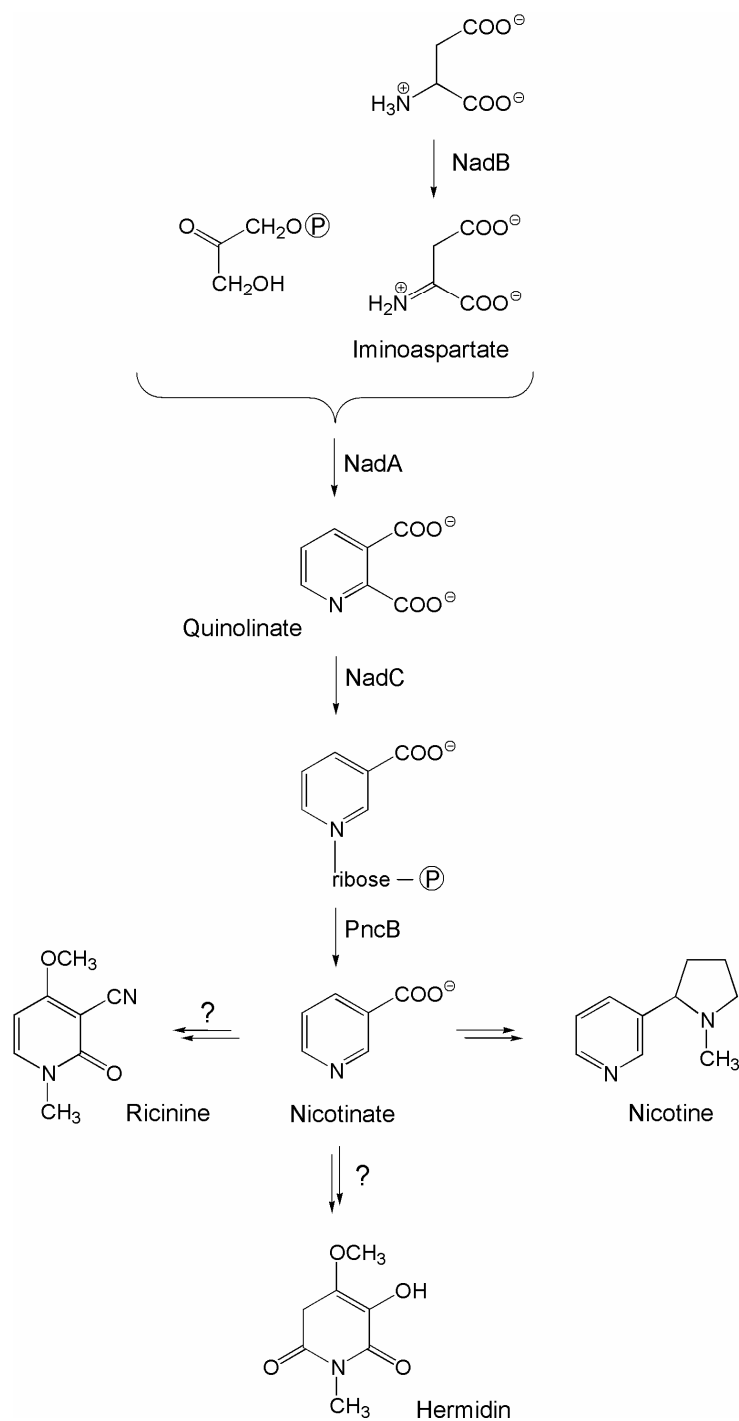


Figure 45. Hypothetical biosynthetic pathway of nicotinic acid and downstream products in plants (for review see, Noctor et al., 2006).

Results and discussion

Table 17. Labelling data of hermidin from the experiment with [1-¹³C₁]glucose

Position	% ¹³ C _{abs}	% ¹³ C ¹³ C	Abundance of multiple-labelled isotopologues, (mol%)
1'	3.8	-	-
2	4.5	11.0 (3) 23.0 (4)	2.9 [2- ¹³ C ₁] 0.5 [2,3- ¹³ C ₂] 1.0 [2,4- ¹³ C ₂]
3	4.5	9.7 (2) 25.8 (4)	3.0 [3- ¹³ C ₁] 0.4 [2,3- ¹³ C ₂] 1.2 [3,4- ¹³ C ₂]
4	4.9	13.6 (3) 13.6 (2)	3.6 [4- ¹³ C ₁] 0.7 [3,4- ¹³ C ₂] 0.7 [2,4- ¹³ C ₂]
5	1.1	8.8 (4)	1.0 [5- ¹³ C ₁] 0.1[4,5- ¹³ C ₂]
6	2.2	-	-
4'	3.8	-	-
OH (3)	-	-	-

As noted above and shown in Figure 40, (**Results and discussion 3.4**), the formation of the pyridine ring of nicotinic acid is assumed to originate from aspartate (**3**) and glyceraldehyde 3-phosphate (**12**) but alternative pathways are thinkable. On the basis of utilization of exogenous [1-¹³C]glucose *via* the glycolytic pathway, glycogenesis, and the pentose phosphate pathway, the labelling patterns of potential building blocs in hermidin biosynthesis can now be predicted. As shown in Figure 46A, the isotopologue compositions of triose phosphate, pyruvate, and acetyl-CoA are characterized by [3-¹³C]glyceraldehyde 3-phosphate, [3-¹³C]pyruvate, and [2-¹³C]acetyl-CoA. [2,3-¹³C₂]-Aspartate is explained *via* the citrate cycle and randomization of the label due to the symmetrical succinate (Fig. 46B).

The labelling pattern for hermidin can now be constructed with the labelling patterns of the early precursors *via* different potential biosynthetic pathways (Fig. 48). As shown in Figure 48, the labelling patterns of hermidin starting from ribulose 5-phosphate (Fig. 48C) or from 1-deoxy-D-xylulose 5-phosphate in a vitamin B₆ – like

Results and discussion

mechanism (Tambasco-Studart *et al.*, 2005) (Fig. 48D) or in a anabasine - like biosynthesis starting from lysine (Mathews *et al.*, 1999) (Fig. 48F) are at odds with the observed pattern in hermidin. However, the observed pattern is in well agreement with the predicted pattern predicted *via* the aspartate route of nicotinic acid biosynthesis (Fig. 48B). The result can be taken as strong evidence that the aspartate route is valid for hermidin biosynthesis.

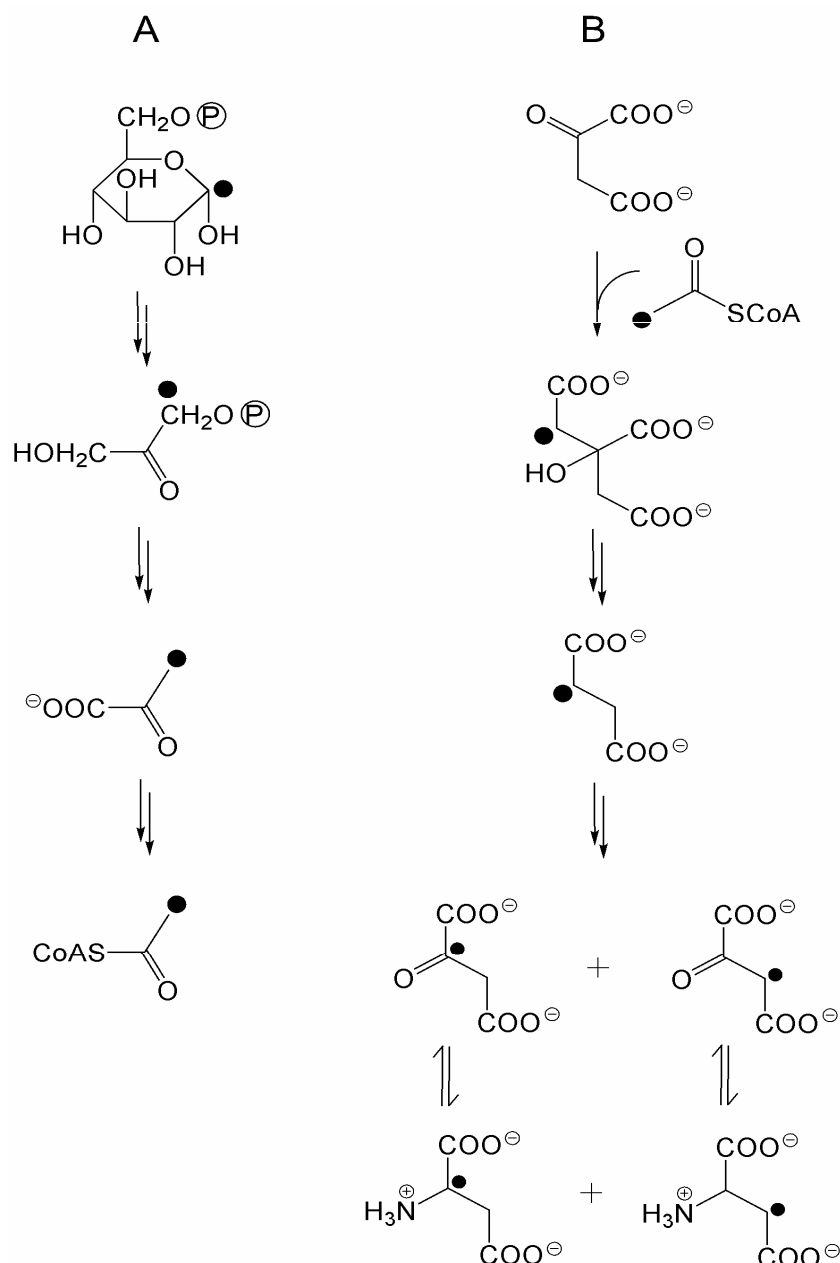


Figure 46. **A**, Biosynthesis of acetyl-CoA *via* glycolysis; **B**, biosynthesis of aspartate *via* citrate cycle. ^{13}C -label is indicated by dots.

Results and discussion

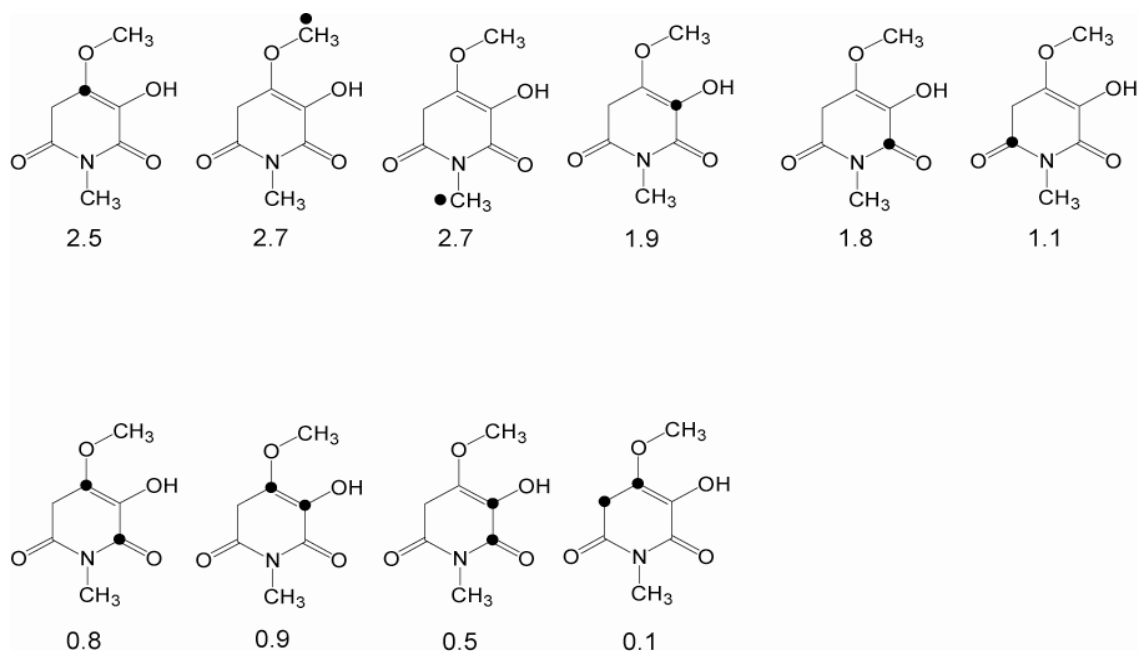


Figure 47. ^{13}C -Enriched isotopologues of hermidin observed in the experiment with $[1-^{13}\text{C}_1]$ glucose isolated from *Mercurialis annua*. ^{13}C -label is indicated by dots.

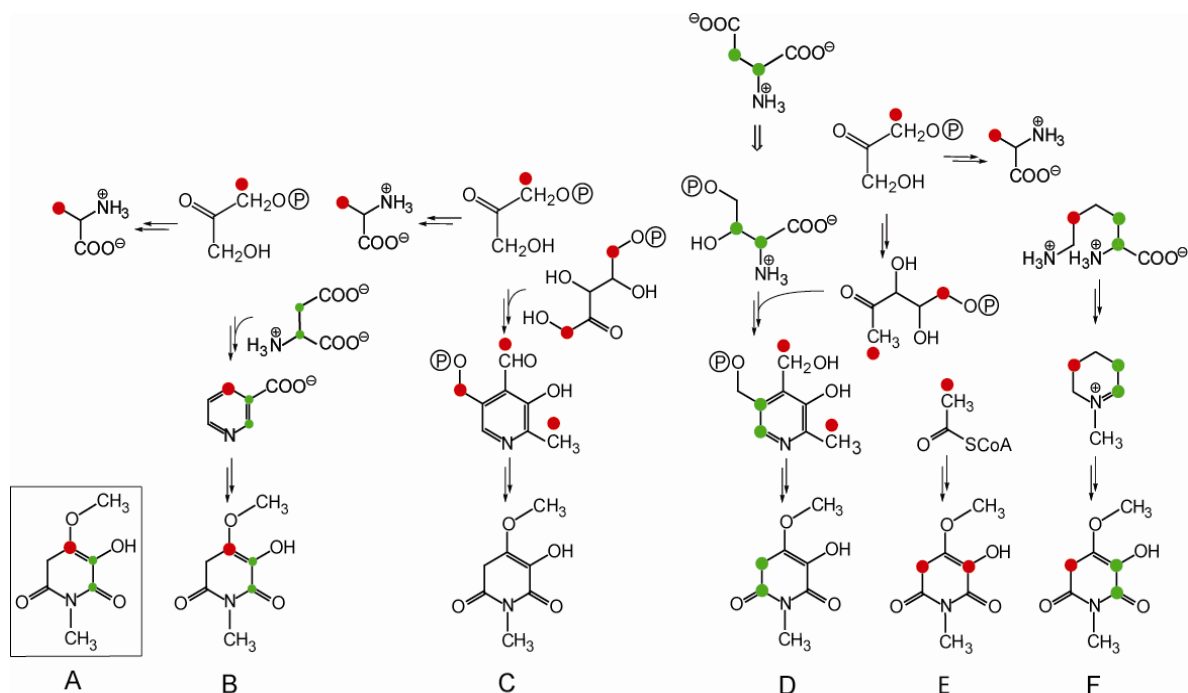


Figure 48. Comparison of the labelling patterns in hermidin from the experiment with $[1-^{13}\text{C}_1]$ glucose, (A) observed by quantitative NMR spectroscopy with (B-F) predicted patterns (B) via the aspartate route of nicotinic acid biosynthesis; (C), via a vitamin B₆ like biosynthesis starting from ribulose 5-phosphate; (D), via a vitamin B₆

Results and discussion

like biosynthesis starting from aspartate and 1-deoxy-D-xylulose 5-phosphate; **(E)**, *via* a polyketide like biosynthesis starting from acetyl-CoA; **(F)**, *via* anabasine like biosynthesis starting from lysine. ¹³C-label is indicated by dots.

3.5.4. Experiments with [¹³C₄, ¹⁵N₁]aspartate

Another support for hermidin biosynthesis *via* aspartate and nicotinic acid was elaborated in incorporation experiments with ¹³C₄, ¹⁵N₁ – labelled aspartate.

Specifically, cut seedlings of *M. annua* L. were supplied with solutions containing 5 mM [U-¹³C₄, ¹⁵N₁]aspartate as described under **Methods 2.3.11.5**. Hermidin was isolated and analyzed by NMR spectroscopy.

Carbon NMR signals of hermidin are shown in Figure 49. Satellites resulting from ¹³C¹³C or ¹³C¹⁵N coupling were detected only for C-2 and C-3 (Table 19).

This demonstrates that the biosynthesis of hermidin can be *via* biosynthetic pathway of nicotinic acid starting from aspartate.

Table 18. Labelling data of hermidin from the experiment with [U-¹³C₄, ¹⁵N₁]aspartate

Position	Chemical shifts,		J Coupling		% ¹³ C ¹³ C	rel. %
	ppm		constants ^a , Hz			
	¹ H	¹³ C	¹³ C ¹³ C	¹³ C ¹⁵ N		
1'	3.2	26.9	-	-	-	-
2		165.9	72.9 (3)	6.6	12.3	2.1
3		122.7	73.4 (2)	3.5	15.3	2.0
4		140.1	-	-	-	1.1
5	3.5	35.8	-	-	-	1.3
6		167.5	-	-	-	1.4
4'	4.1	58.8	-	-	-	1.2
OH (3)	5.6	-	-	-	-	-

As shown in Table 18 and Figure 49, the pairwise incorporation of low adjacent ¹³C atoms in the experiment with [U-¹³C₄, ¹⁵N₁]aspartate was only observed into carbon atoms 2 and 3.

Results and discussion

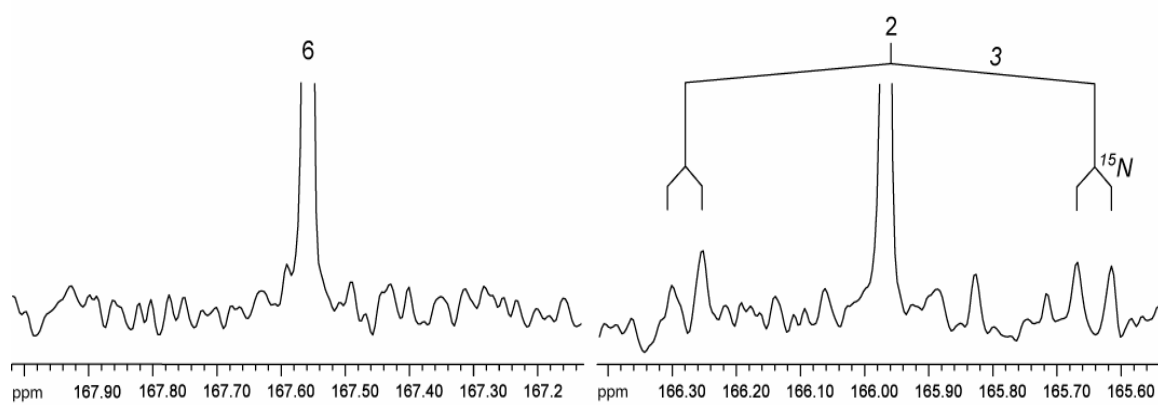


Figure 49. ^{13}C NMR signals of hermidin from the experiment with $[\text{U-}^{13}\text{C}_4, ^{15}\text{N}_1]\text{aspartate}$.

4. Summary

The term metabolomics refers to the systematic study of the unique chemical fingerprints that specific cellular processes generate. Specifically, metabolomics relate to small-molecule metabolite profiles, but can be extended to isotopologue profiles due to labelling experiments using stable-isotope enriched precursors. Indeed, tracer studies using isotopes are among the most important methods for the study of biosynthetic pathways in both primary and secondary metabolism.

Stable isotope experiments monitored by NMR spectroscopy and/or mass spectrometry have also been adapted to studies with plant systems. A major aim of these studies is to provide a rational basis for the improvement of biomass and/or specific plant products. Specifically or uniformly ^{13}C -labelled glucose and sucrose have been used, but in principle any labelled metabolite, such as amino acids, mevalonate or acetate that are absorbed by the cells or tissues at a sufficient rate is suitable.

In this thesis, we have treated plants of *Allium schoenoprasum* with cadmium salt at a concentration of 50 mM. After extraction of shoots and roots with perchloric acid, the extracts were analysed by NMR spectroscopy. The concentrations of polar compounds were assessed by ^1H NMR spectroscopy using a spectral library comprising ^1H NMR spectra of over 260 reference compounds (Chenomx NMR Suite 4,6). Several aliphatic amino acids including asparagine, aspartate, glutamine, glutamate, proline, serine, and threonine were identified as major compounds in the extracts. The concentration of asparagine was approximately 7 times higher in the shoots of Cd-treated plants than in the shoots of control plants. We suppose that asparagine serves as a complexing agent for Cd^{2+} ions in the shoots.

In a second experiment, we have treated plants of *Mercurialis annua* with 0.9% sodium chloride (salinity). After extraction with perchloric acid, the concentrations of polar compounds were again determined by ^1H NMR spectroscopy. Specifically, we have compared the concentrations of polar compounds in the leaves and the roots of salt-stressed and control plants of female or male origin. The concentrations were similar in the extracts of female and male plants. However, the concentrations of glucose and sucrose in the leaves and the roots of salt-treated plants were higher than in the respective control plants. This can be explained by an osmolytic effect. The concentration of malate was approximately 2-5 times higher in the leaves and in the

roots of control than in salt-treated plants. On the other hand, the concentrations of aspartate and oxalacetate were higher upon salinity stress.

Metabolite profiling can be complemented with isotopologue profiles obtained from labelling experiments. The concept was challenged in several model studies focussed on the elucidation of terpenoid and alkaloid biosynthesis.

Using $^{13}\text{CO}_2$ as precursor, the biosynthesis of hyperforin from *Hypericum perforatum*, a commercially important medicinal plant, was studied. The isotopologue compositions of the prenyl and polyketide moieties of hyperforin were analysed. In order to describe the complex isotopologue space of prenyl moieties, a six-digit binary number of the carbon skeleton was used. The low standard deviations indicate that all prenyl units in hyperforin originate from common precursor units. The labelling patterns showed that the isoprenoid units in prenyl moieties are predominantly of non-mevalonate origin.

The biosynthesis of the psychoactive diterpene salvinorin A in *Salvia divinorum* plants was studied using $[\text{U-}^{13}\text{C}_6]\text{glucose}$ and $^{13}\text{CO}_2$ as precursors. The isotopologue composition of salvinorin A from the $^{13}\text{CO}_2$ experiment was analysed by ^{13}C NMR spectroscopy. The presence of multiply ^{13}C -labelled isotopologues in considerable excess over their natural occurrence showed that the ^{13}C labelling pulse had afforded multiply ^{13}C -labeled compounds. The presence of triple labelled isotopologues demonstrated that IPP and DMAPP precursors of the diterpene were predominantly biosynthesized *via* the non-mevalonate pathway. The labelling patterns also showed that the methyl groups C-19 and C-20 were shifted to the neighboured carbon atoms in an allylic diphosphate intermediate (**24**, Fig. 37) of salvinorin A. The exclusive ^{13}C enrichment of the acetyl carbon atoms in salvinorin A from $[\text{U-}^{13}\text{C}_6]\text{glucose}$ indicates that unlabelled salvinorin B is converted into salvinorin A by acetylation.

In perturbation-relaxation experiments with *Nicotiana tabacum*, the plants were grown on agar containing a mixture of $[\text{U-}^{13}\text{C}_6]\text{glucose}$ and unlabelled sucrose. The isotopologue profiles of nicotine were determined by ^{13}C NMR spectroscopy. Specifically, no $[3,4\text{-}^{13}\text{C}_2]$ -isotopologue of nicotine (reflecting $[2,3\text{-}^{13}\text{C}]\text{glyceraldehyde 3-phosphate}$) was detected in the wild-type plants. This suggests that the transketolase reaction of the pentose phosphate pathway (conducive to the formation of $[2,3\text{-}$

Summary

$^{13}\text{C}_2$]glyceraldehyde 3-phosphate from [U- $^{13}\text{C}_6$]glucose) does not contribute to glucose cycling in the root system of the wild-type plant. Therefore, it appears that an active photosynthetic system modulates the carbohydrate fluxes in the metabolic network of the roots.

In labelling experiments with *M. annua* plants, we used [U- $^{13}\text{C}_6$]glucose, $^{13}\text{CO}_2$, [1- $^{13}\text{C}_1$]glucose, and [$^{13}\text{C}_4$, $^{15}\text{N}_1$]aspartate as precursors. The pyridinone type chromogen, hermidin, was isolated and analyzed by NMR spectroscopy. Since only ^1H NMR assignments for hermidin were available from the literature, the ^{13}C signals were assigned by HMQC and HMBC experiments.

The labelling pattern in the experiment with [U- $^{13}\text{C}_6$]glucose showed that up to three ^{13}C atoms can be incorporated en bloc into carbon atoms 4-6 of the pyridinone ring of hermidin. A more detailed analysis showed the presence of a triple-labelled as well as two different double-labelled isotopologues in the hermidin sample. NMR analysis of amino acids obtained by acid hydrolysis of labelled biomass demonstrated the presence of [U- $^{13}\text{C}_3$]alanine, whereas aspartate was found to be virtually unlabelled. Photosynthetic pulse labelling of *M. annua* plants with $^{13}\text{CO}_2$ followed by a chase period in normal air afforded [4,5,6- $^{13}\text{C}_3$]- and [2,3- $^{13}\text{C}_2$]hermidin with significant abundance. [U- $^{13}\text{C}_3$]Alanine and multiply ^{13}C -labelled aspartate isotopologues were also found in significant abundance.

The labelling patterns of hermidin obtained in the experiments with [U- $^{13}\text{C}_6$]glucose and $^{13}\text{CO}_2$ closely resemble those observed for the pyridine ring of nicotine under similar experimental conditions. This suggests that hermidin, like nicotine, is biosynthesized *via* the nicotinic acid pathway from dihydroxyacetone phosphate and aspartate.

In an experiment with [1- $^{13}\text{C}_1$]glucose, hermidin was again isolated and analyzed by NMR spectroscopy. The ^{13}C -enrichment of carbon C-4 was higher than at carbons C-2, C-3 or C-5. On the basis of utilization of exogenous [1- ^{13}C]glucose *via* the glycolytic pathway, glycogenesis, and the pentose phosphate pathway, the labelling patterns of potential building units in hermidin biosynthesis were predicted. The observed pattern in hermidin was in good agreement with the predicted pattern *via* the aspartate route of nicotinic acid biosynthesis. Another support for hermidin biosynthesis *via* aspartate and nicotinic acid was elaborated in incorporation experiments with $^{13}\text{C}_4$, $^{15}\text{N}_1$ – labelled aspartate. Satellites resulting from $^{13}\text{C}^{13}\text{C}$ or $^{13}\text{C}^{15}\text{N}$ coupling were

Summary

detected only for C-2 and C-3 demonstrating that aspartate can be used as a biosynthetic precursor in a pathway *via* nicotinic acid.

Although the use of general precursors (e.g. $^{13}\text{CO}_2$ and ^{13}C -glucose) afforded detailed information about metabolic pathways and fluxes, the synthesis and employment of specific precursors is still important to identify individual steps in pathways. In this context, ^{13}C -labelled 4-diphosphocytidyl-2C-methyl-D-erythritol 2-phosphate was synthesized for identifying downstream metabolites as well as mechanisms of the non-mevalonate pathway enzymes. The non-mevalonate pathway of isoprenoid biosynthesis serves as the unique source of terpenoids in numerous pathogenic eubacteria and apicoplast-type protozoa. It is therefore an attractive target for anti-infective chemotherapy. In photometric and NMR spectroscopy assays, the synthesized substrates were used to screen extracts of Mediterranean plants for inhibitors of the enzymes. In case of IspC protein, strongest inhibitory activity was found in leaf extracts of *Cercis siliquastrum*.

References

- Adam, K.P. and Zapp, J., 1998. Biosynthesis of the isoprene units of chamomile sesquiterpenes. *Phytochemistry* 48, 953-959.
- Adam, P., Arigoni, D., Bacher, A., Eisenreich, W., 2002. Biosynthesis of hyperforin in *Hypericum perforatum*. *J. Med. Chem.* 45, 4786-4793.
- Akhila, A., Rani, K., Thakur, R.S., 1991. Biosynthesis of the clerodane furano-diterpene lactone skeleton in *Tinospora cordifolia*. *Phytochemistry* 30, 2573-2576.
- Alm, E. and Arkin, A.P., 2003. Biological networks. *Curr. Opin. Struct. Biol.* 13, 193-202.
- Aranibar, N., Ott, K.-H., Roongta, V., Müller, L., 2006. Metabolomic analysis using optimized NMR and statistical methods. *Anal. Biochem.* 355, 62-70.
- Arigoni, D., Sagner, S., Latzel, C., Eisenreich, W., Bacher, A., Zenk, M.H., 1997. Terpenoid biosynthesis from 1-deoxy-D-xylulose in higher plants by intramolecular skeletal rearrangement. *Proc. Natl. Acad. Sci. USA* 94, 10600-10605.
- Arlt, K., Brandt, S., Kehr, J., 2001. Amino acids analysis in five pooled single plant cell samples using capillary electrophoresis coupled to laser-induced fluorescence detection. *Journal of Chromatography A* 926, 319-325.
- Bacher, A., Eisenreich, W., Fellermeier, M., Fischer, M., Hecht, S., Herz, S., Kis, K., Lüttgen, H., Rohdich, F., Sagner, S., Schuhr, C.A., Wungsintaweekul, J., Zenk, M.H., 2001. Isoprenoid biosynthesis. International Patent Application No. WO2000EP, 07548.
- Bacher, A., Rieder, C., Eichinger, D., Fuchs, G., Arigoni, D., Eisenreich, W., 1999. Elucidation of biosynthetic pathways and metabolic flux patterns via retrobiosynthetic NMR analysis. *FEMS Microbiol. Rev.* 22, 567-598.

References

- Bagget, B.R., Cooper, J.D., Hogan, E.T., Carper, J., Paiva, N.L., Smith, J.T., 2002. Profiling isoflavonoids found in legume root extracts using capillary electrophoresis. *Electrophoresis* 23, 1642-1651.
- Bailey, N.J., Stanley, P.D., Hadfield, S.T., Lindon, J.C., Nicholson, J.K., 2000. Mass spectrometrically detected directly coupled high performance liquid chromatography/nuclear magnetic resonance spectroscopy/mass spectrometry for the identification of xenobiotic metabolites in maize plants. *Rapid Communications in Mass Spectrometry* 14, 679-684.
- Baker, A.J.M. and Brooks, R.R., 1989. Terrestrial higher plants which hyperaccumulate metallic elements. *Biorecovery* 1, 81-126.
- Bales, J.R., Bell, J.D., Nicholson, J.K., Sadler, P.J., Timbrell, J.A., Hughes, R.D., Bennet, P.N., Williams, R., 1988. Metabolic profiling of body fluids by proton NMR: self-poisoning episodes with paracetamol (acetaminophen). *Magnetic Resonance in Medicine* 6, 300-306.
- Bales, J.R., Higham, D.P., Howe, I., Nicholson, J.K., Sadler, P.J., 1984. Use of high resolution proton nuclear magnetic resonance spectroscopy for rapid multi-component analysis of urine. *Clinical Chemistry* 30, 426-432.
- Barazani, O., Dudai, N., Khadka, U.R., Golan-Goldhirsh, A., 2004. Cadmium accumulation in *Allium schoenoprasum* L. grown in an aqueous medium. *Chemosphere* 57, 1213-1218.
- Bassham, J.A., 2003. Mapping the carbon reduction cycle: a personal retrospective. *Photosynth. Res.* 76, 35-52.
- Bax, A., Davis, D.G., 1985a. MLEV-17-based two-dimensional homonuclear magnetization transfer spectroscopy. *J. Magn. Reson.* 65, 355-360.
- Bax, A., Davis, D.G., 1985b. Practical aspects of two-dimensional transverse NOE spectroscopy. *J. Magn. Reson.* 63, 207-213.

References

- Bax, A., Griffey, R.H., Hawkins, B.L., 1983. Correlation of proton and nitrogen-15 chemical shifts by multiple quantum NMR. *J. Mag. Reson.* 55, 301-315.
- Bax, A., Summers, M.F., 1986. Proton and carbon-13 assignments from sensitivity-enhanced detection of heteronuclear multiple-bond connectivity by 2D multiple quantum NMR. *J. Am. Chem. Soc.* 108, 2093-2094.
- Beerhues, L. Hyperforin. *Phytochemistry* 67, 2201-2207.
- Bernal, C., Mendez, E., Terencio, J., Boronat, A., Imperial, S., 2005. A spectrophotometric assay for the determination of 4-diphosphocytidyl-2-C-methyl-D-erythritol kinase activity. *Anal. Biochem.* 340, 245-251.
- Bodenhausen, G., Ruben, D.J., 1980. Natural abundance nitrogen-15 NMR by enhanced heteronuclear spectroscopy. *Chem. Phys. Lett.* 69, 185-189.
- Boger, D. L., Baldino, C. M. 1993. *d,l*- and *meso*-isochrysohermidin: total synthesis and interstrand DNA cross-linking. *J. Am. Chem. Soc.* 115, 11418-11425.
- Bother-By., A.A, Stephens, R.L., Lee, J., Warren, C.D., Jeanloz, R.W., 1984. Structure determination of a tetrasaccharide: transient nuclear Overhauser effects in the rotating frame. *J. Am. Chem. Soc.* 106, 811-813.
- Braunschweiler, L., Ernst, R.R., 1983. Coherence transfer by isotopic mixing: application to proton correlation spectroscopy. *J. Magn. Reson.* 53, 521-528.
- Broers, S.T.J., 1994. Über die frühen Stufen der Biosynthese von Isoprenoiden in *Escherichia coli*. PhD Thesis, ETH Zürich, Switzerland.
- Butterweck, V., 2003. Mechanism of action of St. John's wort in depression. *CNS Drugs* 17, 539-562.
- Buttschardt, T.K., 2001. Extensive Dachbegrünung und Naturschutz. *Karlsruher Schriften Geogr. Geoökol.* 13, 1-272.

References

- Cannan, R. K., 1926. Electrode potentials of hermidin, the chromogen of *Mercurialis perennis*. *Biochem. J.* 20, 927-937.
- Cheeke, P.R. and Shull, L.R., 1985. Natural toxicants in feeds and poisonous plants. AVI Publishing Company, Inc., Westport.
- Choi, Y.H., Kim, H.K., Linthorst, H.J.M., Hollander, J.G., Lefeber, A.W.M., Erkelens, C., Nuzillard, J.-M., Verpoorte, R., 2006. NMR metabolomics to revisit the tobacco mosaic virus infection in *Nicotiana tabacum* leaves. *J. Nat. Prod.* 69, 742-748.
- Clemens, S., 2001. Molecular mechanisms of plant tolerance and homeostasis. *Planta* 212, 457-486.
- Cordovilla, M.P., Ligeró, F., Lluch, C., 1994. The effect of salinity on nitrogen fixation and assimilation in *Vicia faba*. *J. of Experimental Botany* 45, 1483-1488.
- Covello, P.S., Teoh, K.H., Polichuk, D.R., Reed, D.W., Nowak, G., 2007. Functional genomics and the biosynthesis of artemisinin. *Phytochemistry* 68, 1864-1871.
- Cunnick, W.R., Cromie, J.B., Cortell, R., Wright, B., Beach, E., Selzer, F., Miller, S., 1972. Value of biochemical profiling in a periodic health examination program: analysis of 1,000 cases. *Bulletin of New York Academy of Medicine* 18, 5-22.
- Das, P., Samantaray, S., Rout, G.R., 1997. Studies on cadmium toxicity in plants. *Environ. Poll.* 98, 29-36.
- Dauner, M., Sauer, U., 2000. GC-MS analysis of amino acids rapidly provides rich information for isotopomer balancing. *Biotechnol. Progr.* 16, 642-649.
- David, S., Estramareix, B., Fischer, J.-C., Therisod, M., 1981. 1-Deoxy-D-threo-2-pentulose: the precursor of the five-carbon chain of the thiazole of thiamine. *J. Am. Chem. Soc.* 103, 7341-7342.

References

- David, S., Estramareix, B., Fischer, J.-C., Therisod, M., 1982. The biosynthesis of thiamine. Syntheses of [1,1,1,5-²H₄]-1-deoxy-D-threo-2-pentulose and incorporation of this sugar in biosynthesis of thiazole by *Escherichia coli* cells. L. Chem. Soc. Perkin Trans. I, 2131-2137.
- Daviss, B., 2005. Growing pains for metabolomics. *The Scientist*, 1925-1928.
- Dawson, R. F., Christman, D. R., D'Adamo, A., Solt, M. L., Wolf, A. P., 1960. Biosynthesis of nicotine from isotopically labelled nicotinic acids. *J. Am. Chem. Soc.* 82, 2628-2633.
- Delgado, M.J., Garrido, J.M., Ligeró, F., Lluch, C., 1993. Nitrogen fixation and carbon metabolism by nodules and bacterioids of pea plants under odium chloride stress. *Physiologia Plantarum* 89, 824-829.
- Devaux, P.G., Horning, M.G., Horning, E.C., 1971. Benzyl-oxime derivative of steroids; a new metabolic profile procedure for human urinary steroids. *Analytical Letters* 4, 151.
- Dunn, W.B., Bailey, N.J.C., Johnson, H.E., 2005. Measuring the metabolome: current analytical technologies. *Analyst* 130, 606-625.
- Eguchi, T., Dekishima, Y., Hamano, Y., Dairi, T., Seto, H., Kakinuma, K., 2003. A new approach for the investigation of isoprenoid biosynthesis featuring pathway switching, deuterium hyperlabeling, and ¹H NMR spectroscopy. The reaction mechanism of a novel *Streptomyces* diterpene cyclase. *JOC Articles* 68, 5433-5438.
- Eichinger, D., Bacher, A., Zenk, M.H., Eisenreich, W., 1999. Analysis of metabolic pathways via quantitative prediction of isotope labelling patterns: a retrobiosynthetic ¹³C NMR study on the monoterpene loganin. *Phytochemistry* 51, 223-236.

References

- Eisenreich, W., Bacher, A., 2000. Elucidation of biosynthetic pathways by retrodictive/predictive comparison of isotopomer patterns determined by NMR spectroscopy. In: Setlow, J.K. (Ed.), Genetic Engineering, Principles and Methods 22, 121-153.
- Eisenreich, W., Bacher, A., 2007. Advances of high-resolution NMR techniques in the structural and metabolic analysis of plant biochemistry. *Phytochemistry* 68, 2799-2815.
- Eisenreich, W., Bacher, A., Arigoni, D., Rodich, F., 2004a. Biosynthesis of isoprenoids via the non-mevalonate pathway. *Cell. Mol. Life Sci.* 61, 1401-1426.
- Eisenreich, W., Ettenhuber, C., Laupitz, R., Theus, C., Bacher, A., 2004b. Isotopolog perturbation techniques for metabolic networks: Metabolic recycling of nutritional glucose in *Drosophila melanogaster*. *Proc. Natl. Acad. Sci. USA* 101, 6764-6769.
- Eisenreich, W., Menhard, B., Hylands, P.J., Zenk, M.H., Bacher, A., 1996. Studies on the biosynthesis of taxol: The taxane carbon skeleton is not of mevalonoid origin. *Proc. Natl. Acad. Sci. USA* 93, 6431-6436.
- Eisenreich, W., Rohdich, F., Bacher, A., 2001. Deoxyxylulose phosphate pathway to terpenoids. Review in *Trends in Plant Science* 6, 78-84.
- Eisenreich, W., Sagner, S., Zenk, M.H., Bacher, A., 1997. Monoterpenoid essential oils are not of mevalonoid origin. *Tetrahedron Lett.* 38, 3889-3892.
- Eisenreich, W., Schwarz, M., Cartayrade, A., Arigoni, D., Zenk, M.H., Bacher, A., 1998. The deoxyxylulose phosphate pathway of terpenoid biosynthesis in plants and microorganisms. *Chem. Biol.* 5, R221-R233.
- Eisenreich, W., Schwarzkopf, B., Bacher, A., 1991. Biosynthesis of nucleotides, flavins, and deazaflavins in *Methanobacterium thermoautotrophicum*. *J. Biol. Chem.* 266, 9622-9631.

References

- Ernst, W.H.O., Verkleij, J.A.C., Schat, H., 1992. Metal tolerance in plants. *Acta Bot. Neerl* 41, 229-248.
- Ettenhuber, C., Radykewicz, T., Kofer, W., Koop, H.U., Bacher, A., Eisenreich, W., 2005a. Metabolic flux analysis in complex isotopomer space. Recycling of glucose in tobacco plants. *Phytochemistry* 66, 323-335.
- Ettenhuber, C., Spielbauer, G., Margl, L., Hannah, L. C., Gierl, A., Bacher, A., Genschel, U., Eisenreich, W., 2005b. Changes in flux pattern of the central carbohydrate metabolism during kernel development in maize. *Phytochemistry* 66, 2632-2642.
- Facchini, P.J., 2001. Alkaloid biosynthesis in plants: biochemistry, cell biology, molecular regulation, and metabolic engineering applications. *Annu. Rev. Plant Physiol. Plant Mol. Biol.* 52, 29-66.
- Fan, T.W.-M., 1996. Metabolite profiling by one- and two-dimensional NMR analysis of complex mixtures. *Progress in Nuclear Magnetic Resonance Spectroscopy* 28, 161-219.
- Fiehn, O., 2002. Metabolomics – the link between genotypes and phenotypes. *Plant Mol Biol.* 48, 155-171.
- Fraser, P.D., Pinto, M.E., Holloway, D.E., Bramley, P.M., 2000. Application of high-performance liquid chromatography with photodiode array detection to the metabolic profiling of plant isoprenoids. *Plant Journal* 24, 551-558.
- Forrester, A.R., 1984. Autoxidation of hermidin: an ESR study. *Experientia.* 40, 688-689.
- Fougère, F., Rdulier, D., Streeter, J.G., 1991. Effects of salt stress on amino acids, organic acids, and carbohydrate composition of roots bacteroids and cytosol of alfalfa (*Medicago sativa* L.). *Planta Physiol.* 96, 1228-1236.

References

- Gates, S.C., Sweeley, C.C., 1978. Quantitative metabolic profiling based on gas chromatography. *Clinical Chemistry* 24, 1663-1673.
- Gekeler, W., Grill, E., Winnacker, E.-L., Zenk, M.H., 1989. Survey of the plant kingdom for the ability to bind heavy metals through phytochelatins. *Z. Naturforsch.* 44c, 361-369.
- Giner, J.-L., Kiemle, D.J., Kutrzeba, L., Zjawiony, J. 2007. Unambiguous NMR spectral assignments of salvinin A. *Magn. Reson. Chem.* 45, 351-354.
- Glawischnig, E., Gierl, A., Tomas, A., Bacher, A., Eisenreich, W., 2002. Starch biosynthesis and intermediary metabolism in maize kernels. Quantitative analysis of metabolite flux by nuclear magnetic resonance. *Plant Physiol.* 130, 1717-1727.
- Goese, M., Kammhuber, K., Bacher, A., Zenk, M.H., Eisenreich, W., 1999. Biosynthesis of bitter acids in hops. A ^{13}C NMR and ^2H NMR study on the building blocks of humulone. *Eur. J. Biochem.* 263, 447-454.
- Goodacre, R., Vaidyanathan, S., Dunn, W.B., Harrigan, G.G., Kell, D.B., 2004. Metabolomics by numbers: acquiring and understanding global metabolite data. *Trends in Biotechnology* 22, 245-252.
- Gordon, A.J., Minchin, F.R., Skot, L., James, C.L., 1997. Stress-induced declines in soybean N_2 fixation are related to nodule sucrose synthase activity. *Plant Physiol.* 114, 937-946.
- Griesinger, C.; Otting, G., Wüthrich, K., Ernst, R.R., 1988. Clean TOCSY for ^1H spin system identification in macromolecules. *J. Am. Chem. Soc.* 110, 7870-7872.
- Haas, P., Hill, T.G., 1925. *Mercurialis*. III. A consideration of the physiological significance of the chromogen. *Ann. Bot.* 39, 861-865
- Hatata M., 1982. Specific effect of certain salts on nitrogen metabolism of young corn seedlings. *Acta Botanica Polonia* 51, 263-273.

References

- Hecht, S.H.K., 2002. Intermediate and Enzyme des alternativen Terpenbiosyntheseweges. PhD Thesis, Lehrstuhl für Organische Chemie und Biochemie, Technische Universität München, Germany.
- Hecht, S., Kis, K., Eisenreich, W., Amslinger, S., Wungsintaweekul, J., Herz, S., Rohdich, F., Bacher, A., 2001. Enzyme-assisted preparation of isotope-labeled 1-deoxy-D-xylulose 5-phosphate. *J. Org. Chem.* 66, 3948-3952.
- Herz, S., 2000. Expression von Gene der Riboflavin- und Terpenbiosynthese und Charakterisierung der entsprechenden Proteine. PhD Thesis, Technische Universität München, Germany.
- Hill, R.E., Sayer, B.G., Spenser, J.D., 1989. Biosynthesis of vitamin B₆: incorporation of D-1-deoxyxylulose. *J. Am. Chem. Soc.* 111, 1916-1917.
- Horning, E.C., Horning, M.G., 1970. Metabolic profiles: chromatographic methods for isolation and characterization of a variety of metabolites in man. In: Olson, R.E. (Ed.), *Methods in Medicinal Research*. Year Book Medicinal Publishers, Chicago, p. 369.
- Horning, E.C., Horning, M.G., 1971. Human metabolic profiles obtained by GC and GC/MS. *Journal of Chromatographic Science* 9, 129-140.
- Human, D.V., Sumner, L.W., 2002. Metabolic profiling of saponins in *Medicago sativa* and *Midicago truncatula* using HPLC coupled to an electrospray ion-trap mass spectrometer. *Phytochemistry* 59, 347-360.
- Hutchinson, C.R., Hsia, M.T. Stephen, C.R.A., 1976. Biosynthetic studies with carbon-13 dioxide of secondary plant metabolites. *Nicotiana* alkaloids. 1. Initial experiments. *J. Am. Chem. Soc.* 98, 6006-6011.
- Illarionova, V., Kaiser, J., Ostrozhenkova, E., Bacher, A., Fischer, M., Eisenreich, W., Rohdich, F., 2006. Nonmevalonate terpene biosynthesis enzymes as antiinfective drug targets: substrate synthesis and high-throughput screening methods.

References

- Irigoyen, J.J., Emerich, D.W., Sánchez-Díaz, M., 1992. Phosphoenolpyruvate carboxylase malate and alcohol dehydrogenase activities in alfalfa (*Medicago sativa* L.) nodules under water stress. *Physiologia Plantarum* 84, 61-66.
- Jork, H., Funk, W., Fischer, W., Wimmer, H., 1998. *Dünnschicht Chromatographie: Reagenzien und Nachweismethoden*. VCH Verlagsgesellschaft, Weinheim, Basel, Cambridge, New York.
- Kaiser, J., Yassin, M., Prakash, S., Safi, N., Agami, M., Lauw, S., Ostrozhenkova, E., Bacher, A., Rohdich, F., Eisenreich, W., Safi, J., Golan-Goldhirsh, A., 2007. Anti-malarial drug targets: screening for inhibitors of 2C-methyl-D-erythritol 4-phosphate synthase (IspC protein) in Mediterranean plants. *Phytochemistry* 14, 242-249.
- Kim, S.A., Copelaand, L., 1996. Enzymes of poly- β -hydroxybutyrate metabolism in soybean and chickpea bacteroids. *Applied and Environmental Microbiology* 62, 4186-4190.
- Knappe, S., Flügge, U.I., Fischer, K., 2003. Analysis of the plastidic phosphate translocator gene family in *Arabidopsis* and identification of new phosphate translocator-homologous transporters, classified by their putative substrate-binding side. *Plant Physiology* 131, 1178-1190.
- Krause, K., Maier, R.M., Kofer, W., Krupinska, K., Herrmann, R.G., 2000. Disruption of plastid-encoded RNA polymerase genes in tobacco: expression of only a distinct set of genes is not based on selective transcription of the plastid chromosome. *Mol. Gen. Genet.* 263, 1022-1030.
- Krishnan, P., Kruger, N. J., Ratcliffe, R. G., 2005. Metabolite fingerprinting and profiling in plants using NMR. *J. Exp. Botany* 56, 255-265.
- Kruger, N. J., Ratcliffe, R. G., Roscher, A., 2003. Quantitative approaches for analysing fluxes through plant metabolic networks using NMR and stable isotope labelling. *Phytochemistry Rev.* 2, 17-30.

References

- Kruger, N.J., von Schaewen, A., 2003. The oxidative pentose phosphate pathway: structure and organisation. *Current Opinion in Plant Biology* 6, 236-246.
- Kurth, H., Spreemann, R., 1998. Phytochemical characterization of various St. John's Wort extracts. *Adv. Ther.* 15, 117-128.
- Kutrzeba, L., Dayan, F.E., Howell, J.L., Feng, J., Giner, J.-L., Zjawiony, J.K., 2007. Biosynthesis of salvinorin A proceeds via the deoxyxylulose phosphate pathway. *Phytochemistry* 68, 1872-1881.
- Kuzuyama, T., Takagi, M., Takahashi, S., Seto, H., 2000a. Cloning and characterization of 1-deoxy-D-xylulose 5-phosphate synthase from *Streptomyces* sp. Strain CL190, which uses both the mevalonate and non-mevalonate pathways for isopentenyl diphosphate biosynthesis. *J. Bacteriol.*, 182, 891-897.
- Kuzuyama, T., Takahashi, S., Takagi, M., Seto, H., 2000b. Characterization of 1-deoxy-D-xylulose 5-phosphate reductoisomerase, an enzyme involved in isopentenyl diphosphate biosynthesis, and identification of its catalytic amino acid residues. *J. Biol. Chem.* 275, 19928-19932.
- Last, R.L., Jones, A.D., Shachar-Hill, Y., 2007. Towards the plant metabolome and beyond. *Nat. Rev. Mol. Cell Biol.* 8, 167-174.
- Lee, W.N., Byerley, L.O., Bergner, E.A., Edmond, J., 1991. Mass isotopomer analysis: theoretical and practical considerations. *Biol. Mass Spectrom.* 20, 451-458.
- Leete, E., 1992. The biosynthesis of nicotine and related alkaloids in intact plants, isolated plant parts, tissue cultures, and cell-free systems. *Environmental Science Research* 44, (Secondary-Metabolite Biosynthesis and Metabolism), 121-139.
- Lewis, I.A., Schommer, S.C., Hodis, B., Robb, K.A., Tonelli, M., Westler, W.M., Sussman, M.R., Markley, J.L., 2007. Method for determining molar concentrations of metabolites in complex solutions from two-dimensional ^1H - ^{13}C NMR spectra. *Analytical Chemistry* 79, 9385-9390.

References

- Lichtenthaler, H.K., Schwender, J., Disch, A., Rohmer, M., 1997. Biosynthesis of isoprenoids in higher plant chloroplasts proceeds via a mevalonate-independent pathway. *FEBS Lett.* 400, 271-274.
- Lindon, J.C., Holmes, E., Nicholson, J.K., 2003. So what's the deal with metabolomics? Metabolomics measures the fingerprinting of biochemical perturbations caused by disease, drugs, and toxins. *Anal. Chem.* 75, 384A-391A.
- Lindon, J.C., Holmes, E., Nicholson, J.K., 2007. Metabolomics in pharmaceutical R&D. *FEBS J.* 274, 1140-1151.
- Lois, L.M., Campos, N., Putra, S.R., Danielsen, K., Rohmer, M., Boronat, A., 1998. Cloning and characterization of a gene from *Escherichia coli* encoding a transketolase-like enzyme that catalyzes the synthesis of D-1-deoxyxylulose 5-phosphate, a common precursor for isoprenoid, thiamin, and pyridoxol biosynthesis. *Proc. Natl. Acad. Sci. USA*, 95, 2105-2110.
- Łoś-Kuczera, M., 1990. Composition and nutritive value. *Food Products*, 167.
- Macura, S., Ernst, R.R. 1980. Elucidation of cross-relaxation in liquids by two-dimensional NMR spectroscopy. *Mol. Phys.* 41, 95-117.
- Manandhar A., Gresshoff, P.M., 1980. Blue spruce (*Picea pungens*) tissue and cell culture. *Cytobiosphere* 29, 175-182.
- Margl, L., Eisenreich, W., Adam, P., Bacher, A., Zenk, M.H., 2001. Biosynthesis of thiophenes in *Tagetes patula*. *Phytochemistry* 58, 875-881.
- Masahiro, I., 2005. Phytochelatins. *Braz. J. Plant Physiol.* 17 (1), 65-78.
- Mathews, C.K., Holde, K.E., Ahern, K.G., 1999. *Biochemistry*. Third edition.
- Merritt, A.T. and Ley, S.V., 1992. Clerodane diterpenoids. *Nat. Prod. Rep.* 243-288.

References

- Mesnard, F., Azaroual, N., Marty, D., Fliniaux, M.-A., Robins, R.J., Vermeersch, G., Monti, J.P., 2000. Use of ^{15}N revers gradient two-dimensional nuclear magnetic resonance spectroscopy to follow metabolic activity in *Nicotiana plumbaginifolia* cell suspension cultures. *Planta* 210, 446-453.
- Mroczek, W.J., 1972. Biochemical profiling and the natural history of hypertensive diseases. *Circulation* 45, 1332-1333.
- Müller, L., 1979. Sensitivity enhanced detection of weak nuclei using heteronuclear multiple quantum coherence. *J. Am. Chem. Soc.* 101, 4481-4484.
- Müller, W.E., 2003. Current St. John's wort research from mode of action to clinical efficacy. *Pharmacol. Res.* 47, 101-109.
- Nabeta, K., Ishikawa, T., Okuyama, H., 1995. Sesqui- and di-terpene biosynthesis from ^{13}C labelled acetate and mevalonate in cultured cells of *Heteroscyphus planus*. *J. Chem. Soc. Perkin. Trans. I*, 3111-3115.
- Neuhaus, H.E., Emes, M.J., 2000. Nonphotosynthetic metabolism in plastids. *Annual Review of Plant Physiology and Plant Molecular Biology* 51, 111-140.
- Nicholson, J.K., Wilson, I.D., 2003. Understanding 'global' systems biology: metabolomics and the continuum of metabolism. *Nat. Rev. Drug Discov.* 2, 668-676.
- Noctor, G. and Foyer C.H., 1998. Ascorbate and glutathione: keeping active oxygen under control. *Plant Physiol. Mol. Biol.* 49, 249-279.
- Noctor, G., Queval, G., Gakière, B., 2006. NAD(P) synthesis and pyridine nucleotide cycling in plants and their potential importance in stress conditions. *J. Exp. Bot.* 57, 1603-1620.
- Novak, B.H., Hudlicky, T., Reed, J.W., Mulzer, J., Trauner, D., 2000. Morphine synthesis and biosynthesis – an update. *Current Organic Chemistry* 4, 343-362.

References

- Oliver, S.G., Winson, M.K., Kell, D.B., Baganz, F., 1998. Systematic functional analysis of the yeast genome. *Trends in Biotechnology* 16, 373-378.
- Ortega, A., Blount, J.F., Manchand, P.S., 1982. Salvinorin, a new trans-neoclerodane diterpene from *Salvia divinorum* (Labiatae). *J. Chem. Soc.* 10, 2505-2508.
- Ostrozhenkova, E., Eylert, E., Schramek, N., Golan-Goldhirsh, A., Bacher, A., Eisenreich, W., 2007. Biosynthesis of the chromogen hermidin from *Mercurialis annua* L. *Phytochemistry* 68, 2816-2824.
- Pessaraki, M., Huber, J.T., Tucker, T.C., 1989. Protein synthesis in green beans under salt stress with two nitrogen sources. *J. of Plant Nutrition* 12, 1261-1277.
- Piantini, U., Sorensen, O.W., Ernst, R.R., 1982. Multiple quantum filters for elucidating NMR coupling networks. *J. Am. Chem. Soc.* 104, 6800-6801.
- Piel, J., Donath, J., Bandemer, K., Boland, W., 1998. Mevalonate-independent biosynthesis of terpenoid volatiles in plants: induced and constitutive emission of volatiles. *Angew. Chemie Int. Ed.* 37, 2478-2481.
- Pietrini, F., Iannelli, M.A., Pasqualini, S., Massacci, A., 2003. Interaction of cadmium with glutathione and photosynthesis in developing leaves and chloroplasts of *Phragmites australis* (Cav.). *Plant Physiol.* 133, 829-837.
- Poeknapo, C., Fisinger, U., Zenk, M.H., Schmidt, J., 2004. Evaluation of the mass spectrometric fragmentation of codeine and morphine after ¹³C-isotope biosynthetic labeling. *Phytochemistry* 65, 1413-1420.
- Poulsen, N., 1990. Chives, *Allium schoenoprasum* L. In: J.L. Brewster & H.D. Rabinowitch (Eds.), *Onions and Allied Crops 3, Biochemistry, Food Science, and minor crops*, 231-250.
- Radykewicz, T., 2005. Störexperimenta an photosynthetisch aktiven Organismen. Untersuchungen zu Primär- and Sekundärstoffbiosynthesen in komplexen

References

- Stoffwechselnetzwerken. PhD Thesis, Lehrstuhl für Organische Chemie und Biochemie, Technische Universität München, Germany.
- Raskin, I., Kumar, P..A.N., Dushenkov, S., Salt, D.E., 1994. Bioconcentration of heavy metals by plants. *Current Opinion in Biotechnology* 5, 285-290.
- Ratcliffe, R. G., Shachar-Hill, Y., 2001. Probing plant metabolism with NMR. *Ann. Rev. Plant Physiol. Plant Mol. Biol.* 52, 499-526.
- Ratcliffe, R. G., Shachar-Hill, Y., 2006. Measuring multiple fluxes through plant metabolic networks. *Plant J.* 45, 490-511.
- Ratcliffe, R.G., Shachar-Hill, Y., 2005. Revealing metabolic phenotypes in plants: inputs from NMR analysis. *Biol. Rev.* 80, 27-43.
- Rausser, W.E., 1990. Phytochelatins. *Ann. Rev. Biochem.* 59, 61-86.
- Reisfield, A. S.: The Botany of *Salvia divinorum* (Labiatae). *Sida* 1993, 15, 349–366.
- Robinson, S.P., Downton, W.J.S., Millhouse, J.A., 1983. Photosynthesis and ion content of leaves and isolated chloroplasts of salt-stressed spinach. *Plant Physiol.* 73, 238-242.
- Robinson, N.J., Tommey, A.M., Kuske, C., Jackson, P.J., 1993. Plant metallothioneins. *Biochem. J.* 295, 1-10.
- Rohdich, F., Bacher, A., Eisenreich, W., 2004. Perspectives in anti-infective drug design. The late steps in the biosynthesis of the universal terpenoid precursors, isopentenyl diphosphate and dimethylallyl diphosphate. *Bioorganic Chemistry* 32 (5), 292-308.
- Rohdich, F., Bacher, A., Eisenreich, W., 2005. Isoprenoid biosynthetic pathways as anti-infective drug targets. *Biochem. Soc. Trans.* 33, 785-791.

References

- Rohdich, F., Hecht, S., Bacher, A., Eisenreich, W., 2003. Deoxyxylulose phosphate pathway of isoprenoid biosynthesis. Discovery and function of ispDEFGH genes and their cognate enzymes. *Pure Appl. Chem.* 75, 393-405.
- Rohdich, F., Schuhr, C.A., Hecht, S., Herz, S., Wungsintaweekul, J., Eisenreich, W., Zenk, M.H., Bacher, A., 2000. Biosynthesis of isoprenoids. A rapid method for the preparation of isotope-labeled 4-Diphosphocytidyl-2C-methyl-D-erythritol. *J. Amer. Chem. Soc.* 122, 9571-9574.
- Rohdich, F., Wungsintaweekul, J., Fellermeier, M., Sagner, S., Herz, S., Kis, K., Eisenreich, W., Bacher, A., Zenk, M.H., 1999. Cytidine 5'-triphosphate-dependent biosynthesis of isoprenoids: YgbP protein of *Escherichia coli* catalyzes the formation of 4-diphosphocytidyl-2-C-methylerythritol. *Proc. Natl. Acad. Sci.*, 96, 11758-11763.
- Rohmer, M., 2007. Diversity in isoprene unit biosynthesis: the methylerythritol phosphate pathway in bacteria and plastids. *Pure Appl. Chem* 79, 739-751.
- Rohmer, M., Knani, M., Simonin, P., Sutter, B., Sahm, H., 1993. Isoprenoid biosynthesis in bacteria: a novel pathway for the early steps leading to isopentenyl diphosphate. *Biochem. J.* 295, 517-524.
- Rodriguez-Hahn, L.; Esquivel, B.; Cardenas, J.: Neo-clerodane diterpenoids from American *Salvia* species. *Recent Adv. Phytochem.* 1995, 29, 311-332.
- Römisch-Margl, W., Schramek, N., Radykewicz, T., Ettenhuber, C., Eylert, E., Huber, C., et al., 2007. ¹³CO₂ as a universal metabolic tracer in isotopologue perturbation experiments. *Phytochemistry* 68, 2273-2289.
- Roscher, A., Kruger, N. J., Ratcliffe, R. G., 2000. Strategies for metabolic flux analysis in plants using isotope labelling. *J. Biotechnol.* 77, 81-102.

References

- Roth, B.L., Baner, K., Westkaemper, R., Siebert, D., Rice, K.C., Steiberg, S.A., Ernsberger, P., Rothman, R.B., 2002. Salvinorin A: A potent naturally occurring nonnitrogenous κ opioid selective agonist. PNAS 99, 11934-11939.
- Salt, D.E., Blaylock, M., Kumar, N.P:B.A., Dushenkov, V., Ensley, B., Chet, I., Raskin, I., 1995. Phytoremediation: a novel strategy for the removal of toxic metals from the environment using plants. Biotechnology 13, 468-474.
- Salt, D.E. and Wagner G.J., 1993. Cadmium transport across tonoplast of vesicles from oat roots. Evidence for a $\text{Cd}^{2+}/\text{H}^{+}$ antiport activity. J. Biol. Chem. 268, 12297-12302.
- Schaefer, J., Kier, L.D., Stejskal, E.O., 1980. Characterization of photorespiration in intact leaves using carbon-13 carbon dioxide labeling. Plant Physiol. 65, 254-259.
- Schaefer, J., Stejskal, E.O., Beard, C.F., 1975. Carbon-13 nuclear magnetic resonance analysis of metabolism in soybeans labeled by $^{13}\text{CO}_2$. Plant Physiol. 55, 1048-1053.
- Schuhr, C.A., Radykewicz, T., Sagner, S., Latzel, C., Zenk, M.H., Arigoni, D. et al., 2003. Quantitative assessment of metabolite flux by NMR spectroscopy. Crosstalk between the two isoprenoid biosynthesis pathways in plants. Phytochemistry Rev. 2, 3-16.
- Swan, G.A., 1984. Hermidin, a chromogen from *Mercurialis perennis* L. Experientia 40 (7), 687-688.
- Schwarz, M.K., 1994. Terpen-Biosynthese in *Ginkgo biloba*: Eine überraschende Geschichte. PhD Thesis, ETH Zürich, Switzerland.
- Schwender, J., Ohlrogge, J., Shachar-Hill, Y., 2004. Understanding flux in plant metabolic networks. Curr. Opinion Plant Biol. 7,309-317.

References

- Seeman, J.R., Critchley, C., 1985. Effects of salt stress on the growth, ion content, stomatal behaviour and photosynthetic capacity of salt-sensitive species, *Phaseolus vulgaris* L. *Planta* 164, 151-162.
- Seger, C. and Sturm, S., 2007. Analytical aspects of plant metabolite profiling platforms: current standings and future aims. *J. of Proteome Research* 6, 480-497.
- Shachar-Hill, Y., 2002. Nuclear magnetic resonance and plant metabolic engineering. *Metabolic Engineering* 4, 90-97.
- Shachar-Hill, Y., Pfeffer, P.E., Germann, M.W., 1996. Following plant metabolism in vivo and in extracts with heteronuclear two-dimensional nuclear magnetic resonance spectroscopy. *Analytical Biochemistry* 243, 110-118.
- Sitzung 841 des Bundesrates, 2008. Stellungnahme des BND zur Aufnahme von *Salvia divinorum* in das Betäubungsmittelgesetz. Berlin.
- Soga, Y., Ueno, Y., Naraoka, H., Ohashi, Y., Tomita, M., Nishioka, T., 2002. Simultaneous determination of anionic intermediates for *Bacillus subtilis* metabolic pathways by capillary electrophoresis electrospray ionization mass spectrometry. *Analytical Chemistry* 74, 2233-2239.
- Spielbauer, G., Margl, L., Hannah, L. C., Römisch, W., Ettenhuber, C., Bacher, A., Gierl, A., Eisenreich, W., Genschel, U., 2006. Robustness of central carbohydrate metabolism in developing maize kernels. *Phytochemistry* 67, 1460-1475.
- Sprenger, G. A., Schörken U; Wiegert, T., Grolle, S., de Graaf, A., Taylor, S.V., Begley, T.P., Bringer-Meyer, S., Sahm, H., 1997. Identification of a thiamin-dependent synthase in *Escherichia coli* required for the formation of the 1-deoxy-D-xylulose 5-phosphate precursor to isoprenoids, thiamin, and pyridoxol. *Proc. Natl. Acad. Sci. USA*, 94, 12857-12862.
- Steffens, J.C., 1990. The heavy metal-binding peptides of plants. *Annu Rev. Plant Physiol. Mol Biol.* 41, 553-575.

References

- Steinmetz, K.A., 1996. Vegetables, fruits, and cancer prevention: A review. *J. Am Diet Assoc.* 96, 1027-1039.
- Sumner, L.W., Mendes, P., Dixon, R.A., 2003. Plant metabolomics: large-scale phytochemistry in the functional genomics era. *Phytochemistry* 62, 817-836.
- Sun., J.X., Sun, X.F., Zhao, H., Sun, R.C., 2004. Isolation and characterization of cellulose from sugarcane bagasse. *Polymer Degradation and Stability* 84, 331-339.
- Swan, G.A., 1984. Hermidin, a chromogen from *Mercurialis perennis* L. *Experientia.* 40 (7), 687-688.
- Swan, G.A., 1985. Isolation, structure, and synthesis of hermidin, a chromogen from *Mercurialis perennis* L. *J. Chem. Soc. Perkin Trans. 8*, 1757-1766.
- Tambasco-Studart, M., Titiz, O., Raschle, T., Forster, G., Amrhein, N., Fitzpatrick, T.B., 2005. Vitamin B₆ biosynthesis in higher plants. *PNAS* vol. 102, 13687-13692.
- Thompson, J.A., Markey, S.P., 1975. Quantitative metabolic profiling of urinary organic acids by gas chromatography-mass spectrometry: comparison of isolation methods. *Analytical Chemistry* 47, 1313-1321.
- Tweeddale, H., Notley-McRobb, L., Ferenci, T., 1998. Effect of slow growth on metabolism of *Escherichia coli*, as revealed by global metabolite pool ("Metabolome") analysis. *Journal of Bacteriology* 180, 5109-5116.
- Umehara, M., Sueyoshi, T., Shimomura, K., Iwai, M., Shigyo, M., Hirashima, K., Nakahara, T., 2006. Interspecific hybrids between *Allium fistulosum* and *Allium schoenoprasum* reveal carotene-rich phenotype. *Euphytica* 148, 295-301.
- Valdés, III, L. J. J.; Díaz, J. L.; Paul, A. G.: Ethnopharmacology of *ska Maria Pastora* (*Salvia divinorum*, Epling and Játiva-M.). *J. Ethnopharmacol.* 1983, 7, 287-312.

References

- Valdés, III, L. J. J.; Hatfield, G. M.; Koreeda, M.; Paul, A. G.: Studies of *Salvia divinorum* (Lamiaceae), an Hallucinogenic Mint from the Sierra Mazateca in Oaxaca, Central Mexico. *Econ. Bot.* 1987, 41, 283–291.
- Verpoorte, R., Choi, Y.H., Kim, H.K., 2007. NMR-based metabolomics at work in phytochemistry. *Phytochemistry Review* 6, 3-14.
- Vogeli-Lange R. and Wagner, G.J., 1990. Subcellular localization of cadmium-binding peptides in tobacco leaves. Implication of a transport function for cadmium-binding peptides. *Plant Physiol.* 92, 1086-1093.
- Ward, J.L., Baker, J.M., Beale, M.H., 2007. Recent applications of NMR spectroscopy in plant metabolomics. *FEBS J.* 274, 1126-1131.
- Weiss, R., Fintelmann V., 2000. *Herbal Medicine*, 2nd ed. New York: Thieme.
- Werner, I., Bacher, A., Eisenreich, W., 1997. Formation of gallic acid in plants and fungi. A retrobiosynthetic study with ¹³C-labelled glucose. *J. Biol. Chem.* 272, 25474-25482.
- White, R.H., 1978. Stable isotope studies on the biosynthesis of the thiazole moiety of thiamine in *Escherichia coli*. *Biochemistry* 17, 3833-3840.
- Widarto, H.T., Meijden, E.V.D., Lefeber, A.W.M., Erkelens, C., Kim, H.K., Choi, Y.H., Verpoorte, R., 2006. Metabolomic differentiation of *Brassica rapa* following herbivory by different insect instars using two-dimensional nuclear magnetic resonance spectroscopy. *J. Chem. Ecol.* 32, 2417-2428.
- Wungsintaweekul, J., 2001. Enzymes of the alternative terpenoid pathway in *Escherichia coli*. PhD Thesis, Technische Universität München, Germany.
- Yang, J.-W. and Orihara, Y, 2002. Biosynthesis of abietane diterpenoids in cultured cells of *Torreya nucifera* var. *radicans*: biosynthetic inequality of the FPP part and the terminal IPP. *Tetrahedron* 58, 1265-1270.

References

- Yang, S.Y., Kim, H.K., Lefeber, A.W.M., Erkelens, C., Angelova, N., Choi, Y.H., Verpoorte, R., 2006. Application of two-dimensional nuclear magnetic resonance spectroscopy to quality control of Ginseng commercial products. *Planta Med.* 72, 364-369.